pennsylvania
DEPARTMENT OF TRANSPORTATION

STRUCTURAL EVALUATION OF SLAB REHABILITATION BY THE METHOD OF HYDRODEMOLITION AND LATEX MODIFIED OVERLAY

FINAL REPORT

December 2013

Kent A Harries, PhD, FACI, PEng
Matthew McCabe, BSCE
Michael Sweriduk, BSCE
University of Pittsburgh

COMMONWEALTH OF PENNSYLVANIA
DEPARTMENT OF TRANSPORTATION

CONTRACT # 4400004037
WORK ORDER # PIT WO 01

SWANSON school of engineering
civil and environmental engineering
structural engineering and mechanics
Watkins Haggart structural engineering laboratory

The contents of this report reflect the views of the author(s) who is(are) responsible for the facts and the accuracy of the data presented herein. The contents do not necessarily reflect the official views or policies of the US Department of Transportation, Federal Highway Administration, or the Commonwealth of Pennsylvania at the time of publication. This report does not constitute a standard, specification or regulation.

This work was sponsored by the Pennsylvania Department of Transportation and the U.S. Department of Transportation, Federal Highway Administration.

Technical Report Documentation Page

1. Report No.	2. Government Accession No.	3. Recipient's Catalog No.
FHWA-PA-2013-006-PIT WO 01		

4. Title and Subtitle STRUCTURAL EVALUATION OF SLAB REHABILITATION BY THE METHOD OF HYDRODEMOLITION AND LATEX MODIFIED OVERLAY	**5. Report Date** December 2013 **6. Performing Organization Code**
7. Author(s) Kent Harries, Matthew McCabe and Michael Sweriduk	**8. Performing Organization Report No.** CE/ST 43
9. Performing Organization Name and Address University of Pittsburgh Civil and Environmental Engineering 742 Benedum Hall, Pittsburgh, PA 15261	**10. Work Unit No. (TRAIS)** **11. Contract or Grant No.** 4400004037 – PIT WO 01
12. Sponsoring Agency Name and Address The Pennsylvania Department of Transportation Bureau of Planning and Research Commonwealth Keystone Building 400 North Street, 6th Floor Harrisburg, PA 17120-0064	**13. Type of Report and Period Covered** Final Report: December 21, 2012 – December 31, 2013 **14. Sponsoring Agency Code**

15. Supplementary Notes

16. Abstract

The primary objective of this study was to assess the validity of PennDOT Publication 15 Section 5.5.5.1, specifically that "a latex overlay is not considered structurally effective", in terms of the structural response of the bridge superstructure. Experimental evidence from this study clearly demonstrates that the LMC overlay is structurally effective in terms of load carrying capacity. Specifically a) the anticipated capacity of an LMC overlaid deck may be estimated as that of the original full-depth deck. Experimental capacities were seen to exceed this value in all cases. Simple plane sections analyses are suitable for obtaining these capacities; b) the LMC interface has essentially no impact on the behavior of the repaired slabs; and, c) the interface shear capacity is expected to exceed the demand for bridge slabs typical of slab-on-girder bridges. The use of pull-off testing to assess interface bond is promulgated and acceptance criteria proposed. This study has demonstrated the effectiveness of PennDOT Method 2 LMC overlays for Type 1 and 2 bridge deck repairs.

17. Key Words	18. Distribution Statement
hydrodemolition, latex-modified concrete, overlay, slab	No restrictions. This document is available from the National Technical Information Service, Springfield, VA 22161

19. Security Classif. (of this report)	20. Security Classif. (of this page)	21. No. of Pages	22. Price
Unclassified	Unclassified	118	N/A

Form DOT F 1700.7 (8-72) Reproduction of completed page authorized

EXECUTIVE SUMMARY

The primary objective of this study was to assess the validity of *PennDOT Publication 15 Section 5.5.5.1*, specifically that "a latex overlay is not considered structurally effective", in terms of the structural response of the bridge superstructure. Experimental evidence from this study clearly demonstrates that the LMC overlay is structurally effective in terms of load carrying capacity. Several parameters were varied amongst full-scale test specimens in the experimental program: overlay depth, removal of concrete 'shadows' under primary reinforcement bars, and the direction of bending. The LMC-repaired slabs acted as monolithic slabs in all cases and the capacity was uniform regardless of LMC depth. The capacity of the LMC-repaired slabs tested in positive flexure exceeded their predicted ultimate capacities and the capacity of the unrepaired control slab in all cases. Finally, it was demonstrated based on fundamental mechanics and shear friction theory that LMC interface stresses are relatively low and unlikely to exceed reasonable values of capacity for properly constructed LMC overlay repairs. It is therefore recommended that LMC overlays exceeding 1.25 inches in depth may be considered structurally effective in load rating a bridge deck. This assumes that the overlay in question has been constructed to an appropriate standard using 'best practices' described in the document. A number of specific conclusions were drawn from the experimental study of full-scale slab specimens:

- The anticipated capacity of an LMC overlaid deck may be estimated as that of the original full-depth deck. Experimental capacities were seen to exceed this value in all cases. Simple plane sections analyses are suitable for obtaining these capacities.
- The LMC interface has essentially no impact on the behavior of the repaired slabs.
- The interface shear capacity is expected to exceed the demand for bridge slabs typical of slab-on-girder bridges.

It is further recommended that a pull-off testing program be establish for quality assurance purposes in accordance with ASTM C1583. A 'commentary' on this test method is provided to clarify its use for this specific application. Additionally, acceptance criteria for such testing are proposed as follows:

- If the pull-off strength exceeds 200 psi, it is believed that the interface shear capacity will be adequate and the overlay will behave in a fully composite manner with the substrate concrete. For pull-off capacities less than 200 psi, the mode of failure is telling. If the failure remains in the substrate (Mode S), the interface is stronger than the substrate and the shear capacity is at least that of the residual substrate concrete. In such a case, composite behavior of the overlay is likely. Pull-off tests indicating an interface failure (Mode I) are cause for further investigation. Pull-off tests less than 100 psi, regardless of failure mode should not be accepted.

This study has demonstrated the effectiveness of PennDOT Method 2 LMC overlays for Type 1 and 2 bridge deck repairs. The LMC clearly contributes to the load carrying capacity of the rehabilitated deck slab. With this conclusion, it is envisioned that more bridges that would otherwise be subject to complete deck replacement may be viable candidates for overlay repair. This, it is believed, will conserve resources directed to an individual bridge and significantly speed the deck rehabilitation process.

ACRONYMS

AASHTO	American Association of State Highway and Transportation Officials
ACI	American Concrete Institute
ASTM	American Society for Testing and Materials
BMS	Bridge Management System
DC	Dead Load of Structural Components and nonstructural attachments (AASHTO)
DW	Dead Load, Wearing Surface and Utilities (AASHTO)
FHWA	Federal Highway Administration
GPR	Ground Penetrating Radar
HD	Hydrodemolition
HMWM	High Molecular Weight Methacrylate
ICRI	International Concrete Repair Institute
LMM	Latex Modified Mortar
LMC	Latex Modified Concrete
LRFD	Load and Resistance Factor Design
MSC	Microsilica Modified Concrete
NDE	Non-Destructive Evaluation
PCC	Portland Cement Concrete
PennDOT	Pennsylvania Department of Transportation
SCS	Siva Corrosion Services
SDC	Super-dense Plasticized Concrete
SHRP	Strategic Highway Research Program
SSD	Saturated Surface Dry

NOMENCLATURE

A	area of material above interface
A_c	horizontal area of concrete in the shear span
A_{cv}	area of concrete interface
A_s	area of tension reinforcement
A_v	area of steel crossing shear interface
b	slab width
b_f	flange width
c	cohesion factor
c	concrete cover
d_b	reinforcement bar diameter
d_o	target depth of hydrodemolition
f'_c	concrete compressive strength
f_r	modulus of rupture
f_t	direct tensile strength (pull-off strength)
f_{sp}	split cylinder strength of concrete
f_y	steel reinforcement yield strength
h	height of slab
I	moment of inertia of gross cross section
K	generic limiting factor-shear friction
L	span length
M	moment
M_{DL}	dead load design moment
M_{LL}	live load design moment
N	normal forces
P	applied Load
Pc	externally applied loads normal to the interface
S	girder spacing
T	tension in Reinforcement
t	width of cross-section at the interface
V	internal shear

V_{ni}	shear Friction Capacity
w	shear interface crack width
y	distance from centroid of A to centroid of gross section
γ	normal force factor
Δ	shear interface displacement or slip
ε_s	shear interface steel reinforcement strain
μ	friction factor
ρ	slab longitudinal steel reinforcement ratio
φ	curvature

U.S. customary units were used throughout this report. The following conversion factors were used:

1 inch = 25.4 mm

1 kip = 4.448 kN

1 ksi = 6.895 MPa

Reinforcing bar was also designated using U.S. standard notation. This notation consists of a "#" symbol followed by a number (e.g. #5). The number refers to the bar diameter in eighths of an inch.

TABLE OF CONTENTS

1 INTRODUCTION AND LITERATURE REVIEW

1.1 OBJECTIVE

The objective of this work is to provide laboratory-based experimental verification and assessment of the performance of reinforced concrete deck slabs rehabilitated by means of hydrodemolition (HD) followed by the application of a latex modified concrete (LMC) overlay. The fundamental objective is to determine whether the overlay may be considered composite with the residual deck and under what conditions composite behavior may be assumed in load rating of the rehabilitated deck.

1.2 INTRODUCTION AND BACKGROUND

Chapter 5 of PennDOT Publication 15[1] *Design Manual Part 4: Structures*, provides guidance for rehabilitation strategies for bridge deck structures (specifically, Figure 5.5.2.3-3). Section 1040 of PennDOT Publication 408[1] *Construction Specifications* provides the necessary specifications and identifies three levels of bridge deck repair (Section 1040.1):

Type 1: Areas where deteriorated concrete extends to a maximum depth of the top of the top mat of reinforcement bars, exposing no more than one-quarter bar diameter.

Type 2: Areas where deteriorated concrete extends beyond the depth of the top of the top mat of reinforcement bars or where reinforcement bars are unbonded. Regardless of the extent of concrete deterioration, A Type 2 repair requires that 0.75 in (20 mm) clearance be provided all around top mat reinforcing bars (*Pub. 408*. Section 1040.3b)

Type 3: Areas where deteriorated concrete or patching extends to the full depth of the deck, including deck overhang areas.

The focus of the present work are Type 1 and Type 2 repairs carried out by the method of hydrodemolition (HD) followed by the application of a latex modified concrete (LMC) overlay material. The construction requirements for LMC are provided in *Pub. 408* Section 1040.3 and the specifications for LMC and its application are provided in Section 1042. Section 1040.3f.1b provides two methods of executing a Type 2 repair with LMC overlay:

Method 1: provides an LMC overlay (of unspecified, although presumably thin, thickness) on top of a Class AAA concrete repair. This method requires two complete cycles of surface preparation and material application (concrete followed by LMC), and requires that the AAA concrete achieve a compressive strength of 3300 psi (23 MPa) before subsequent scarification and LMC overlay application.

Method 2: provides that Type 2 repairs up to 2 in. (50 mm) deep may be completed as a single monolithic LMC overlay.

[1] citations are to May 2012 edition of *Publication 15* and April 2011 edition of *Publication 408*

Section 1042.3, to which Method 2 refers, does not, however, appear to specify a maximum thickness of LMC overlay and specifically provides guidance for minimum thickness greater than 50 mm (in Table A, for instance). From the perspective of time and labor required, clearly Method 2 repairs are preferred. The present study will consider Method 2 Type 2 repairs having LMC overlay depths ranging from 0.5 to 3.75 in. (12 – 95 mm), thereby extending the range of depths of LMC-only repairs from that suggested by *Pub. 408*.

Publication 408 Section 1042.2f requires that latex modified ***mortar*** (LMM) be used for depths less than 1.25 in. (30 mm) and latex modified ***concrete*** (LMC) be used for thicker applications. Mix requirements for both LMM and LMC are provided in Section 1042.2f. Anecdotally, field practice is to use only LMC and place a depth of at least 1.25 in.

Both *Publications. 408* Sections 1040 and 1042 permit power-driven hand tools, sandblasting or water blasting (i.e.: hydrodemolition (HD)) as a means of surface preparation prior to repair and overlay. Section 1040.3c restricts power tools to those less than 30 lbs (13.6 kg) and limits their use, particularly in cases where reinforcing steel is exposed (i.e. Type II repairs). Hydrodemolition is therefore attractive, particularly where large areas of repair are required.

Both *Publications 408* and *15* are silent on specific requirements for the replacement of reinforcing steel exposed during the HD process. Anecdotally, steel having more than 25% section loss due to corrosion is cut out and replaced. Additionally, PennDOT reports that for LMC applications thicker than about 4 in. (100 mm), an additional layer of welded wire fabric is added, presumably to provide improved crack control.

LMC overlays are reported as having a targeted service life of 20 years (*Pub. 15* Section 5.5.4(a)(3)). Nonetheless, *Pub. 15* Section 5.5.5.1 states that “a latex overlay is not considered structurally effective” in terms of superstructure load carrying capacity. The primary objective of this study is to challenge this last statement by identifying the extent to which Method 2 LMC overlays used in Type 1 and 2 repairs contribute to the load carrying capacity of the rehabilitated deck slab.

1.2.1 Latex-Modified Bridge Deck Concrete

Latex-modified concrete (LMC) is defined as “hydraulic cement and aggregates combined at the time of mixing with organic polymers that are dispersed or redispersed in water.” (ACI 548.4-11). Mortar and concrete incorporating natural (developed in 1930’s) and synthetic (1932) latex were initially deployed in the 1950’s in overlays intended only as protection against chloride ion penetration. In 1969, Virginia DOT demonstrated the first application of LMC as a bridge deck overlay. FHWA *Report RD-78-35 Styrene-Butadiene Latex Modifiers for Bridge Deck Overlays* was published in 1978 and remains the *de facto* specification for LMC additives in the United States highway industry. Today, more than 10,000 LMC overlays have been placed in the United States (Bertrand 2012). Reviews of performance of LMC bridge deck overlays in the United States (Sprinkel 2003 and 2009) and Canada (Bertrand and Sprinkel 2009) indicate that LMC has “excellent” resistance to chloride ion penetration, freeze-thaw durability, and resistance to scaling. LMC also exhibits “excellent” bond to the concrete substrate and can be expected to “extend the useful life of a bridge deck 25 years or more.”

ACI 548.3R-09 *Report on Polymer-Modified Concrete* provides an overview of the use of LMC. LMC itself is a ‘mature technology’; the main body of knowledge was developed in the 1980’s and 1990’s and now resides in specification documents such as ACI 548.4-11 *Specification for Latex-Modified Concrete Overlays* and DOT specifications.

1.3 LITERATURE REVIEW

Approximately 70 % of the bridges in the United States have concrete decks (this number is likely higher since 18% of bridge structures have no deck type reported) (FHWA 2011). Concrete overlays provide many benefits for extending the service life of concrete bridge structures. Overlays can be used to improve wearing surface performance, add load carrying capacity to the structure, and repair regions of concrete damaged by corroding reinforcing steel or other deleterious processes. Overlays are a more time and cost efficient solution than full deck replacement. The objective of this review is to identify best practices and means that may extend the applicability and utility of LMC overlays in lieu of full deck replacement. A recent RILEM (2011) state-of-the-art report, *Bonded Cement-Based Material Overlays for the Repair, the Lining or the Strengthening of Slabs or Pavements* provides an excellent overview of the subject matter.

1.3.1 Overlay Construction Process

The first step in the overlay construction process is to evaluate the concrete deck to determine which portions are in need of repair. Conventionally, an adequate assessment of a deck will consist of a visual inspection and 'chain dragging' (ASTM D4580). The visual inspection will identify cracking, spalling, erosion and other types of physical or chemical deterioration. Other means of non-destructive evaluation (NDE) are available but are rarely used. A review of NDE methods appropriate for concrete bridge structures is beyond the scope of the present study but was recently completed by the principle investigator for another PennDOT-funded study (Harries et al. 2009).

Once areas of deteriorated concrete are identified, they are removed to the level of sound concrete. There are many different methods for concrete removal on a bridge deck: sandblasting, shotblasting, pneumatic hammers, cutting, explosives, hydro-demolition, etc. (ACI Committee 546 2004). Silfwerbrand (2009) argues that hydrodemolition is the best method of concrete removal. Hydrodemolition (HD) enables concrete to be removed selectively based on the water pressure used. Essentially, water pressure builds inside the concrete and the concrete will begin to spall when the water pressure exceeds the *in situ* tensile strength of the concrete (Silfwerbrand 2009). Pressure builds in cracks and microcracks in deteriorated concrete and will be resisted in regions of sound concrete removing the former, leaving the latter in place and unaffected. Furthermore, HD can be carried out in a directional manner, making relatively 'focused' concrete removal possible. In addition to being faster and more focused, HD surfaces have a greater exposed aggregate area (since cement paste is selectively removed in deference to the tougher aggregate) than other mechanical means of concrete removal enhancing subsequent overlay bond. HD additionally cleans the steel of cement paste and corrosion product allowing good inspection of steel condition and enhancing bond of the overlay to the newly exposed 'bright' steel. Finally, unlike the use of pneumatic hammers, HD does not result in vibrations which may result in microcracking of the exposed surface or underlying slab.

Once damaged concrete is removed the exposed concrete must be cleaned and prepared to accept the overlay. The purpose of cleaning and prepping the substrate concrete is to ensure that there will be a sound monolithic connection between the substrate and the concrete overlay. Cleaning removes dirt and laitance that will affect the performance of the overlay. Common concrete surface cleaning techniques include sandblasting, shotblasting and high-pressure water blasting (Vaysburd and Bissonnette 2011). These methods not only clean the concrete of debris but also leave behind a rough and relatively uniform surface on the substrate concrete. The roughness of the substrate level provides the mechanical bond crucial for good overlay performance. The amplitude of the resulting substrate should be relatively uniform across the surface (to avoid stress raisers) and be sufficient to fully engage the coarse aggregate in the substrate concrete.

Similarly, exposed reinforcement steel must be cleaned, inspected and possibly replaced prior to placement of the overlay. Cleaning of reinforcement usually occurs during the concrete surface cleaning procedures but practitioners should pay careful attention to the reinforcement condition once it is exposed (Vaysburd and Bissonnette 2011). Standard practice dictates that epoxy coated reinforcing steel should be recoated prior to overlay placement. Where reinforcing steel is found to be corroded, the source or cause of corrosion should be determined. In some cases, removing and overlaying (usually chloride-) contaminated concrete will simply initiate corrosion immediately adjacent the patched region (Vaysburd and Bissonnette 2011). Thus remedial measures such as cathodic protection are necessary in addition to the overlay if long term performance is to be assured.

Another advantage of the use of overlays is that there is minimal need for formwork or falsework since the substrate deck remains intact. For relatively thick overlays that project above the original slab thickness (i.e.: cover to existing top steel is increased over that in the original deck), additional reinforcing steel (usually a welded wire fabric mat) should be provided to provide shrinkage and temperature crack control. Research has shown that reinforcing steel in concrete overlays performs just as well in pull-out tests as reinforcement placed at mid-thickness of a conventional concrete slab (Fowler and Trevino 2011).

Concrete overlays are generally selected to have similar mechanical properties as the sound substrate concrete (Silfwerbrand 2009). Latex modified concrete (LMC) is the preferred overlay material due to its low permeability and better bond to the substrate concrete (Fowler and Trevino 2011). Selection of an LMC overlay comes with inherent benefits of having mixing and batching controls that are generally more controlled than for conventional concrete. More stringent quality control should ultimately lead to a better performing overlay.

Like any concrete flatwork, there are a variety of environmental factors during placement and cure that must be controlled. High initial evaporation rates lead to plastic shrinkage cracks. Additionally, since the overlay is supported by, and eventually is expected to be composite with the substrate concrete, large temperature gradients or differentials that may result in thermal cracking of large overlay areas should be avoided. For this reason, overlay placement is often conducted overnight. Conventional best curing practices, such as curing blankets and membranes, are appropriate for overlay construction.

If proper construction techniques are followed, concrete overlays can be a very effective way to repair bridge decks. All stages of overlay construction can impact the ultimate performance of the overlay. However current best practices, as described briefly in the preceding will result in sound overlay performance.

1.3.2 Interface Stresses

Sound bond between the substrate and LMC concrete is crucial to maintaining composite action. The stresses that occur at the interface are complex due to the irregularity of the interface and complexity of loading (Silfwerbrand 2009). Fundamental mechanics of a slab in flexure, however, allow the interface stresses to be assessed. Horizontal shear must be engaged to transfer the principal horizontal tension and compression forces: this is a so-called *VAy/It* shear. The tension force developed in the primary longitudinal reinforcing steel shear is resisted over the interface area of the shear span. Due to the self-weight of the overlay and the fact that transient loads are applied to the top of the overlay, the interface region is also subject to compression, which enhances the shear transfer. Loading that would result in tension across the interface is unlikely.

Shear transfer across a concrete interface is termed ‘shear friction’. Shear friction theory is based on an interface having perpendicular reinforcement to provide ‘clamping’ of the interface. While no perpendicular reinforcement is present in an overlay application, the overlay self-weight and transient gravity loads also serve to provide clamping of the interface to some degree. Thus looking to shear friction approaches for guidance in assessing overlay interface capacity is appropriate.

There are three mechanisms of shear friction resistance: cohesion, aggregate interlock, and clamping force. Figure 1 provides a schematic representation of shear friction as originally proposed by Birkeland and Birkeland (1966).

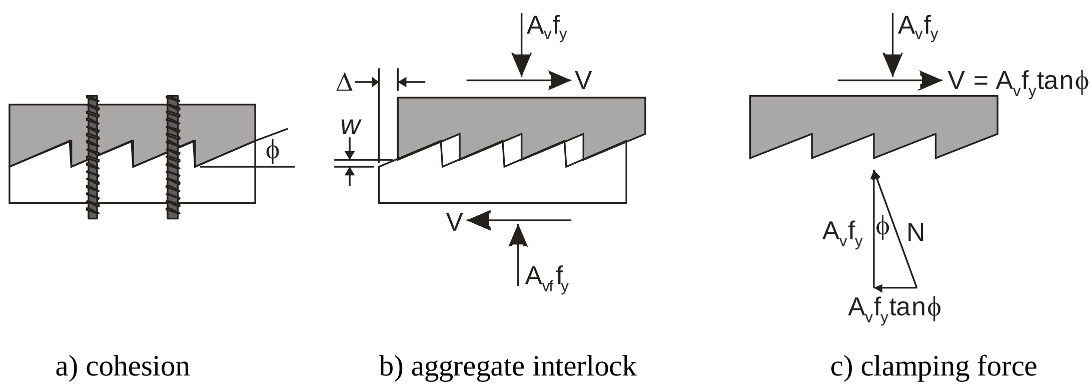

Figure 1: Saw-toothed model for shear friction (redrawn based on Birkeland and Birkeland (1966)).

Cohesion is the pre-cracked shear resistance of the concrete. Aggregate interlock is engaged after the cohesive capacity is exhausted and the interface cracks. In order for a shear crack to displace (Δ), the rough surfaces must pass over each other resulting in a corresponding crack opening (w). This is resisted by ‘interlock’ of the rough surfaces and enhanced by normal forces (N) (thus, the use of the term ‘friction’). The clamping force is provided by reinforcing steel crossing the interface. As the interface crack displaces, the steel is placed in tension, resulting in a clamping force proportional to the resulting steel stress. Provisions for establishing shear friction capacity assume that cohesive bond is negligible (i.e.: the concrete interface is cracked) and that the maximum aggregate interlock and steel clamping forces act simultaneously. This last assumption is not true. The aggregate interlock is initially high and degrades as the interface slips. The slip, however is what engages the steel clamping force. Thus, as shown by Zeno (2009), the aggregate interlock reaches a maximum value and degrades while the clamping force is relatively low and increases. The clamping force is ultimately limited by the yield capacity of the reinforcing steel, however without very large interface slip (exceeding about 0.1 in.), this theoretical maximum clamping force is not achieved (Zeno 2009).

Most shear friction recommendations take the form of Equation 1:

$$V_{ni} = cA_{cv} + \mu A_v f_y + \gamma P_c \leq KA_{cv} \qquad (1)$$

where: V_{ni} = shear friction capacity
A_{cv} = area of concrete interface
A_v = area of reinforcing steel having yield strength equal to f_y crossing interface
P_c = externally applied loads normal to the interface

Table 1 presents shear friction parameters, c, μ, γ and K, from AASHTO (2010), ACI 318 (2011) and two related scholarly works. The equation terms and limits associated with the concrete interface area, A_{cv}, in each case, are the *implied* contributions of aggregate interlock to the shear friction capacity. These provide guidance as to the anticipated shear capacity at the substrate-overlay interface. While the concept of shear friction requires a normal force, this is provided in the case of an overlay by its self-weight and the transient loads resulting in the interface shear. All cases presented in Table 1 assume "normal-weight concrete placed against a clean concrete surface, free of laitance, with surface intentionally roughened to an amplitude of 0.25 in. (6.35 mm)" (AASHTO 2010).

Table 1: Shear friction coefficients and implied aggregate interlock shear capacity.

Source	c	μ	γ	K	implied aggregate interlock interface capacity
AASHTO (§5.8.4)	240 psi (1.65 MPa)	1.0	1.0	$0.25f_c' \leq 1500$ psi (10.3 MPa)	240 psi (1.65 MPa)
ACI 318 (§11.6.4)	0	1.0	0	$0.20f_c' \leq 800$ psi (5.52 MPa)	-
Kahn and Mitchell (2002)	$0.05f_c'$	1.4	0	$0.20f_c'$	$0.05f_c'$
Harries, Zeno and Shahrooz (2012)	$0.06f_c'$	$0.0014E_s$	0	$0.20f_c'$	$0.06f_c'$

f_c' = concrete compressive strength
E_s = modulus of elasticity of reinforcing steel

The implied aggregate interlock capacities shown in Table 1 are very similar. The recommendations of Kahn and Mitchell (2002) were developed for high strength concrete having values of f_c' up to 14 ksi (96.5 MPa) while those of Harries et al. (2012) were based on experiments in which f_c' varied from 5 to 7 ksi (34.5 – 48.3 MPa).

1.3.3 Defining Bond and Methods of Testing Bond Strength

Bonded Portland cement overlays, like unbonded overlays, provide water and corrosive agent protection to underlying structurally sound concrete. Bonded overlays, however are not intended to be 'sacrificial'; rather they should act in a composite manner with the substrate concrete, restoring, or even improving, the original monolithic slab capacity.

As previously described, bond between the overlay and substrate has two components: chemical adhesion and mechanical interlock (Silfwerbrand et al. 2011). Chemical adhesion results from a well-prepared substrate interface while mechanical interlock results from the physical irregularities at the interface.

Adding bonding agents to Portland cement can improve adhesion. Portland cement grout with latex or certain epoxy resins can be added to the overlay concrete mixture to improve adhesion. Using such additives, however, comes with inherent risks including creating a thin interface between the substrate and overlay, introducing two potential planes of bonding (Silfwerbrand et al. 2011). Additionally, latex additives have been associated with finishing problems that have led to shrinkage cracking (ACI Committee 546 2004).

Mechanical interlock stems from the roughness of the interface. The ‘sand area’ method is a simple manner of quantifying this roughness. This method involves pouring a known volume of sand over the concrete surface. The sand is spread over the concrete in a circular fashion until all the cavities on the concrete surface are filled. A smaller circle correlates to a rougher concrete surface (Silfwerbrand 2009).

Bond strength is usually assessed by means of a tensile pull-off tests (ICRI 2004; ASTM C1583). A pull-off test involves isolating a region of the substrate-interface-overlay region using a hole saw (core drill). A test fixture (dolly) is affixed to the overlay and a monotonic concentric tension force is applied until tensile failure of the isolated specimen results. Figure 2 provides a schematic representation of the pull-off test and the failures that may result. There are a variety of available fixtures reported to be suitable for such testing. Vaysburd and McDonald (1999) provide a review of available fixtures and specimen sizes. Eveslage et al. (2010) and others adopt the rule-of-thumb that the specimen size must exceed the maximum coarse aggregate size.

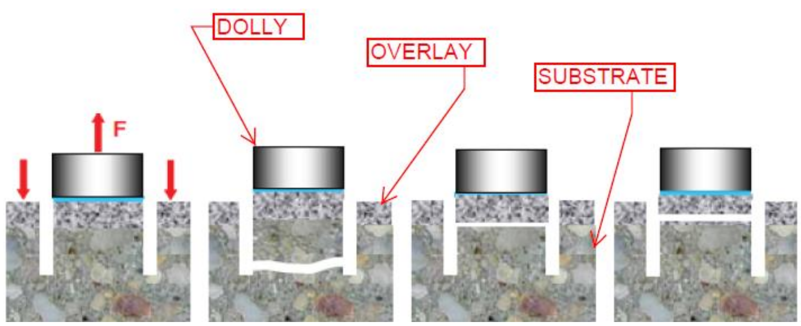

test arrangement | cohesive in substrate concrete | adhesive at interface | cohesive in overlay

failure modes

Figure 2: Bond strength pull-off test (adopted from Germann Instruments Inc.).

Failure in a pull-off test will occur through the weakest material. A cohesive failure in the substrate concrete is the preferred failure mode since this indicates that both the overlay and the interface bond exceed the substrate concrete tensile strength. The substrate material properties essentially limit the outcome of such a test since these are the only values that one has no control over in the design of the repair.

Although, direct tension is not representative of *in situ* forces on an overlay system, the pull-off test is a simple and viable test for quality assurance. Studies have indicated that the tensile bond strength found through the pull-off method is less than the shear strength of the interface. Gillum et al. (2001) reports tensile strength approximately 35% of shear strength while Silfwerbrand (2009), report the value to be approximately one half of the shear bond strength. There is conflicting available guidance on the minimum ‘acceptable’ substrate tension capacity from pull-off tests: Wenzlick (2002) suggests a minimum of 100 psi (0.69 MPa), Basham (2004) recommends 200 psi (1.38 MPa), while ICRI (2004) suggests a value below 175 psi (1.21 MPa) indicates poor bond.

1.3.4 Factors Affecting Bond

A monolithic connection in a bonded concrete overlay is achieved through several means, some of which have greater importance than others. Silfwerbrand (2009) list the five most important factors affecting the performance of this interface as: absence of microcracks, absence of laitance, cleanliness, compaction of overlay, and curing. The following is a summary of Silfwerbrand’s list of factors in chronological order as they occur in the overlay process. Relative importance is given by Silfwerbrand on a scale of 1 through 3 in which 3 is most important.

- *Substrate Properties* (1) Mechanical properties of the substrate concrete include the modulus of elasticity, tensile strength and compressive strength. Silfwerbrand states that composite action of the overlay is best achieved when the overlay properties are designed to closely match those of the substrate concrete.
- *Microcracks* (3) Microcracking is often caused by the method by which deteriorated concrete is removed. Pneumatic hammers are likely to cause more microcracking than other non-impact alternatives, such as hydrodemolition. Regions of microcracks are potential weak zones in which adequate bond strength will not develop.
- *Laitance* (3) Laitance is a layer of fine particles that forms as excess water bleeds to the surface of the concrete during the curing process. Laitance is only an issue when bonding to an existing concrete surface; when any form of demolition is used to remove the substrate concrete, laitance is removed.
- *Roughness* (1) As discussed above, bond strength is developed partially by mechanical interlock. To a degree, the ‘rougher’ the substrate level is, the more mechanical interlock is able to develop. This factor is highly dependent on the method of removing deteriorated concrete.
- *Cleanliness* (3) This factor is perhaps one of the most important and most easily controlled. Both ACI Committee 546 (2004) and Silfwerbrand (2009) agree that surface cleanliness is critical to performance of the repair. Supporting evidence has been found in Sweden, where bonded overlays were used on two bridge decks. The overlays did not perform well due to loose particles found at the interface between the substrate and overlay resulting in poor bond strength (Silfwerbrand et al. 2011).
- *Prewetting* (2) Bond strength is maximized when the substrate surface to which the overlay is applied is saturated and then allowed to superficially dry prior to overlay placement. Silfwerbrand (2009) recommends keeping the substrate wet for 48 hours then letting it dry for 12 hours preceding the overlay placement. This condition is known as saturated, surface-dry (SSD) and is intended to minimize the amount of water that the substrate will wick away from the overlay when it is placed. Conventional practice is similar although the substrate is maintained wet, without standing water; a condition referred to as saturated, surface-wet (SSW). Vaysburd et al. (2011) recommends that the SSD condition be used when testing for the optimum water condition of the substrate cannot be done.

- *Bonding Agents* (1) Silfwerbrand (2009) argues against using bonding agents such as epoxy and grout because they create multiple interfaces, thus increasing the probability of a weak bond.
- *Overlay Properties* (2) Overlay mix design can affect bond strength in the same way as substrate properties. Workability, strength and other products of the mix design can have effects on overall overlay performance.
- *Placement* (1) As with all concrete construction, poor placement techniques can lead to segregation within the overlay.
- *Compacting* (3) Proper compaction leads to fewer and better distributed air voids at the interface. Air voids can detrimentally affect bond strength and result in poor overlay performance.
- *Curing* (3) As in any concrete flatwork construction, improper curing can lead to surface cracks which, while having little effect on bond to the substrate, nonetheless result in poor-performing overlay.
- *Time (2) and Early Traffic (1)* Time and early traffic loading are factors that work hand in hand. If traffic is applied too early, vibrations may cause differential movement between the overlay and the substrate. Studies have shown that bond strength develops at a rate similar to compressive strength (Silfwerbrand 2009). If enough time is allowed for bond strength to develop, composite action should be developed.
- *Fatigue* (1) Low-cycle fatigue tests conducted at high stress levels have shown that bond is not a weakness in the overlay system. Silfwerbrand (2009) comments that provided the static bond strength is adequate and the tension reinforcement does not coincide with the bond interface fatigue performance is not an issue. There is no known data for high cycle fatigue which is the *in situ* condition of an overlay.
- *Environment* (1) Environmental factors, such as temperature, should be taken into consideration during any concrete placement operations including overlay placement.

1.3.5 Experimental Studies of Bond Strength

Several studies have focused on overlay-to-substrate bond strength. The following general conclusions have been drawn:

- Bond strength plays a very important role in overall performance when the interface area is subjected to longitudinal compression (from positive bending of the slab). When the interface is subjected to tension (negative bending areas), bond strength does not play as vital a role in overlay performance.
- Construction procedures, such as the method of concrete removal, affect overlay performance.
- Sealants used on the substrate surface reduce bond strength.

Gillum et al. (1998) presents a comprehensive study performed for the Ohio Department of Transportation investigated bond performance of overlays over concrete sealed with high molecular weight methacrylate (HMVM) and epoxy. The report indicates a limited number of previous studies addressing the effects of substrate surface preparation on bond strength. Critically, the authors report that there are no known studies to determine the bond strength needed for an overlay to be deemed effective. Both field and laboratory specimens were used in a variety of tests: direct shear, direct tension (pull-off), Strategic Highway Research Program (SHRP) interfacial bond and flexural beam tests. Of particular interest are the flexural beam tests, which consisted of a one half-scale model of a 12 in. (300 mm) strip of a typical bridge slab. Overlays used on these specimens were (1.6 in.) 40 mm deep microsilica modified concrete (MSC) overlays. These flexural specimens were subjected to both negative and positive bending. Overlays in positive bending failed as a result of bond failure of the overlay whether the specimens were sealed or not. Figure 3 shows to examples of failures associated with poor overlay bond (from Cole et al. 2002). Negative bending did not cause specimens to fail due to bond failure since the overlay is in tension (Figure 4).

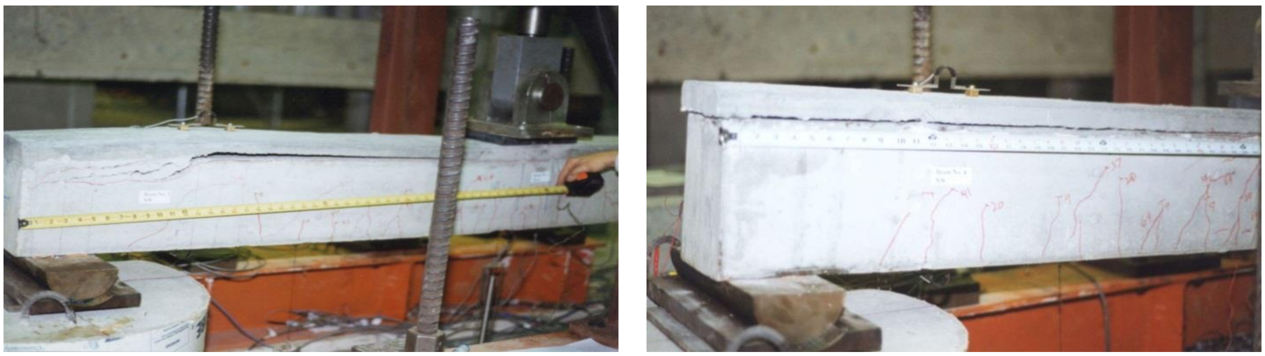

a) ‘buckling’ failure of overlay in compression

b) ‘slip’ failure of overlay characterized by relative movement at the ends of the test slab

Figure 3: Examples of bond failure of overlays subject to positive bending (Cole et al. 2002).

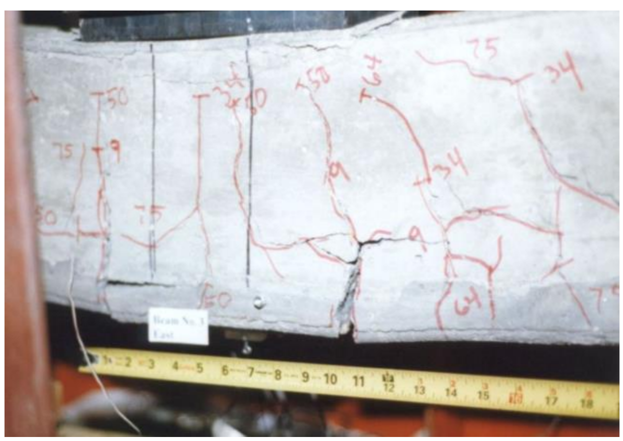

Figure 4: Example of overlaid slab in negative bending - overlaid at the bottom of test slab in tension zone (Cole et al. 2002).

Gillum et al. (2001) continued, focusing on whether the application of low-viscosity sealers affected the bond between Portland cement-based overlays and bridge decks. Bond strength was again tested under four different types of tests: direct shear, direct tension, SHRP interfacial bond and flexural beam tests. Microsilica modified concrete (MSC), super-dense plasticized concrete (SDC) and latex modified concrete (LMC) were tested in both field and laboratory conditions. For the field tests, it was determined that results from the direct tension test are approximately 35% the values of direct shear tests.

Additionally, there was a high level of scatter in bond strength values for the LMC overlay making determination of the bond strength uncertain. Laboratory tests included test beams intended to replicate an overlay bonded to a bridge deck. Flexural tests in both positive and negative three point bending revealed that the overlay seemed to be adequately bonded to the substrate concrete for the case in which no sealer had been applied to the substrate. LMC was found to have the highest bond strength among the three alternatives: 860 psi (5.9 MPa). Four primary conclusions resulted from the study: 1) flexural testing is the most realistic method of testing specimens; 2) sealers reduce bond strength by approximately 50% when compared to unsealed specimens; 3) sandblasting the interface where sealers are applied can increase bond strength of sealed specimens to 80-85% of unsealed specimens (although the authors of the present report suspect that the subsequent sandblasting simply removes the applied sealer); and 4) in negative moment regions it is not as crucial to sandblast sealed areas as it is in positive bending regions, i.e. bond strength is not as significant a concern in negative moment regions such as over piers.

Cole et al. (2002), in a continuation of the Gillum et al. 2001, considered overlays placed over sealed concrete bridge decks and their performance was evaluated in both static and fatigue loading scenarios. Specimens consisted of one-third-scale subassemblages of a steel stringer bridge. HMWM sealers and gravity-fed epoxy resins were found to reduce bond strength by approximately 50%. Sandblasting once the sealer had cured can restore bond strength to 80 to 85% of that without sealers (once again, one suspects that the sandblasting is simply removing the sealer). Broadcasting sand at a rate of 1 kg/m^2 immediately after sealer application was shown to restore bond strength. Bond strength is a function of bending direction. Specimens subject to positive moments exhibited bond failure when sealers were used; bond failure was mitigated when sealers were not used. Specimens subject to negative moments, once again, did not exhibit these failures due to the fact that the interface area is located in the region of flexure-induced tensile stresses. Fatigue testing to 1,000,000 cycles showed that sealers were not detrimental to the overlay performance provided sand is applied to the sealer as it cured.

Wenzlick (2002) reports a study, by the Missouri Department of Transportation conducted in an effort to support the use of hydrodemolition as the preferred method of concrete removal prior to subsequent concrete overlay. Both latex modified and silica fume overlays were considered. The study focused on time, cost and performance of hydrodemolition and compared it to conventional pneumatic hammer removal of concrete. Specimens came from decommissioned bridges and bond strengths were determined using direct tension tests. Hydrodemolition was able to reduce micro-fractures in the substrate concrete, which ultimately was deemed to result in better overlay bond strength. Bond strength of the overlay installed following hydrodemolition ranged from 121 to 161 psi (0.84 – 1.11 MPa), averaging 151 psi (1.04 MPa), whereas pneumatic hammering and milling averaged 80 and 140 psi (0.55 and 0.97 MPa), respectively.

Alhassan and Issa (2010) demonstrated the superiority of synthetic fiber-reinforced latex-modified concrete overlays over other overlay types. Full scale testing was conducted on a two-span prototype bridge having two equal 40 foot (12.2 m) spans. Various AASHTO loading scenarios were tested and it was found that the load-deflection response was improved as a result of overlay application: increasing the 8 in. (200 mm) deck depth with a 2.25 in. (55 mm) thick fiber-reinforced LMC overlay was found to increase the stiffness of the composite bridge by 20%. This improved behavior was attributed to composite action between the substrate concrete and the overlay. Composite action can only be developed through adequate bond strength. The complexities of analyzing stresses at the overlay-substrate interface were also discussed, with several finite-element analyses performed to validate critical issues found in experimental test results.

Silfwerbrand (2009) and Silfwerbrand et al. (2011) report extensive ongoing research and implementation of concrete overlays for the repair of bridge decks in Sweden. During the late 1980s and early 1990s bond strength tests were performed on 20 bridge decks that had been hydrodemolished and repaired with a bonded concrete overlay. The majority of these tests did not fail at the interface and failure strengths averaged over 217 psi (1.5 MPa). Silfwerbrand argues that since most of the specimens did not fail at the interface between overlay and substrate level concrete, the actual bond strength is higher than the recorded values. Most specimens failed within the substrate concrete. Bridges with newer overlays performed slightly better than older overlays in terms of both failure strengths and percentage of bond failures. Silfwerbrand attributes this to the experience of contractors who work in the bridge deck repair arena, recognizing that careful attention must be paid to construction procedures, such as surface preparation.

1.4 SUMMARY

LMC overlays, when correctly constructed, can increase deck capacity, improve deck surface conditions, and provide a long-term lower maintenance solution for repairing degraded concrete deck structures. Appropriate repair and maintenance procedures are those that reduce manpower requirements, time, resource use, and shut-down times. In addition to addressing these issues, LMC deck overlays are also favorable with respect to sustainability when compared to other methods of repair or full deck replacement (Silfwerbrand 2009). Overlay performance is governed mostly by bond of the overlay to the substrate concrete. Good bond is primarily affected by good construction practices in preparing the substrate and installing the overlay. A well-designed and constructed overlay should restore a moderately degraded deck – represented by a Type 1 or Type 2 repair – to its original structural capacity and have a service life on the order of 20 years or more (*Pub. 15* Section 5.5.4(a)(3)).

2 *IN SITU* STRUCTURES IN PENNDOT DISTRICT 11

2.1 REVIEW OF INSPECTION DATA

A review available inspection reports and construction documents was undertaken to assess the condition and performance of latex modified concrete (LMC) overlays in PennDOT District 11 (Allegheny, Beaver and Lawrence Counties in South-western Pennsylvania). Initially, the bridge management system (BMS) was queried to identify bridges within the district that had a LMC overlay applied. This search returned 149 bridges (8% of those in District 11; listed in Appendix A) and represent over 3 million square feet of deck area (20%). Overlays (based on 'year of reconstruction') range from less than one year to 40 years old. Wearing surface (overlay) thicknesses of up to 3.5 in. were reported. Wearing surface ratings range from 4 to 9 with the majority of ratings at or above 6 as shown in Figure 5. Figure 6 plots the wearing surface ratings against the reported year of reconstruction. As one would expect, bridges repaired more recently had slightly better wearing surface ratings than those with older repairs (as shown by trendline).

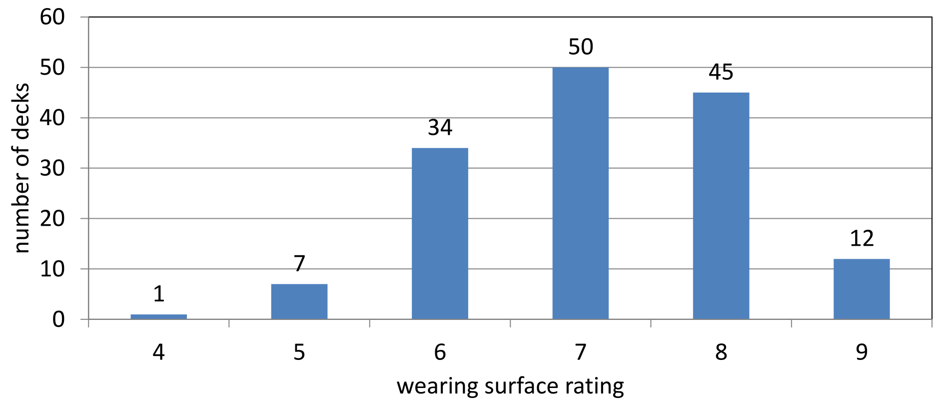

Figure 5: Distribution of wearing surface ratings for LMC-overlaid bridge decks in District 11.

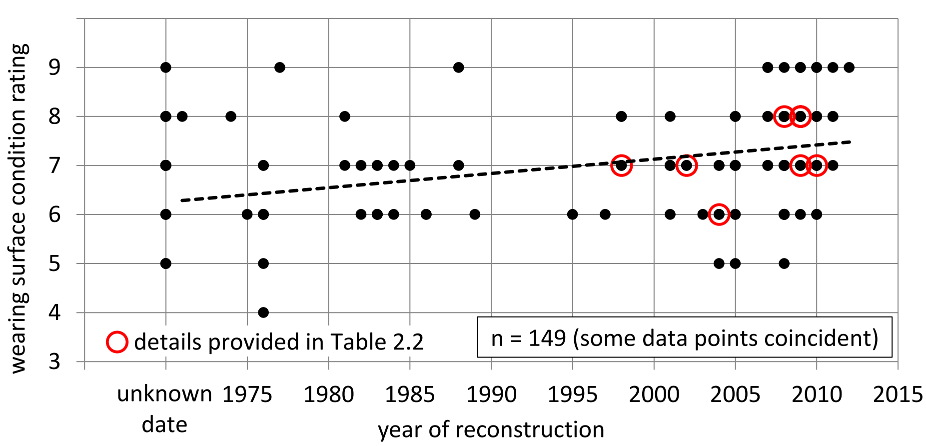

Figure 6: Wearing surface condition vs. year of reconstruction
for LMC-overlaid bridge decks in District 11.

A qualitative review of all comments associated with deck and overlay performance of the 149 sample decks was undertaken; the results are shown in Table 2. Keywords were used to classify the condition of the overlay ("good", "fair" and, "poor"); the extent of cracking ("minor" or "few", "moderate", "widespread" or "numerous", and "severe"); and evidence of surface wear (reported or not). Considering the nature of inspection comments, it is believed reasonable to assume that there were no observed issues if there was no mention of an issue. That is, while 64 of 149 overlays were considered to be "good"; there was no mention of condition in 77 reports – one may assume, therefore, that close to 141 of the 149 decks were "good" or had no condition issues meriting comment.

Considering the 40 cases indicated as having moderate or severe cracking (Table 2), the following observations are made:

- Most comments (30 of 40) refer to 'hairline' or 'map' cracking; both are possible indications of shrinkage cracks associated with inadequate cure conditions (see, for example, Figures 7a, b and d).
- Many comments (18 of 40) refer to longitudinal cracking (see, for example, Figure 7); this may be reflective cracking at girder locations although this cannot be confirmed.
- Some comments (10 of 40) refer to transverse tracks. Without further data it is not possible to assess a likely cause of these, but shrinkage restraint cannot be ruled out.

Overall, the 149 decks with overlays in District 11 are performing well. No major issues for concern are noted. Much of the observed cracking is very likely associated with early-age effects resulting from inadequate curing processes.

Table 2: Qualitative review of inspection comments[1] related to overlay (n=149).

overall condition of overlay	*good*	*fair*		*poor*	no mention
	64	7		1	77
extent of cracking of overlay	*minor* or *few*	*moderate*		*severe*	no mention
	60	36		4	49
reported nature of cracking		*hairline* or *map cracking*	*longitudinal cracking*	*transverse cracking*	
		30	18	10	
evidence of surface wearing	reported				no mention
	28				121

[1]terms in italic text are search words used to categorize qualitative inspection data

Comments associated with the poorly performing decks identified in Table 2 include:

Single deck having 'poor' condition of overlay: (Beaver Valley Expressway over LR 04004 and Brady's Run Park, BMS 04 0376 0340 0000)

"New modified latex overlay installed since 2010 inspection. A 100'L [length] *of the SB* [southbound] *passing lane exhibits poor quality concrete, close-density pop-outs were observed within a 100' length of deck in span 4. Additionally, several 3' length longitudinal hairline cracks were found propagating through a section of haunch adjacent to the center joint, no other problems were noted."* (reported year of overlay: 2011; deck rating in 2012: 7)

This comment appears to indicate a substandard LMC installation.

Four decks having 'severe' cracking:

"Condition rating of the latex modified concrete surface was reduced to Satisfactory, minor deterioration was noted. The left lane has moderate-to-heavy density hairline map cracks." (reported year of overlay: 1982 (more likely 2008 based on incomplete BMS data); deck rating in 2012: 6).

"Integral concrete - heavy longitudinal, map, and transverse cracking." (reported year of overlay: 1995; deck rating in 2012: 6)

"New latex overlay - heavy wide spread hairline map cracking in passing lane and on both shoulders, minor hairline map cracking in travel lane. No plans exist for this wearing surface at time of inspection, actual thickness is unknown." (reported year of overlay: 2008; deck rating in 2012: 7)

"Latex concrete overlay - minor to moderate wear in wheel paths, severe transverse and longitudinal cracking." (reported year of overlay: 1989; deck rating in 2012: 6)

None of these comments highlight any significant issues; simply general deterioration of overlays.

2.1.1 Bridges for Further Study

In consultation with PennDOT District 11, nine bridges were selected for further examination; these are reported in Table 3. Inspection reports and available construction documents were reviewed to establish the data shown. Values of overlay depth vary considerably and are not necessarily consistent with that reported in the BMS. The depth values given in construction documents are assumed to be target depths and likely the basis for calculating pay-quantities. Where available, depth-check records maintained by PennDOT inspectors were reviewed. In most cases spot-depths varied both along and across bridge decks. In some cases, spot depths exceeded two or three times the reported depth. This is likely the result of the requirement to provide hydrodemolition to a 'depth of sound concrete'. Photographs of many of the decks considered, taken January 7, 2013, were provided by PennDOT. Representative photos illustrating the notes on each deck are provided in Figure 7.

Additional photos from two of these bridges are provided in Figure 8. These show a damaged LMC overlay at the acute angle of a skew (Figure 8a), an apparent pop-out (Figure 8b), and a mortar patch of an LMC overlay (Figure 8c). The acute skew location shown in Figure 8a is at the 'low' point of the bridge, suggesting the accumulation and incomplete removal of laitance prior to LMC application although this cannot be confirmed. Apart from some localized damage on Bridge F, no significant areas of concern were identified in the bridges selected for detailed summary.

In consultation with District 11, five of these bridges were selected for field evaluation by SIVA Corrosion Services (see Section 2.2). These are noted in Table 3 (as 'Task 3 Study'). These five bridges have LMC overlays varying from 2 to 15 years old. Wearing surface ratings range from 6 to 8. Based on BMS data, all appear to be Type 1 repairs (i.e.: not extending below top of reinforcing steel). Nonetheless anecdotal evidence and evidence subsequently collected in the field tests (see Section 2.2) suggest that many of these repairs are indeed, at least in some locations, Type II repairs.

2.1.2 Summary of Review of Inspection Data

LMC overlaid decks in District 11 appear to be behaving quite well. Minor hairline cracks are noted in many instances; these are likely attributable to early-age effects resulting from inadequate curing processes and appear to be 'localized' to small regions in many cases. No evidence of LMC delamination from the substrate deck is evident based on this review.

Table 3: Sample D11 bridges selected for potential field study.

ID	A	B	C	D	E	F	G	H	I
Bridge	SR28 over Powers Run	SR28 over SR910	SR79 over SR50	SR79 over Glenfield Rd	SR79 over Red mud Hollow Rd	SR837 to Homestead Ramps	Fort Duquesne Bridge-NB	Fort Duquesne Bridge-SB	Neville Island Bridge
ECMS#		70202		26926	26926	27271	84235	84235	74919
Plan#	S-23750	S-26537	S-22382	S-26795	S-26794	S-25256			S-29389
Project	SR28-A32	SR28-A44/45	SR79-A17	SR79 35M	SR79 35M	SR885 A23	SR-279 A75	SR-279 A75	SR79 A40-A65 A38
BMS #	02-0028-0240-0000-1	SB-02-0028-0271-1085	02-0079-0525-0486	02-0079-0660-0615	02-0079-0690-0106	NB-02-0837-0430-0000	NB-02-0279-0008-0425	SB-02-0279-0009-2108	02-0079-0650-0000
Year of LMC overlay	2002[1]	2008	1998	2009	2009	2004	2009	2009	2010
Type of LMC	-	-	type 1 PCC	conventional LMC	conventional LMC	conventional LMC	rapid set	rapid set	conventional LMC (span) rapid set (S. approach)
Reported depth of HD	-	0.25 in.	0.25	varies: to sound concrete	varies: to sound concrete	varies: to sound concrete	1.50 in.	1.50 in.	1.00 in.
Depth of LMC (construction records)	1.25 in.	1.25 in.	1.5 in.	varies: LMC to increase slab depth 0.5 in.	varies: LMC to increase slab depth 0.5 in.	varies: LMC to match extant elevations	1.5 in., 3.5 in. and 4.5 in.	1.5 in., 3.5 in. and 4.5 in.	1.50 in.
Depth of LMC (BMS)	1.2 in.	0.5 in.	1.20 in.	1.0 in.	0.5 in.	1.5 in.	3.0 in.	3.0 in.	0.5 in.
MPT at LMC placement	-	-	half width closures	one lane maintained	one lane maintained	traffic during project	single lane closures	single lane closures	traffic during project
7 day LMC strength	-	-	4260 psi	-	-	4050-6800 psi	-	-	5 day: 3000 psi
28 day LMC strength	-	-	3200-5900 psi	4140-7240 psi	4140-7241 psi	-	3000-4000	3000-4000	3500 psi
Wearing Surface Rating	7	8	7	8	7	6	8	8	7
Deck Rating	7	9		7	7	4			
Notes	A	B	C	D	E	F	G	H	I
Figure	7a	7b	7c	7d, 8a	7e	7f, 8b, 8c	-	-	-
Cracking analysis?	-	-	-	-	-	-	yes	yes	yes
Task 3 study	yes	yes	yes	no	yes	yes	no	no	no

[1] beyond 7 year retention limit; construction records destroyed.
Empty cells indicate that no data was found during review.

Notes for Table 3

The following notes are transcribed directly from inspection reports

A. several minor cracks (see Figure 7a)
B. minor hairline cracks (see Figure 7b)
C. Integral concrete - moderate wearing and light cracking typical of all spans. Small popouts have been patched with mortar (Figure 1c shows image of deck; no popouts are seen)
D. few small areas of hairline cracking (see Figure 7d)
E. LMC overlay-good condition (see Figure 7e)
F. LMC - fair condition - numerous hairline longitudinal cracks (see Figure 7f)
G. The latex-modified concrete wearing surface exhibits a few longitudinal hairline cracks and small diameter shallow concrete spall.
H. The 3 [in.] thick latex-modified concrete wearing surface was recently replaced as part of the Ft. Duquesne Bridge and Ramp Rehabilitation project and is in very good condition.
I. The Latex Modified Concrete (LMC) wearing surface is in overall good condition. Areas of moderate density hairline mapcracking are present in the Northbound right lane and shoulder areas throughout. Multiple longitudinal hairline cracks are present throughout the Northbound right lane for the full length of the bridge. Random transverse hairline cracking is present throughout. Span 10 Northbound deck right lane exhibits a 6 inch diameter by 3/4 inch deep shallow spall. The deck wearing surface at Pier 12 is chipped along the sawcut paving joint with missing joint filler. No significant change in the wearing surface has been noted since the 2011 Deck Wearing Surface cracking inspection.

The following data was unavailable for any bridge considered in this review:

- strength of substrate concrete
- bond strength between LMC and substrate
- amplitude of HD surface
- whether concrete ‘shadow’ below steel was removed – although most bridges do not report sufficiently deep HD for this to be an issue.
- degree of corrosion of embedded steel
- chloride content of substrate concrete

a) minor hairline cracks (Bridge A)

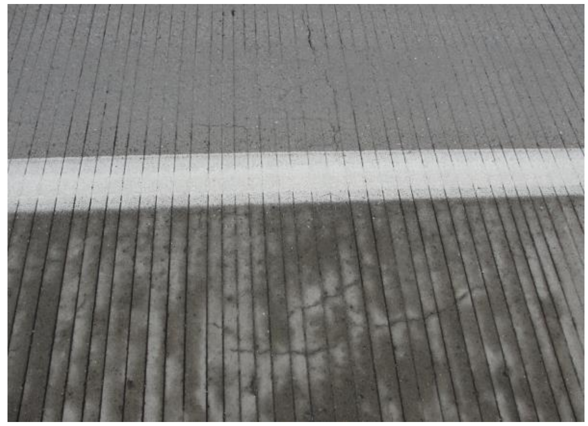

b) minor hairline cracks (Bridge B)

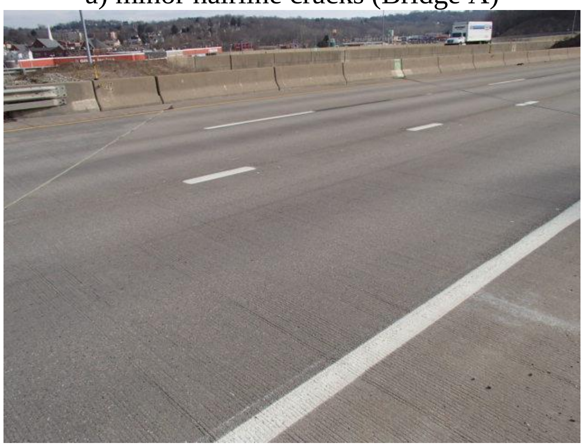

c) LMC overlaid deck of Bridge C
(photo taken 1.14.13)

d) minor hairline cracks (Bridge D)

e) LMC overlaid deck of Bridge E

f) hairline longitudinal cracks (Bridge F)

Figure 7: Photos reflecting inspection notes for bridges reported in Table 3.
(photos courtesy of PennDOT D11 were all taken 01.07.13 except as noted)

a) damage to LMC overlay at location of acute skew (Bridge D)

b) apparent pop-out of LMC (Bridge F)

c) mortar patch of LMC (Bridge F)

Figure 8: Observed local damage to LMC overlays.
(photos courtesy of PennDOT D11 were all taken 01.07.13)

2.2 SUMMARY OF FIELD TESTS CONDUCTED BY SIVA CORROSION SERVICES

Siva Corrosion Services (SCS) conducted an investigation of the *in situ* performance of the LMC repairs of five existing bridges indicated in Table 3. The extent of this investigation included a) initial inspection of the deck, including ground penetrating radar (GPR) to locate reinforcing steel, chain dragging and additional sounding as required; b) pull-off testing (3 per deck) and core extraction (2 per deck); c) visual inspection of all cores, encased reinforcing steel and pull-off specimens; and d) chloride content measurements (2 per core). The complete report submitted by SCS is provided in Appendix D.

SCS collected two types of cores from each bridge: two 4 in. (102 mm) diameter cores (10 total) and three 2 in. (51 mm) diameter pull-off specimens (15 total) from each bridge. The 4 in. diameter cores came from "problem areas" identified by cracking and each contained one top mat reinforcing bar. The 2 in. diameter cores resulted from the pull-off tests and came from sound areas of the deck and did not include reinforcing bar. Average values of overlay depth and reinforcing bar depth for each bridge are summarized in Table 4.

Table 4: Summary of SCS Test Results (values in parentheses indicate COV).

	Bridge ID				
	A	**B**	**C**	**E**	**F**
bridge description	SR28 over Powers Run Rd	SR28 over SR 910	SR79 over SR 50	SR79 over Red Mud Hollow Rd	SR837 to Homestead ramps
age of LMC repair (years)	11	5	15	4	9
depth of overlay (in.)	2.6 (0.29)	2.6 (0.35)	2.4 (0.24)	4.0 (0.21)	3.3 (0.20)
amplitude of interface (in.)	0.9 (0.40)	0.6 (0.34)	0.5 (0.34)	0.9 (0.46)	0.4 (0.34)
depth of reinforcing steel (in.)	3.9 (0.11)	3.6 (0.14)	4.4 (0.08)	4.9 (0.15)	3.2 (0.31)
bar diameter loss due to corrosion	7%	7 – 19%	3 – 6%	0 – 14%	17 – 25%
pull-off strength (psi)	285 (0.26)	348 (0.04)	202 (0.51)	[1]	284 (0.23)
failure modes observed[see foot note 2]	A, I/S, S	A, A, S	I, S, S	A, A, A[1]	A, I, I/S

[1] 3.5 in. test core did not intersect interface having 4 in. depth.

Visual inspection of the cores indicated that out of the 24 viable cores (one core contained only LMC and thus no interface), 17 indicated good bond. Of the 7 remaining cores, 4 were pull-off tests that failed at the bond interface (Failure Mode I)[2], while the other 3 were 4 in. (102 mm) cores that contained cracking likely associated with reinforcing steel corrosion. Vertical cracking and reinforcing bar corrosion were prevalent throughout the 4 in. diameter cores; all 10 cores contained vertical cracking (in 8 of the 10 cores, this was limited to the LMC region, though one core did contain a full-depth crack), and 9 of the 10 cores exhibited corrosion (with loss in steel cross sectional area ranging from 3%-25% as indicated in Table 4.

A total of 15 pull-off tests (the 2-in. (51 mm) diameter cores) were conducted according to ICRI Guideline No. 03739 (ICRI 2004); results are summarized in Table 4. Nine of the eleven pull-off tests exceeded the 175 psi (1.21 MPa) threshold recommended by ICRI. Of the two that did not meet this threshold, one failed in the substrate (S) and the other failed at a tension strength of 153 psi (1.06 MPa) in Mode I. Figure 9 shows the results of the pull-off tests plotted against the reported age of the LMC repair. The results indicate a slight decay in pull-off strength with increasing age; however, some of these failures occurred only in the substrate concrete (S) indicating both LMC overlay and interface strength capacity greater than the reported values in these cases.

---

[2] SCS reports failure modes based on the ICRI notation as indicated in Appendix D; these correlate to the following failure mode notations used in this study (see Section 4.1):

Failure Mode A = ICRI Failure Mode 1
Failure Mode O = ICRI Failure Mode 2
Failure Mode I = ICRI Failure Mode 3
Failure Mode O/I = ICRI Failure Mode 4
Failure Mode I/S = ICRI Failure Mode 5
Failure Mode S = ICRI Failure Mode 6

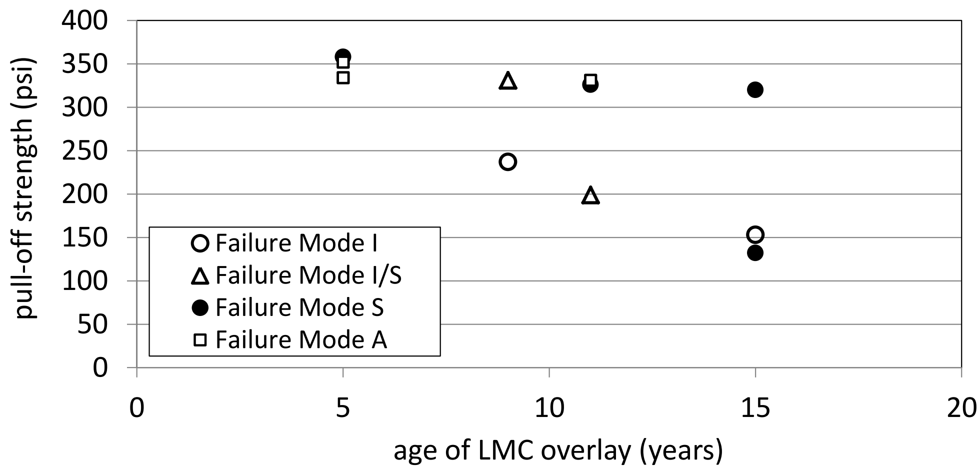

Figure 9 : Pull-off test results vs. age of LMC overlay repair.

Chloride content measurements (ASTM C1152) were performed at two different locations on each of the cores. Chloride content exceeded the recommended limit of 350 ppm at the depth of reinforcing steel in 40% of the tests on 2 in. (51 mm) diameter cores (taken from areas of sound concrete) and in all of the tests on 4 in. (102 mm) diameter cores (taken from areas with vertical cracks). The report notes that the high chloride content is pervasive throughout the samples and will likely lead to "significant corrosion-related concrete damage in the near future (5-10 years)." Finally, the report also notes that in 40% of the tested cores, chloride content did not decrease with increasing depth from the deck surface (as is typical in chloride content profiles). SCS speculates that this could be due to chlorides from the contaminated substrate concrete diffusing into the fresh LMC overlay at the time of LMC placement [and cure], although the sample size of the test is too small to state this with any certainty.

3 FULL-SCALE SLAB FLEXURAL TESTS

3.1 EXPERIMENTAL PROGRAM

The flexural test program comprised two different series of specimens: laboratory cast slabs and field cut slabs (Marshall Ave Slabs). The laboratory slabs are described in Chapter 3, whereas comparable information on the field cut slabs can be found in Appendix C.

3.1.1 Specimen Details

Fourteen 90 in. (2286 mm) by 22 in. (559 mm) slabs, each 7.5 in. (191 mm) deep were cast. Ten were intended for testing, while four were held in reserve for future fatigue tests and to calibrate the HD process. Figure 10 provides details of the control specimen (Slab A; not receiving LMC). The primary flexural reinforcing (i.e.: bridge transverse) steel shown in Figure 10b was bent as a closed tie in order to ensure full development of both top and bottom steel; this mimics continuous deck construction in the simply-supported specimen. Straight secondary reinforcing (bridge longitudinal) steel was placed within the primary steel ties. Figure 11 shows the slab reinforcing cages positioned within formwork, prior to concrete placement.

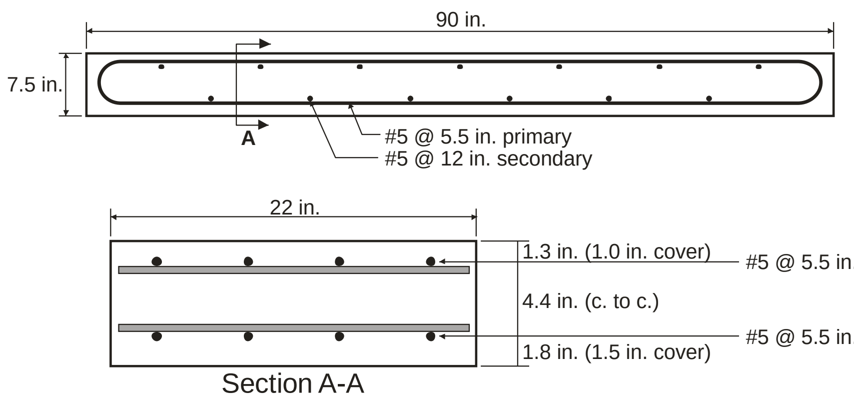

a) slab details

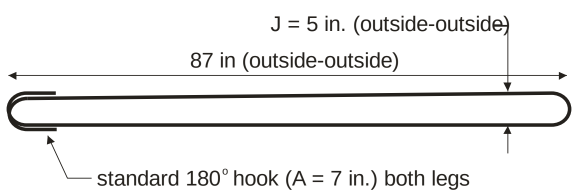

b) #5 primary reinforcing steel bend detail (installed in alternating directions)

Figure 10: Details of slab specimens (Slab A as tested).

Figure 11: Slabs forms prior to placing concrete.

3.1.2 Test Matrix

Slab A is a control specimen and was tested as shown in Figure 1. The remaining slabs were subject to removal of their upper region of concrete by hydrodemolition (HD) and overlaying the affected region with latex-modified concrete (LMC) as shown schematically in Figure 12. The primary variable in this study is the depth of the HD and the subsequent LMC overlay, d_o. Figure 13 provides the as-built slab details for Slabs B through H, all receiving LMC overlays. The 'target' depths of HD and LMC (d_o) were based on the concrete cover, c, and bar diameter, d_b, and are noted in Figure 13. For example, the target depth of HD for Slab D is $d_o \approx c + d_b$; thus the depth of HD should be at the intersection of the primary and secondary reinforcing steel in this section.

Figure 13 indicates the average measured depth of LMC calculated from the recorded depths from six measurement points across the approximately 66 x 22 in. (1676 x 559 mm) extent of HD (Figure 12) as recorded in Table 5. These depths were measured perpendicular to a level placed across the top of the formwork prior to LMC placement. This method is similar to that used by PennDOT to record such depths in the field. In order to be consistent with field practice, a minimum depth of LMC was provided; this required increasing the overall depth of Slabs B and C to 8.5 and 8 in. (216 and 203 mm), respectively.

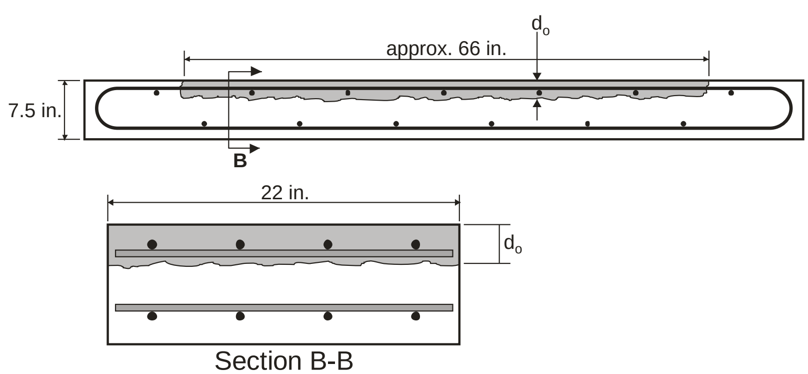

Figure 12: Schematic detail of LMC overlay.

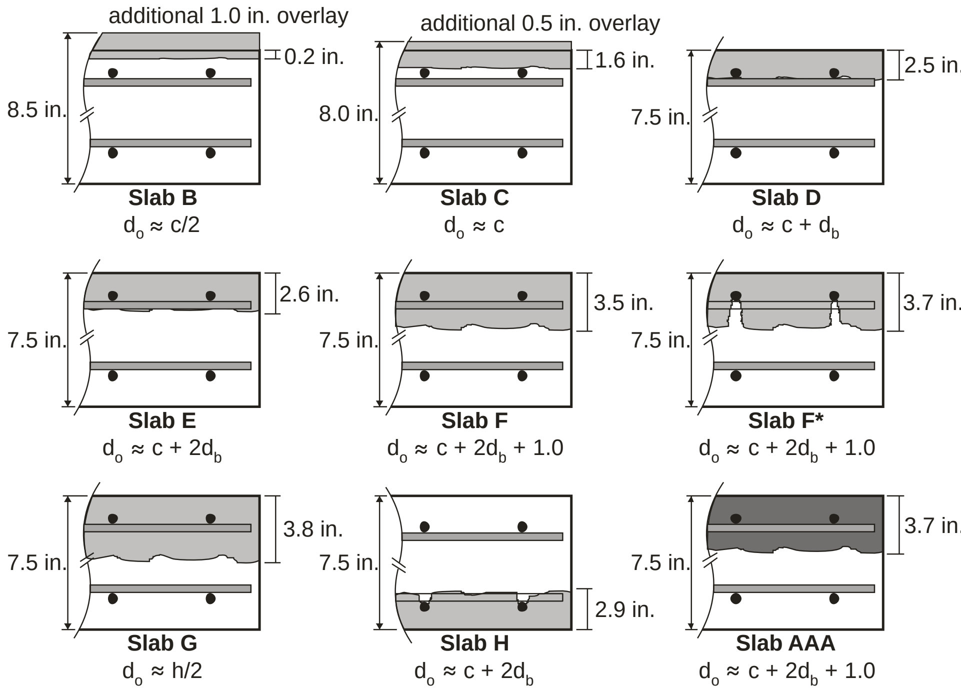

Figure 13: Schematic details of all LMC slabs.

Table 5: Measure depths of HD relative to original 7.5 in. slab thickness.

Slab	**target depth**	**measured depths (in.)**							
		1	**2**	**3**	**4**	**5**	**6**	**Average**	**COV**
B	*c/2 = 0.75*	0.25	0.0	0.0	0.25	0.38	0.25	0.2	0.82
C	*c = 1.5*	1.50	1.75	1.38	1.25	1.75	1.75	1.6	0.14
D	$c+d_b = 2.2$	2.50	2.50	2.75	2.25	2.00	2.75	2.5	0.12
E	$c+2d_b = 2.8$	2.25	2.50	2.25	3.00	3.25	2.50	2.6	0.16
F	$c+2d_b +1 = 3.8$	3.00	3.25	4.25	3.50	3.50	3.25	3.5	0.12
F*	$c+2d_b +1 = 3.8$	4.25	3.75	3.75	3.50	3.25	3.50	3.7	0.09
G	*h/2 = 3.8*	3.75	3.75	4.00	3.50	3.50	4.25	3.8	0.08
H	$c+2d_b = 2.8$	2.25	2.75	3.25	2.50	3.00	3.50	2.9	0.16
AAA	$c+2d_b +1 = 3.8$	3.75	4.00	3.50	4.00	3.50	3.50	3.7	0.07

Slabs E and H and F and F* are identical with the exception that the concrete ‘shadows’ beneath the reinforcing steel that result from the HD process have not been removed in Slabs H and F*. Slab H was tested in the inverted position (i.e. LMC at tension face of slab), representing the behavior of an overlay in the negative moment region of a continuous slab. Finally, Slab AAA is subject to the same HD as slab F but a standard PennDOT AAA concrete mix is used instead of LMC for the overlay.

3.1.3 Specimen Preparation

The substrate slabs were cast January 16, 2013. Conventional hydrodemolition – using a manual wand – was carried out by an approved contractor, Rampart Hydro Services, March 18th to March 20th, 2013 when the substrate concrete was at least 63 days old (Figure 14a).

Following HD, slabs were stored in a surface-saturated condition until LMC application. During this time ‘shadows’ – concrete left below exposed reinforcing steel – were removed in all slabs but F* and H using a hand-held electric chipping hammer (Figure 14c). HD depths were measured as recorded in Table 5. All HD surfaces were cleaned of laitance and loose aggregate with water and high pressure air (Figure 14b). Immediately prior to LMC application, the interface surface is dried of any standing water although the surface itself remains wetted for the LMC application; this is the typical practice of the contractor. Finally, the LMC overlays were applied March 29, 2013 by a PennDOT-approved contractor, Trumbull, (Figure 14d).

Following LMC application, the slabs were kept under wet burlap for 7 days and then allowed to cure in ambient laboratory conditions.

a) slabs during hydrodemolition

b) hydrodemolished surface profile

c) “shadows” removed

d) installing LMC overlay

Figure 14: HD and LMC process.

3.1.4 Material Properties

3.1.4.1 Substrate Concrete and Slab AAA Overlay Concrete

A PennDOT-approved AAA mix was provided by local ready-mix supplier Frank Bryan Concrete for both the substrate slabs and the overlay for slab AAA. The mix design reported by the supplier is shown in Table 6. Measured 28-day concrete compression strength (f_c' per ASTM C39), split cylinder tension strength (f_{sp} per ASTM C496) and modulus of rupture (f_r per ASTM C78) are given in Table 7. All cylinders were standard 4 in. (102mm) diameter cylinders and the modulus of rupture specimens were standard 6 in. (152 mm) beams. It is noted that the AAA overlay strength was lower than the substrate concrete strength.

2.25 inch (57 mm) diameter cores were taken from Slab A following all testing in order to confirm *in situ* concrete strength. Compressive strength from these cores is also shown in Table 7 and agree well with the 28-day strength.

A rule of thumb is that the direct tension capacity of conventional concrete is approximately $0.70f_{sp}$ and $0.50f_r$. Therefore the direct tension capacity of the concrete in the test specimens is on the order of 320 - 400 psi (2.2-2.8 MPa) ($4\sqrt{f_c'} - 5\sqrt{f_c'}$ in psi units). The recommended value of direct tension strength is typically given as $4\sqrt{f_c'}$(psi units), in this case, 320 psi (2.2 MPa).

3.1.4.2 Latex-Modified Overlay Concrete

A PennDOT-approved latex-modified concrete was provided by Trumbull for all overlays. The mix design reported by the supplier is shown in Table 6. Measured 7- and 28-day concrete compression strength and split cylinder tension strength are given in Table 7. All cylinders were standard 4 in. (102 mm) diameter cylinders. The LMC was made with *Styrofan 1186*, an aqueous styrene-butadiene copolymer dispersion manufactured by BASF and pre-qualified under FHWA RD-78-35 (FHWA 1978). This prequalification is considered acceptable per PennDOT *Pub*. 408 Section 1042.2e.

3.1.4.3 Reinforcing Steel

The #5 A615 reinforcing steel had experimentally-determined yield and tensile strengths of 67.8 ksi (467 MPa) and 107.9 ksi (744 MPa), respectively.

Table 6: Mix designs for PennDOT AAA concrete and LMC overlay.

<table>
<tr><th></th><th colspan="2">AAA Concrete</th><th colspan="2">LMC Concrete</th></tr>
<tr><td>Supplier</td><td colspan="2">Frank Bryan Concrete</td><td colspan="2">Trumbull</td></tr>
<tr><td></td><td>material</td><td>mix (lbs/yd^3)</td><td>material</td><td>mix (lbs/yd^3)</td></tr>
<tr><td>cement</td><td>Type I/II (Lehigh)</td><td>540</td><td>Type I/II (CEMEX)</td><td>658</td></tr>
<tr><td>pozzolan</td><td>Class C flyash (CEMEX)</td><td>110</td><td>-</td><td>-</td></tr>
<tr><td>coarse aggregate</td><td>#57
(Greer Limestone)<table><tr><th>screen</th><th>% passing</th></tr><tr><td>1-1/2”</td><td>100</td></tr><tr><td>1”</td><td>99</td></tr><tr><td>1/2"</td><td>46.5</td></tr><tr><td>#4</td><td>2.2</td></tr><tr><td>#8</td><td>1.0</td></tr></table></td><td>1776</td><td>A8
(Allegheny Minerals)<table><tr><th>screen</th><th>% passing</th></tr><tr><td>1/2”</td><td>100.0</td></tr><tr><td>3/8”</td><td>91.5</td></tr><tr><td>#4</td><td>25.7</td></tr><tr><td>#8</td><td>3.5</td></tr><tr><td>#16</td><td>0.8</td></tr></table></td><td>1070</td></tr>
<tr><td>fine aggregate</td><td>A
(Tri State River Prod.)<table><tr><th>screen</th><th>% passing</th></tr><tr><td>#4</td><td>99</td></tr><tr><td>#8</td><td>83</td></tr><tr><td>#16</td><td>61</td></tr><tr><td>#30</td><td>41</td></tr><tr><td>#50</td><td>14</td></tr><tr><td>#100</td><td>3</td></tr></table></td><td>1172</td><td>A
(Hanson Agg.)<table><tr><th>screen</th><th>% passing</th></tr><tr><td>3/8”</td><td>100.0</td></tr><tr><td>#4</td><td>98.6</td></tr><tr><td>#8</td><td>83.5</td></tr><tr><td>#16</td><td>69.1</td></tr><tr><td>#30</td><td>55.6</td></tr><tr><td>#50</td><td>20.9</td></tr><tr><td>#100</td><td>5.3</td></tr></table></td><td>1706</td></tr>
<tr><td>mix water</td><td></td><td>267</td><td></td><td>124</td></tr>
<tr><td>admixture water</td><td></td><td>-</td><td></td><td>109</td></tr>
<tr><td>AEA</td><td>AIR-260 (SIKA)</td><td>1 oz/cwt</td><td>-</td><td>-</td></tr>
<tr><td>RR</td><td>Plastocrete 10N (SIKA)</td><td>3.5 oz/cwt</td><td>-</td><td>-</td></tr>
<tr><td>latex</td><td>-</td><td>-</td><td>Styrofan 1186 (BASF)</td><td>210</td></tr>
<tr><td>w/c</td><td></td><td>0.410</td><td></td><td>0.354</td></tr>
<tr><td>unit weight</td><td></td><td>143</td><td></td><td>140</td></tr>
<tr><td rowspan="2">reported trial mix strength</td><td>7 day</td><td>4776 psi</td><td>5 day</td><td>4622 psi</td></tr>
<tr><td>28 day</td><td>6559 psi</td><td>28 day</td><td>6481 psi</td></tr>
</table>

Table 7: Concrete material properties.

age (days)	**ASTM C39 compression tests**			**ASTM C496 split cylinder tests**			**ASTM C78 modulus of rupture**		
	n	f_c (psi)	COV	n	f_{sp} (psi)	COV	n	f_r (psi)	COV
	AAA substrate slab concrete								
28	3	6501	3.4%	3	$453 = 5.6\sqrt{f_c'}$	13.1%	3	$790 = 9.8\sqrt{f_c'}$	5.6%
132	3 cores	6647	8.4%	-	-	-	-	-	-
	latex-modified concrete overlay								
7	3	4718	0.7%	-	-	-	-	-	-
28	3	6568	4.4%	3	$641 = 7.9\sqrt{f_c'}$	11.7%	-	-	-
	AAA overlay (Slab AAA only)								
28	3	4676	5.2%	3	$441 = 6.4\sqrt{f_c'}$	6.4%	-	-	-

3.1.5 Test Set-Up and Instrumentation

The slabs are tested over a simple span of 84 in. (2134 mm) as shown in Figure 15. The selection of an 84 in. (2134 mm) simple span is based on a slab-on-steel girder bridge having a girder spacing S = 8 ft (2.44 m) and a top flange dimension b_f = 12 in. (305 mm). In such a case, the clear span of the slab is 84 in. (2134 mm). In all slabs but H, the LMC is placed in compression representing positive flexure typical of a slab spanning between girders. Slab H was tested in the inverted position (i.e. LMC at tension face of slab), representing the behavior of an overlay in the negative moment region of a continuous slab. Support points are full-width 4 in. (102 mm) diameter rockers transitioned to the slab through 3/8 in. (10 mm) steel plates. The load location is a 2 in. (50 mm) wide by 1/2 in. (13 mm) deep neoprene pad. Load is applied through a full-width spreader beam and single 60 kip (267 kN) hydraulic ram with a ball joint between the ram and spreader beam. Applied load is calculated from hydraulic pressure with a precision of 72 pounds (320 N). Displacement at midspan is measured manually with a precision of 1/32 in. (0.8 mm). The combined 130 pound (578 N) weight of the ball joint and spreader beam is included in all reported applied loads.

DEMEC targets having an 8 in. (203 mm) gauge length are applied at midspan on both sides of the slab. Target locations vary vertically for each slab but were selected to capture the following:

- centroid of tensile steel (1.82 in. (46.2 mm) above soffit)
- immediately above the LMC interface
- immediately below the LMC interface
- as near to the extreme compression fiber as possible (1/2 in. (13 mm) below top of slab)
- a fifth location selected to provide good data distribution

The DEMEC instrument used (Figure 15c) has a resolution of 8 microstrain (0.000008 in/in).

Load was applied to the slabs in increments of approximately 1000 pounds (4.45kN) at which time a complete set of instrument readings were recorded. Following yield of the slab, instruments were recorded at displacement increments not exceeding 1/16 in (1.6 mm).

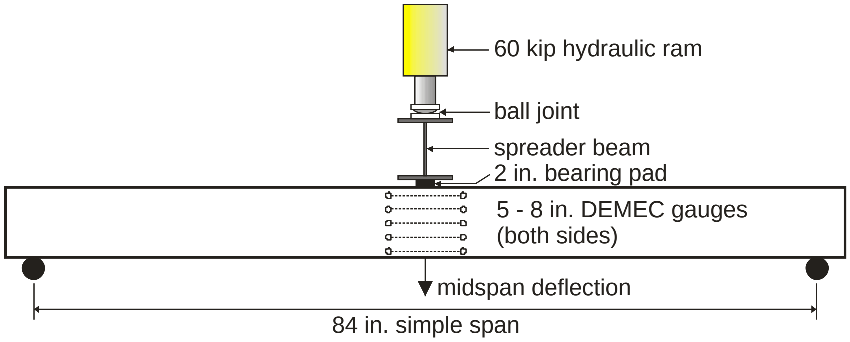

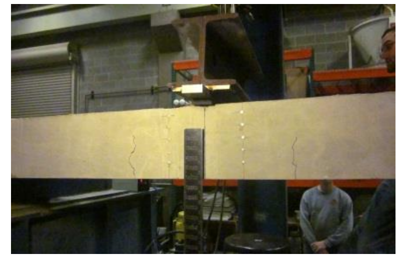

b) DEMEC and vertical deflection instrumentation

a) test set-up

c) DEMEC reader (wexham-developments.co.uk)

Figure 15: Test set up and instrumentation.

3.1.6 Predictions of Slab Behavior

In order to verify the control slab behavior and establish a baseline against which to compare test data, a fiber-element model of the control test slab was analyzed. This and all subsequent analysis were conducted using program RESPONSE (Bentz 2000), a fiber-element plane-sections analysis tool which incorporates the modified compression field theory. RESPONSE is well established in both the research and consulting communities.

Figure 16 shows the moment-curvature response predicted for the control slabs calculated using measured material properties and as-tested dimensions. Also shown are AASHTO slab design moments determined based on the AASHTO 'strip method' calculations (*AASHTO LRFD* §4.6.2.1.1 as tabulated in AASHTO Appendix A4). The positive live load design moment for S = 8 ft (2.44 m) is M_{LL} = 5.69 kipft/ft (25.31 kNm/m). Dead load moment for the 7.5 in. (191 mm) thick slab, M_{DL} = 0.75 kipft/ft (3.34 kNm/m) is added to this value. These values are multiplied by 22/12 to account for the 22 in. (559 mm) specimen width. The moments shown are based on the AASHTO SERVICE I and STRENGTH I load combinations as summarized in Table 8.

Table 8: Slab specimen design moments.

'strip method' moments (AASHTO§ 4.6.2.1.1)		22 in. wide specimen moments	
		SERVICE I	STRENGTH I
M_{LL}	M_{DL}	(22/12)(M_{DL} + M_{LL})	(22/12)(1.25M_{DL} + (1.33 x 1.75M_{LL})
5.69 kipft/ft	0.75 kipft/ft	11.8 kipft	26.0 kipft

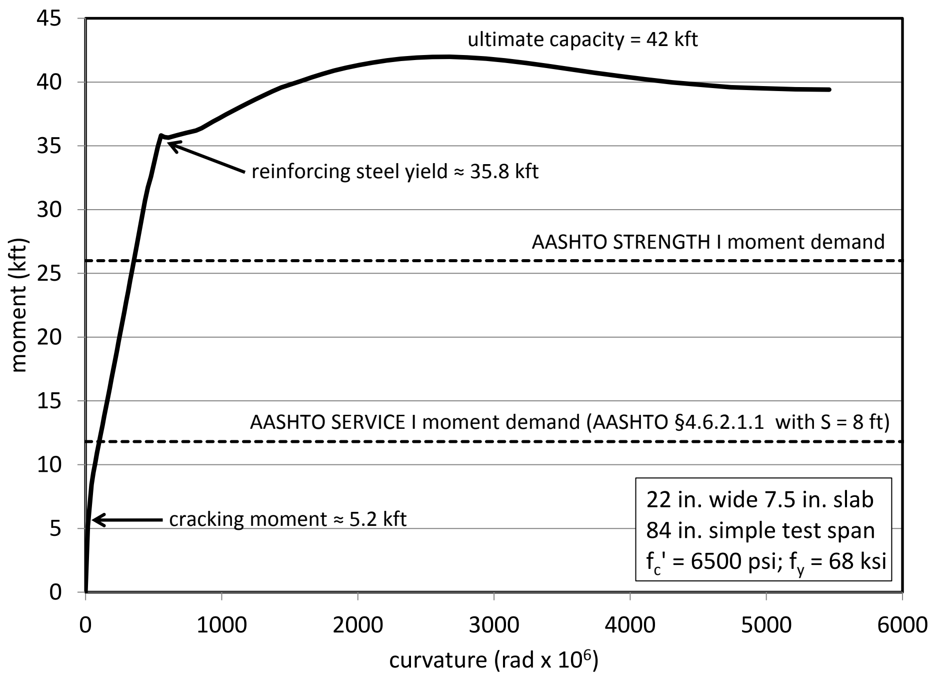

Figure 16: Predicted moment-curvature behavior of slab specimens.

Figure 17 (left axis) presents the slab moment capacity with decreasing concrete depth as concrete is removed from the top of the slab; essentially the capacity of the slab as it is subject to HD. The data shown represents a series of plane sections analyses conducting using program RESPONSE. The slab depth is measured from the soffit. Once the slab depth falls below the layer of the top reinforcing steel (at 6.2 in. (157 mm)), the contribution of the top steel is neglected (hence the step in the ultimate capacity curve). In terms of capacity, Figure 17 demonstrates that a slab of 6.0 in. (152 mm) is required to resist the factored load demand (STRENGTH I) while a 4 in. (102 mm) slab is adequate to resist the nominal demand (SERVICE I). The predicted ultimate deflection (Figure 17, right axis) for a 7.5 in. (191 mm) slab is *S*/225; this falls to *S*/112 and *S*/77 for the slabs having a thickness of 6 and 4 in. (152 and 102 mm), respectively. The slab span is *S* = 84 in. (2134 mm).

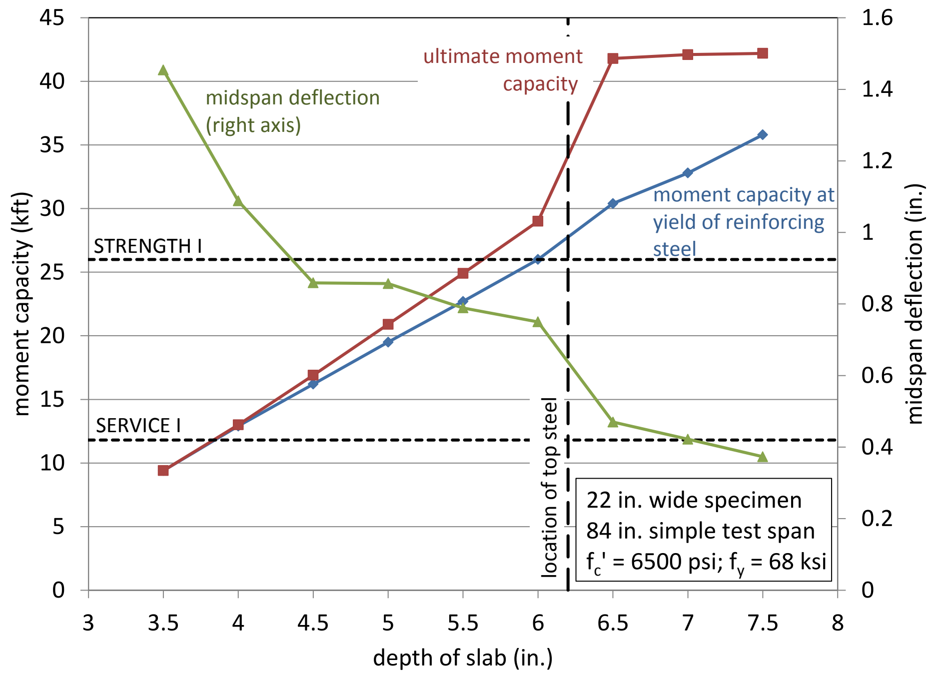

Figure 17: Predictions of slab behavior in LMC **does not** contribute to slab capacity.

3.2 RESULTS OF SLAB FLEXURAL TESTS

Table 9 summarizes key results from all test slabs while Figures 19 through 28 provide details of each test slab. The data shown in these figures is described as follows:

Figures a show the moment-curvature (M-φ) diagrams; both experimental (solid line) and analytical (dashed line) predictions are presented. Moment is the applied moment, neglecting self-weight of the slab, and is calculated as: $M = PL/4 = 1.75P$ (kipft) (where L is the span length of 7 ft). The curvature is calculated from the individual strain profiles (see below) by dividing the absolute difference in strain between the top- and bottom-most DEMEC gages by the vertical distance between the gage lines. The analytical curves are generated using RESPONSE as described above (see Figure 16) using the geometry and material properties of each slab.

Figures b show the strain profiles determined directly from DEMEC readings plotted at their appropriate vertical locations. For clarity, profiles at all loading intervals are not shown. Although DEMEC readings were recorded from both sides of each test slab, results from only one side are shown. The results shown are from the side capturing uniform cracking. The location of the LMC interface is also shown in each instance

DEMEC gages report the *average strain* over their 8 in. (203 mm) gage length. It is expected that multiple cracks will intersect the gage length and the strain reading is therefore essentially the sum of the crack widths since concrete strain between cracks is negligible. In cases were a crack passes from outside the gage length to inside the gage length between gages – as shown in the circled region of Figure 18a – the DEMEC reading between adjacent gages is affected as shown in Figure 18b. In the case shown in Figure 18, three cracks are included in the top four gages. The right-most crack passes outside the gage at the bottom DEMEC gage; the associated crack width (strain) is therefore not captured in the reading and the apparent bottom strain falls. In this case, the curvature is calculated over the linear section from the top gage to the fourth gage.

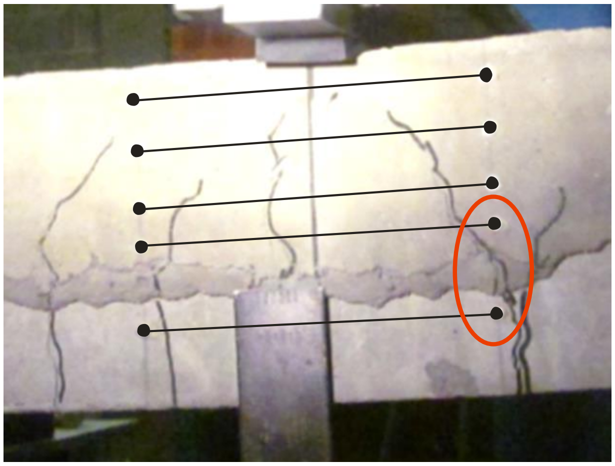

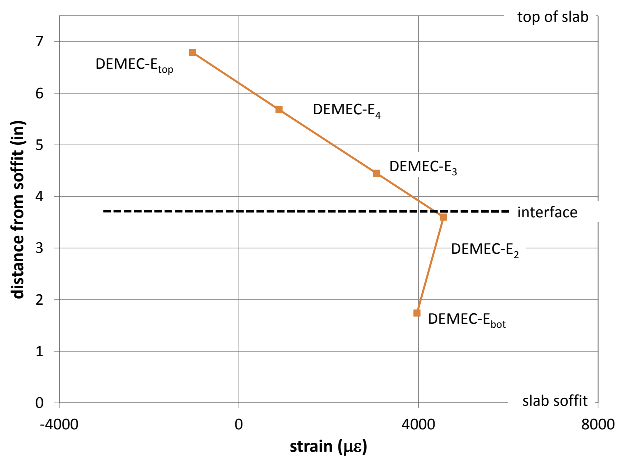

a) crack pattern on Slab AAA (gages enhanced) b) strain profile of Slab AAA (at 35.4 kipft)

Figure 18: Example of the effect of crack location on strain profiles (Slab AAA shown).

Figures c show the location of the neutral axis derived from the slope of the strain profiles. This calculation was made by assuming linearity between two points on the strain profile and using a linear equation to calculate the y-axis intercept. In all cases, the y-axis is given as the distance from the slab soffit. The location of the LMC interface is also shown in each instance.

Figures d, e and f show photographs at key milestones in the load application process: reinforcement yield, final DEMEC reading (DEMEC gages have a limit of about 15000 με), and ultimate load, respectively.

Table 9: Summary of key test results.

	Slab									
	A	**B**	**C**	**D**	**E**	**F**	**F***	**G**	**H**	**AAA**
depth of slab (in.)	7.5	8.5	8.0	7.5	7.5	7.5	7.5	7.5	7.5	7.5
depth of overlay (in)	none	1.2	2.1	2.5	2.6	3.5	3.7	3.8	2.9	3.7
load at first crack (kips)	5.08	7.13	3.10	5.15	5.13	4.11	5.13	5.13	6.14	-
moment at first crack (kipft)	8.89	12.47	5.42	9.01	8.97	7.19	8.97	8.97	10.74	-
load at reinforcing yield (kips)	18.19	27.13	23.15	20.18	20.18	20.08	20.13	20.23	20.15	20.15
moment at reinforcing yield (kipft)	31.83	47.47	40.51	35.31	35.31	35.14	35.22	35.40	35.26	35.26
ratio yield capacity to Slab A	-	1.49 1.16[1]	1.27 1.12[1]	1.11	1.11	1.10	1.11	1.11	-	1.11
deflection at reinforcing yield (in.)	0.375	0.375	0.343	0.406	0.406	0.406	0.406	0.406	0.343	0.469
curvature at reinforcing yield (rad/in^6)	651	572	571	640	806	622	845	600	565	537
ultimate load (kips)	28.03	39.38	34.13	30.21	29.31	29.17	28.23	31.13	29.24	25.19
ultimate moment (kipft)	49.05	68.91	59.72	52.86	51.29	51.04	49.40	54.47	51.17	44.08
ratio ultimate capacity to Slab A	-	1.40 1.09[1]	1.22 1.07[1]	1.08	1.05	1.04	1.01	1.11	-	0.90
deflection at ultimate load (in.)	-	3.50	2.125	1.81	2.56	2.81	2.5	3.00	2.00	2.25
failure mode	flexural	flexural	flexural	flexural	flexural	flexural	flexural	flexural	flexural	flexural

[1] value normalized to 7.5 in. slab depth; i.e.: Slab B ratio multiplied by $(7.5/8.5)^2$ and Slab C by $(7.5/8.0)^2$

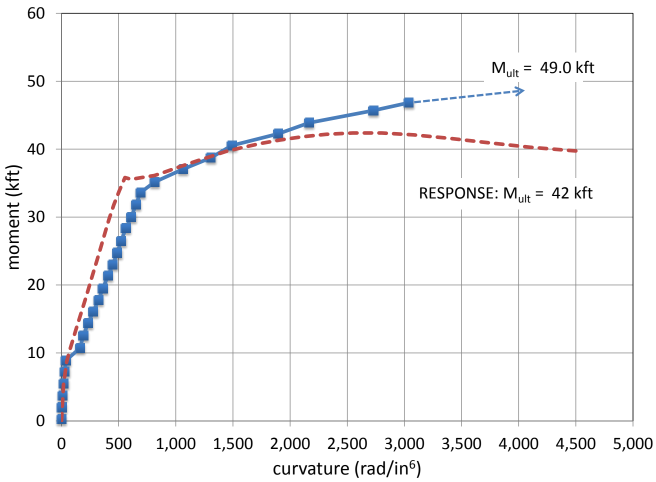

a) moment-curvature plot

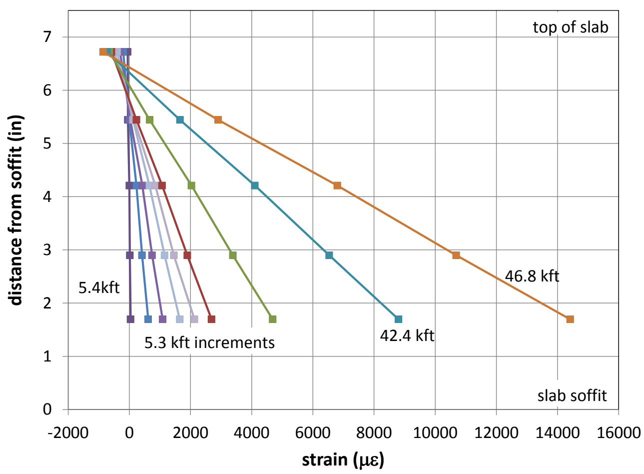

b) strain profiles

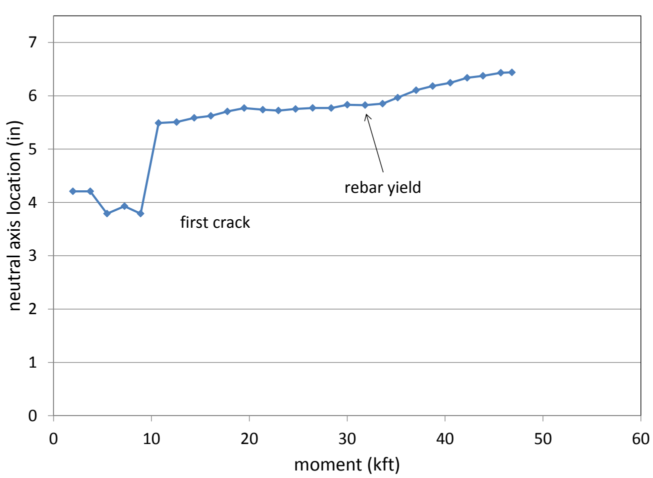

c) location of neutral axis

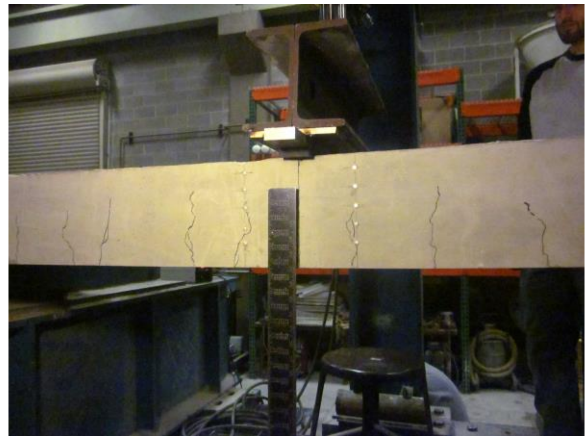

d) reinforcement yield (31.8 kipft)

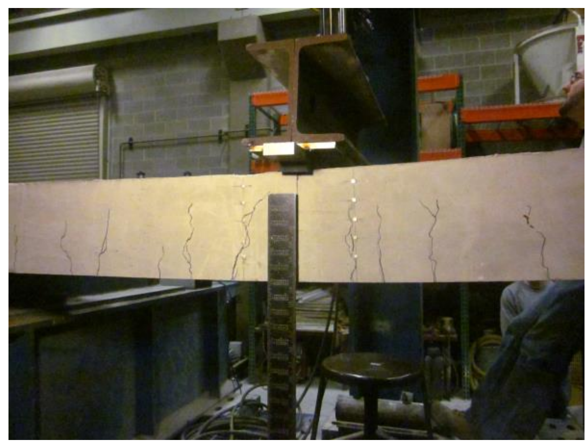

e) final DEMEC reading (46.8 kipft)

f) ultimate load (49.0 kipft)

Figure 19: Slab A results.

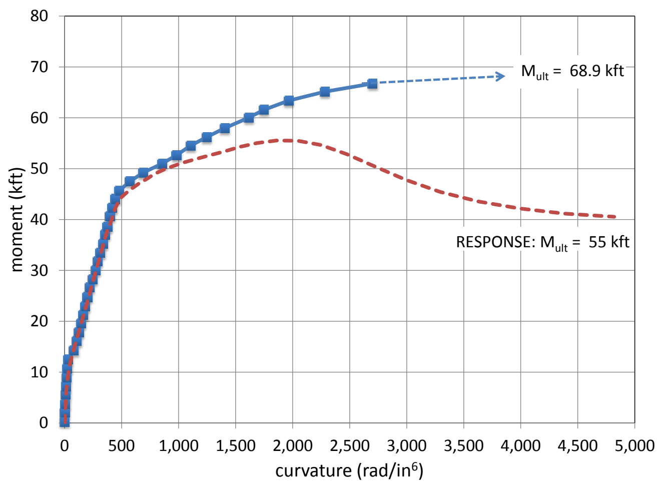

a) moment-curvature plot

d) reinforcement yield (47.5 kipft)

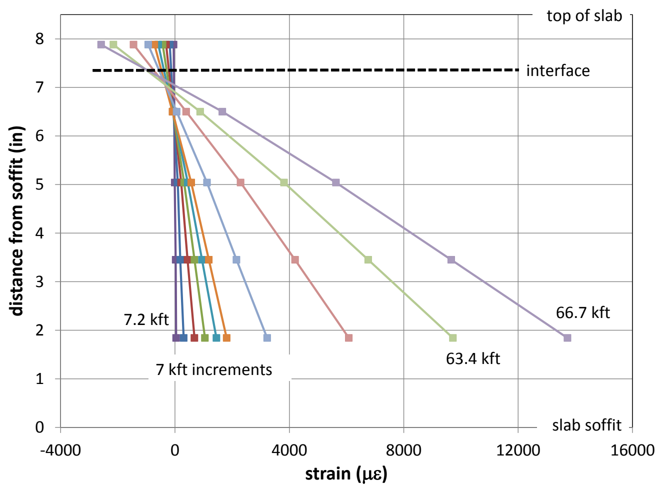

b) strain profiles

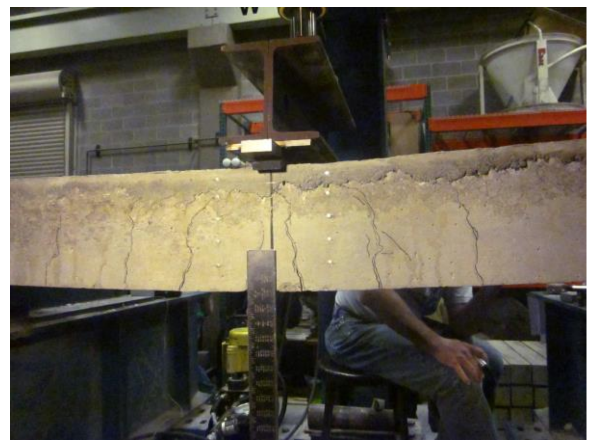

e) final DEMEC reading (66.7 kipft)

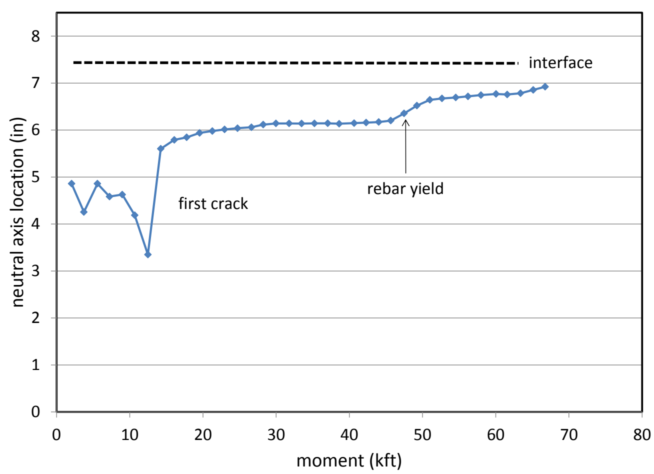

c) location of neutral axis

f) ultimate load (68.9 kipft)

Figure 20: Slab B results.

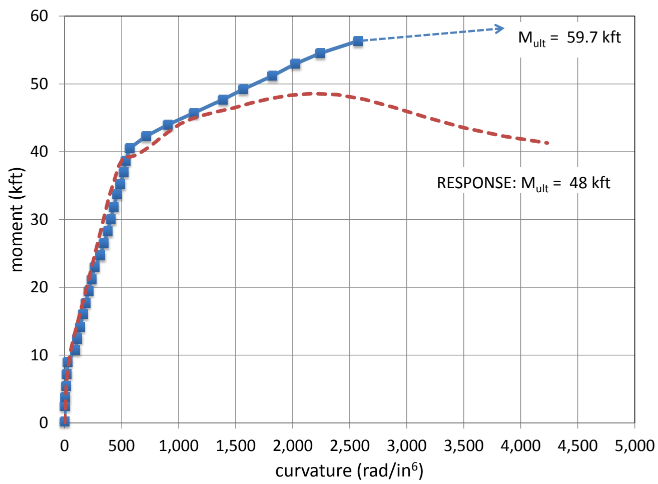

a) moment-curvature plot

d) reinforcement yield (40.5 kipft)

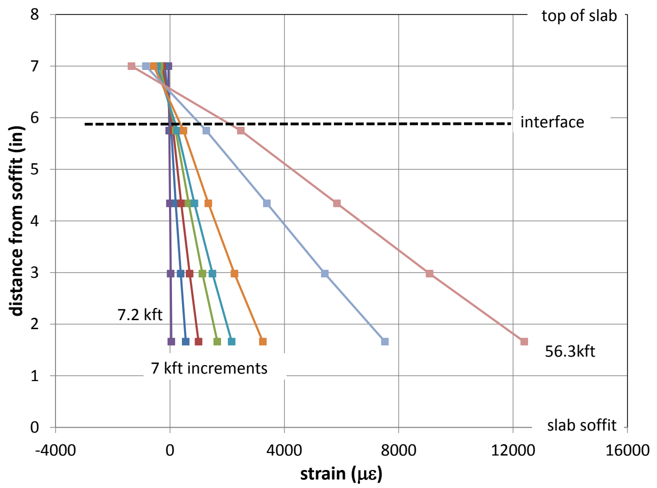

b) strain profiles

e) final DEMEC reading (56.3 kipft)

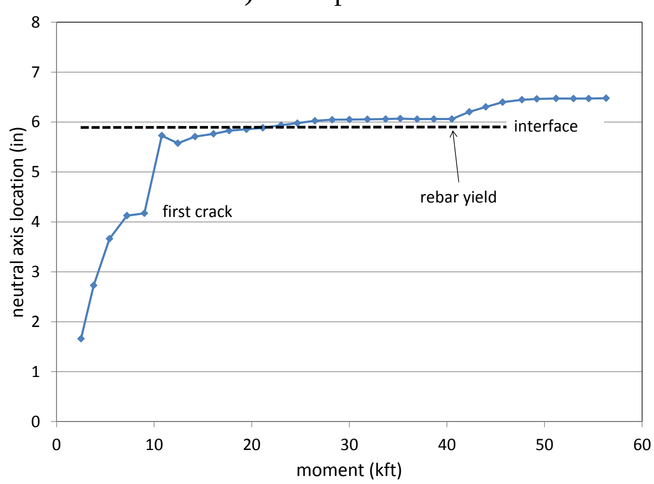

c) location of neutral axis

f) ultimate load (59.7 kipft)

Figure 21: Slab C results.

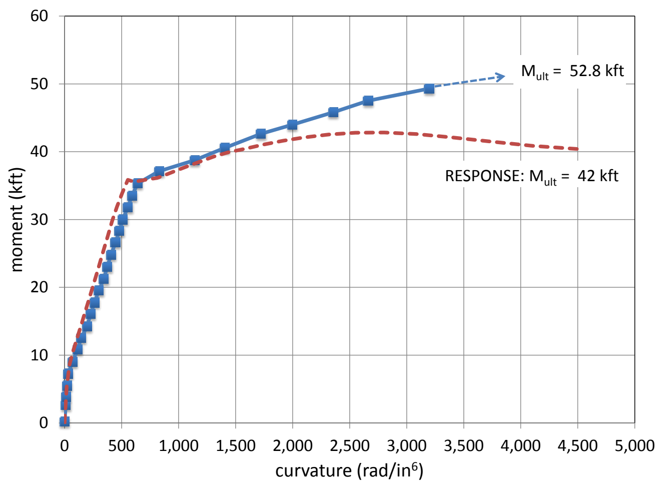

a) moment-curvature plot

d) reinforcement yield (35.3 kipft)

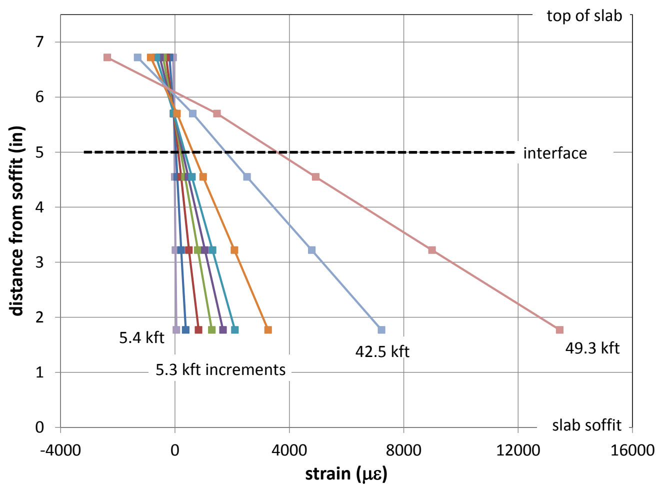

b) strain profiles

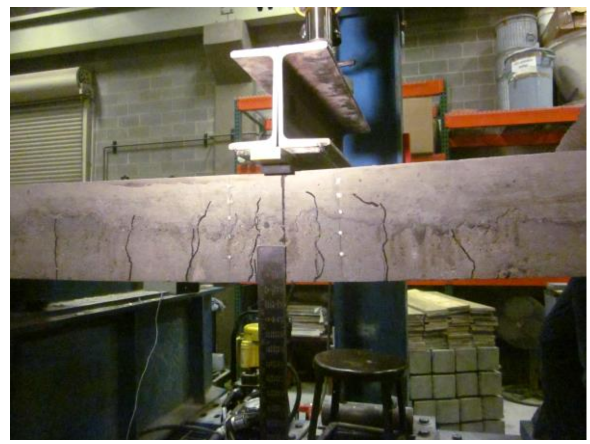

e) final DEMEC reading (49.3 kipft)

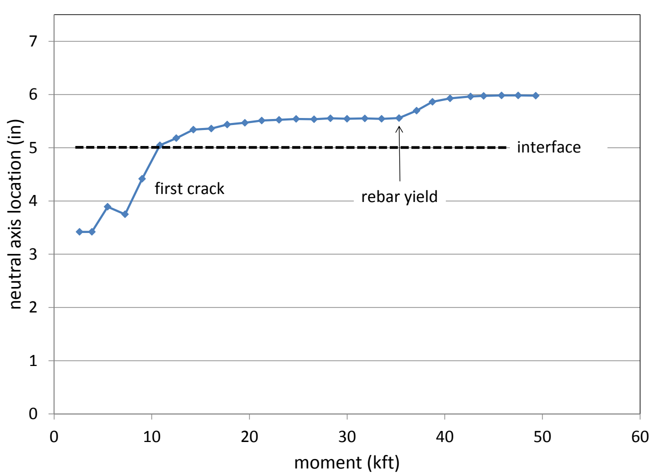

c) location of neutral axis

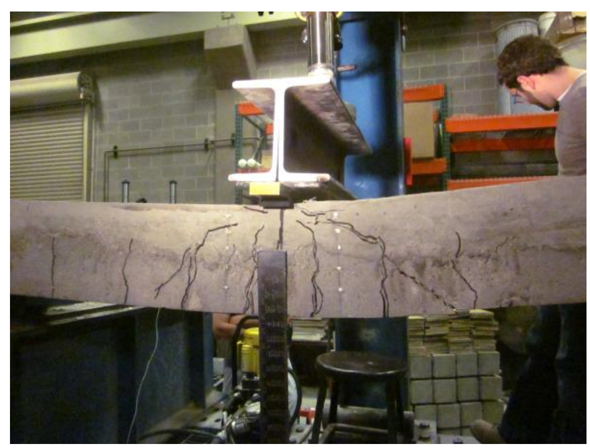

f) ultimate load (52.8 kipft)

Figure 22: Slab D results.

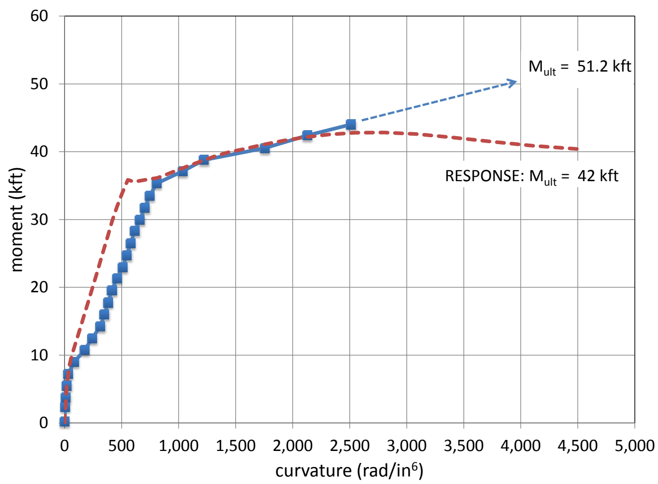

a) moment-curvature plot

d) reinforcement yield (35.3 kipft)

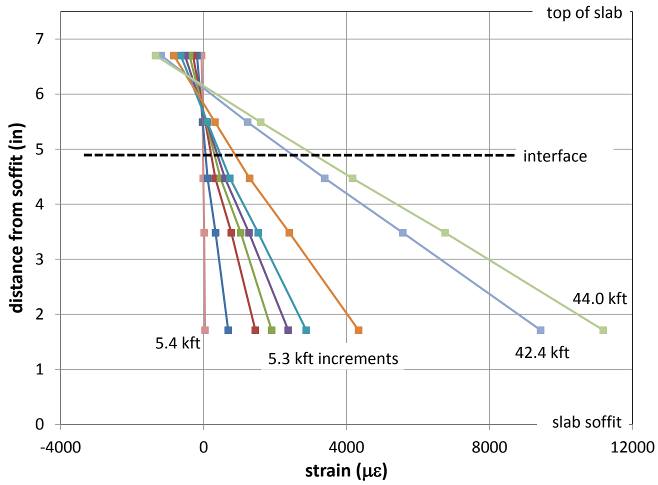

b) strain profiles

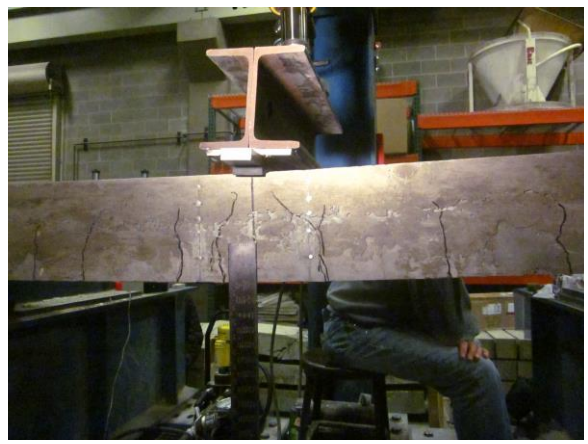

e) final DEMEC reading (44.0 kipft)

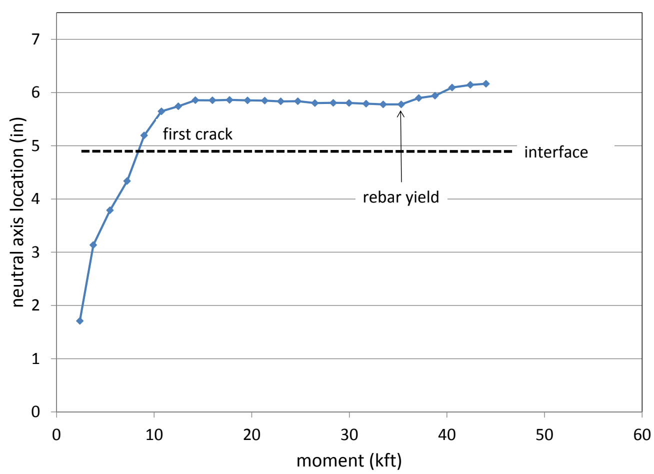

c) location of neutral axis

f) ultimate load (51.2 kipft)

Figure 23: Slab E results.

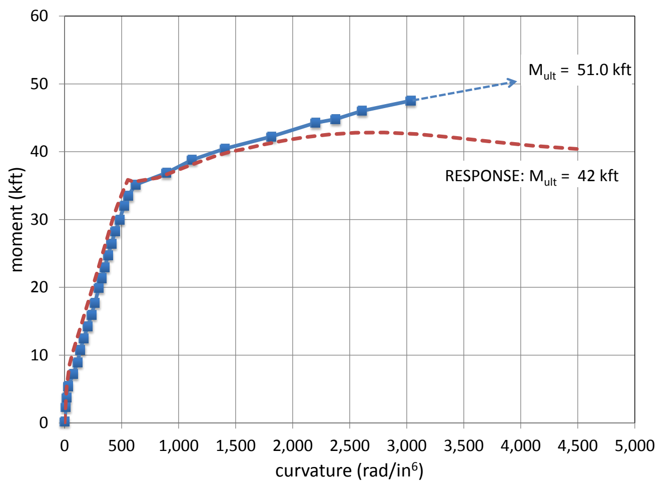

a) moment-curvature plot

d) reinforcement yield (35.1 kipft)

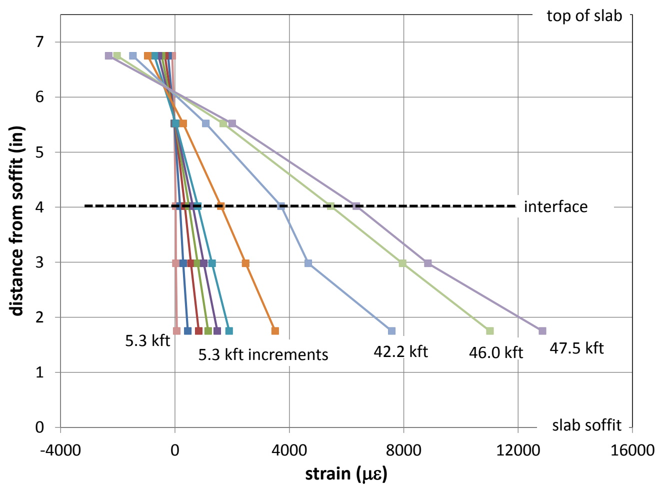

b) strain profiles

e) final DEMEC reading (47.5 kipft)

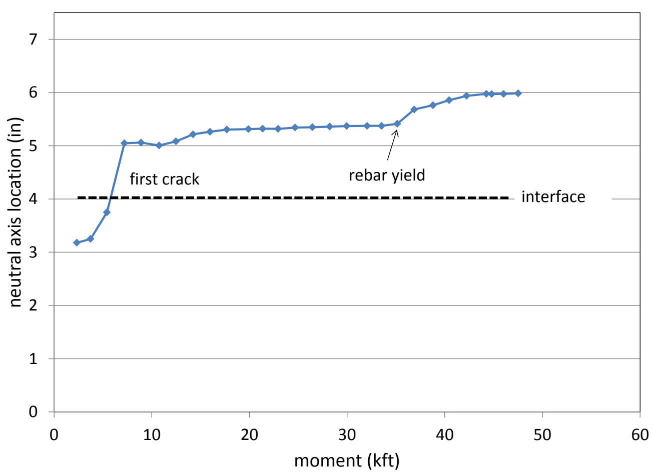

c) location of neutral axis

f) ultimate load (51.0 kipft)

Figure 24: Slab F results.

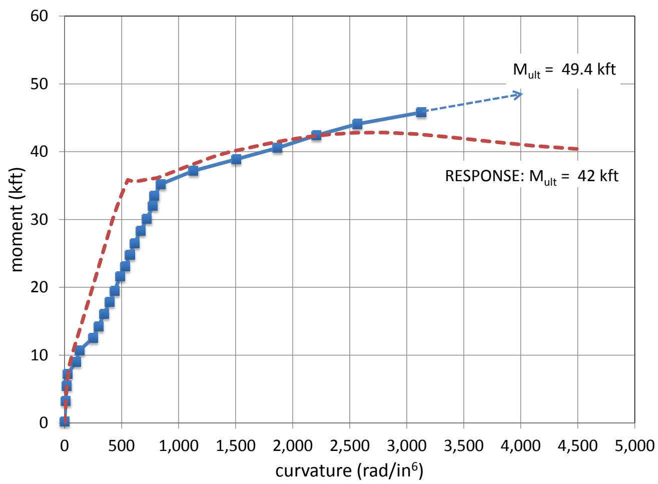

a) moment-curvature plot

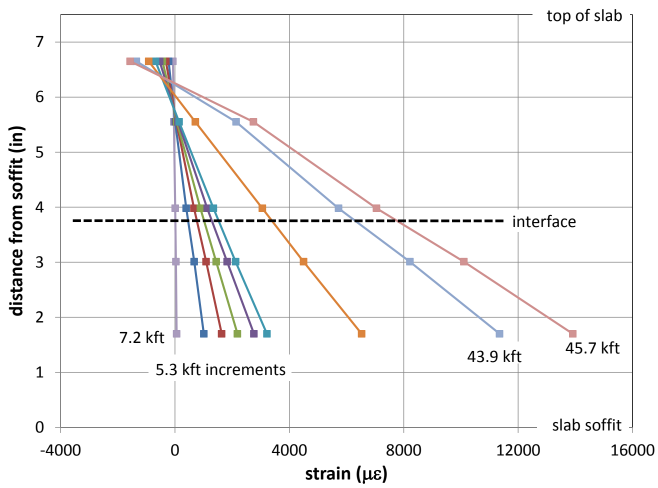

b) strain profiles

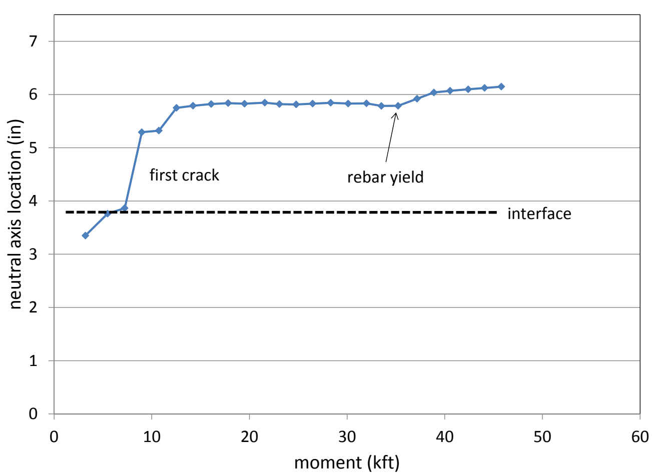

c) location of neutral axis

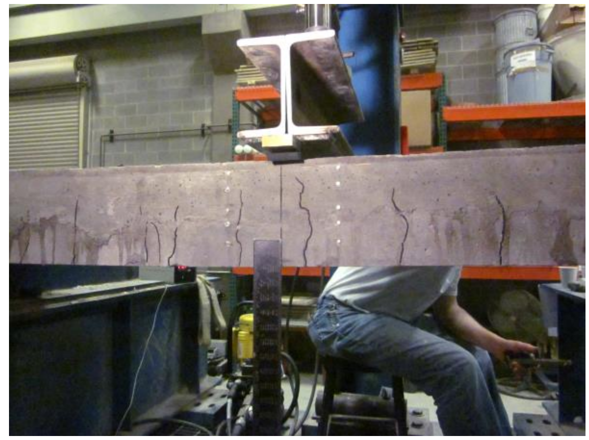

d) reinforcement yield (35.2 kipft)

e) final DEMEC reading (45.7 kipft)

f) ultimate load (49.4 kipft)

Figure 25: Slab F* results.

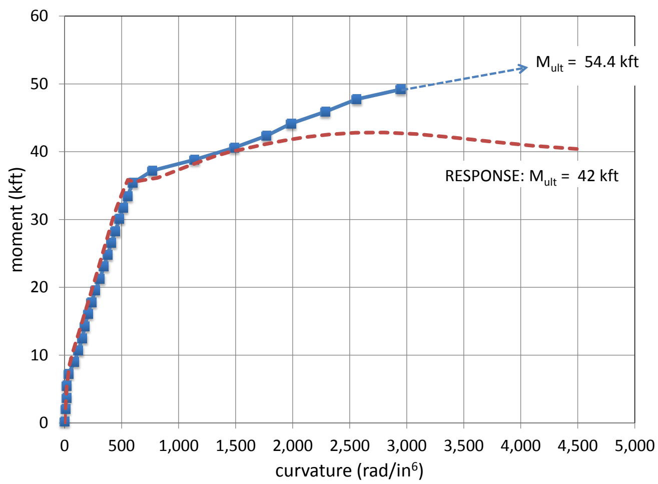

a) moment-curvature plot

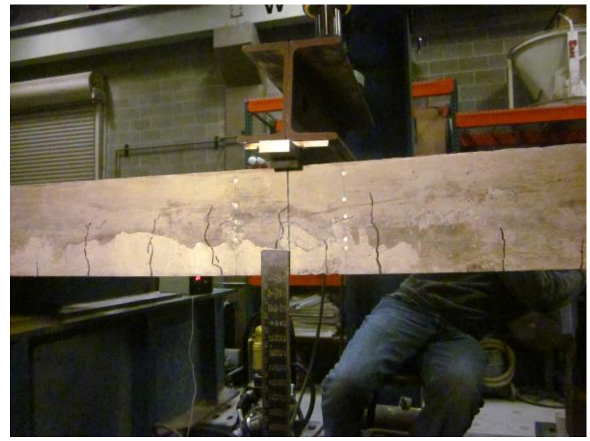

d) reinforcement yield (35.4 kipft)

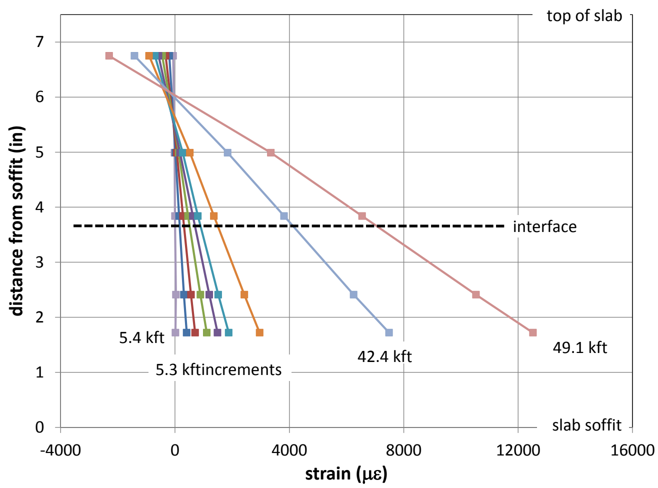

b) strain profiles

e) final DEMEC reading (49.1 kipft)

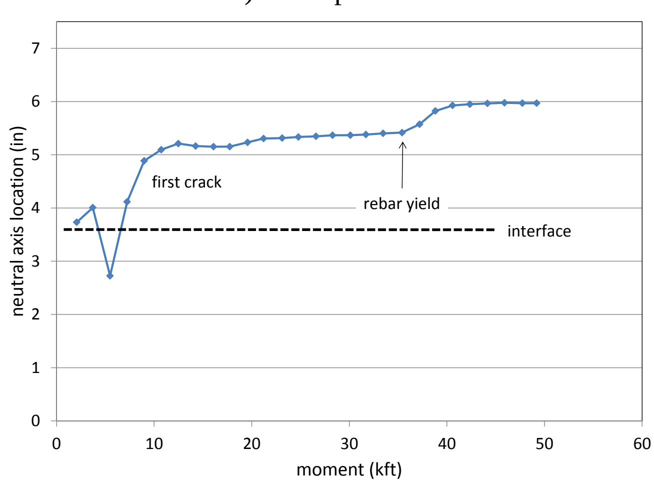

c) location of neutral axis

f) ultimate load (54.4 kipft)

Figure 26: Slab G results.

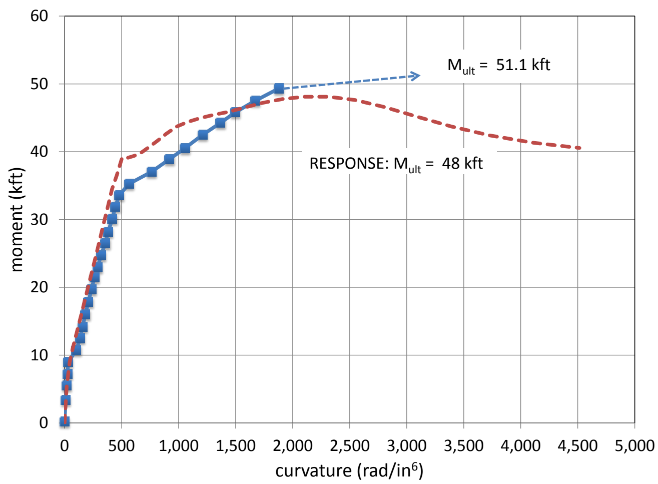

a) moment-curvature plot

d) reinforcement yield (35.3 kipft)

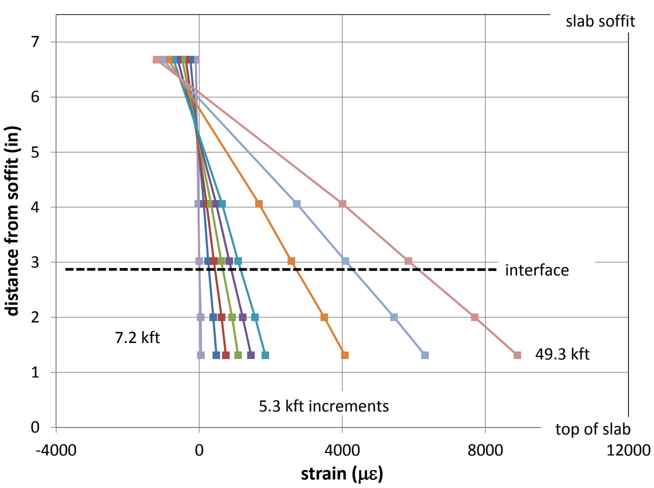

b) strain profiles

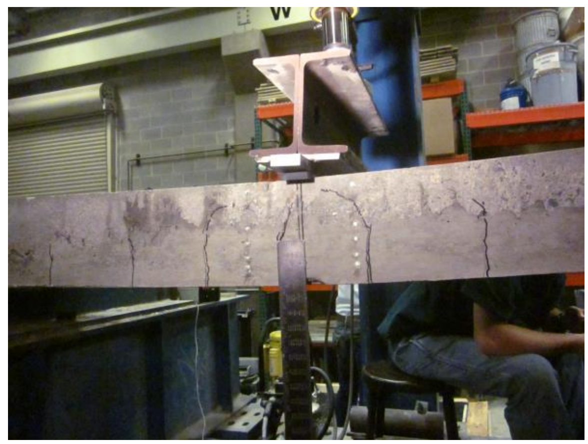

e) final DEMEC reading (49.3 kipft)

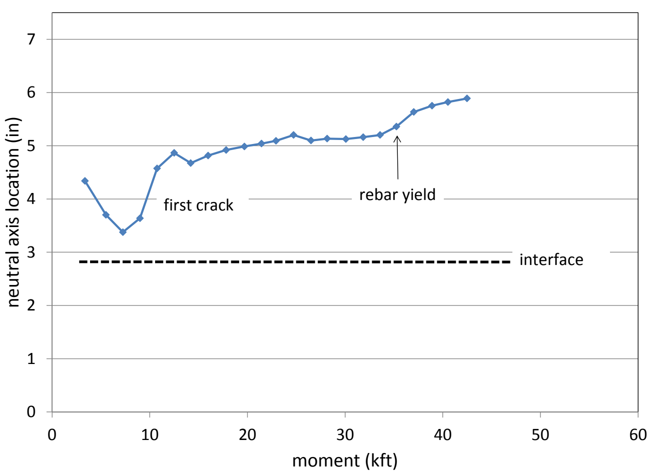

c) location of neutral axis

f) ultimate load (51.1 kipft)

Figure 27: Slab H results.

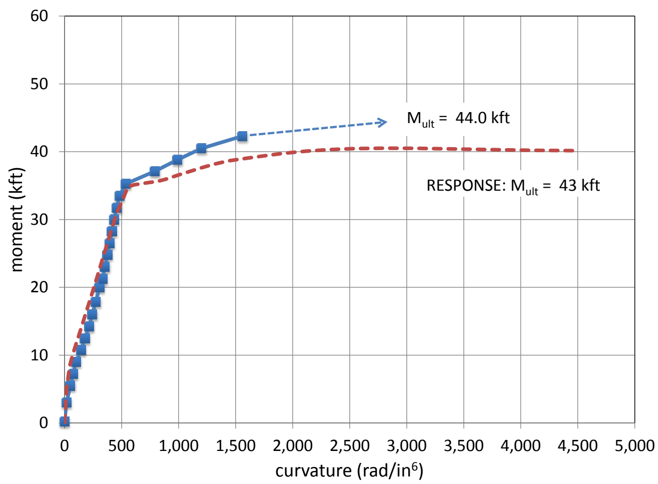

a) moment-curvature plot

d) reinforcement yield (35.3 kipft)

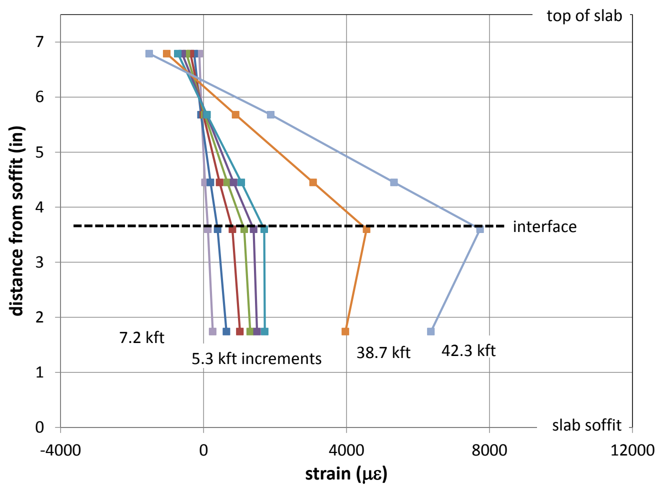

b) strain profiles

e) final DEMEC reading (42.3 kipft)

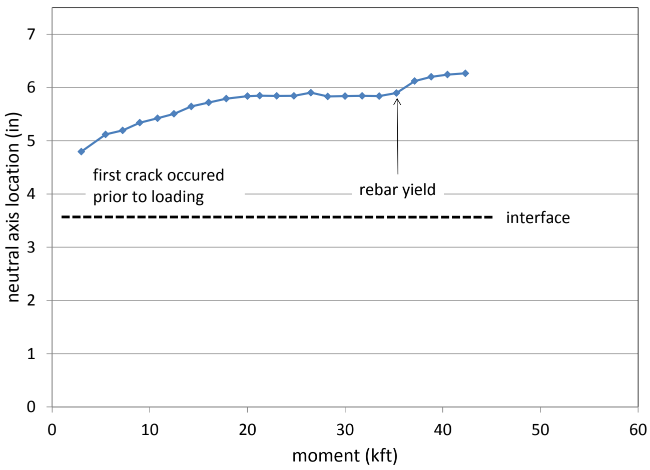

c) location of neutral axis

f) ultimate load (44.0 kipft)

Figure 28: Slab AAA results.

3.3 FLEXURAL TEST DISSCUSION

The following discussion is based on experimental results presented in the previous section. Analytical models as well as material from the literature review supplement the discussion.

3.3.1 Experimental vs. Predicted Capacities

In the course of the experimental program, analytical models (described previously in Section 3.1.6) were generated for each of the test specimens using RESPONSE. Slab capacities predicted from these plane-sections analyses were generated for the control slab and each tested specimen. Although the laboratory slabs are all under-reinforced (i.e.: behavior governed by reinforcing steel), each analysis considered the actual geometry of the slab, particularly the location of the LMC overlay interface and the different concrete and LMC material properties (Table 7). For instance, the uncracked and cracked moments of inertia will shift slightly because of the small difference in compressive strengths (and therefore moduli) of the substrate and LMC. This affects the sectional response to a small degree.

Figure 29 compares predicted moment capacities for the laboratory specimens generated using RESPONSE, to the experimentally obtained capacities noted in Table 9. Most data falls to the right of the 45 degree line indicating that the experiments uniformly exhibited strengths greater than predicted. This is the 'desired' result of this comparison since the analytical model necessarily makes simplifying assumptions, particularly in terms of material behavior. Two comparisons are presented in Figure 29: a) solid circles and triangles represent comparisons made between experimental and analytical data that reflect the unique geometries of the individual slabs; whereas b) the open data points represent comparisons between experimental data and predictions for Slab A. The latter is more appropriate to design or rating procedures since it considers the 'as-built' capacity of the monolithic slab.

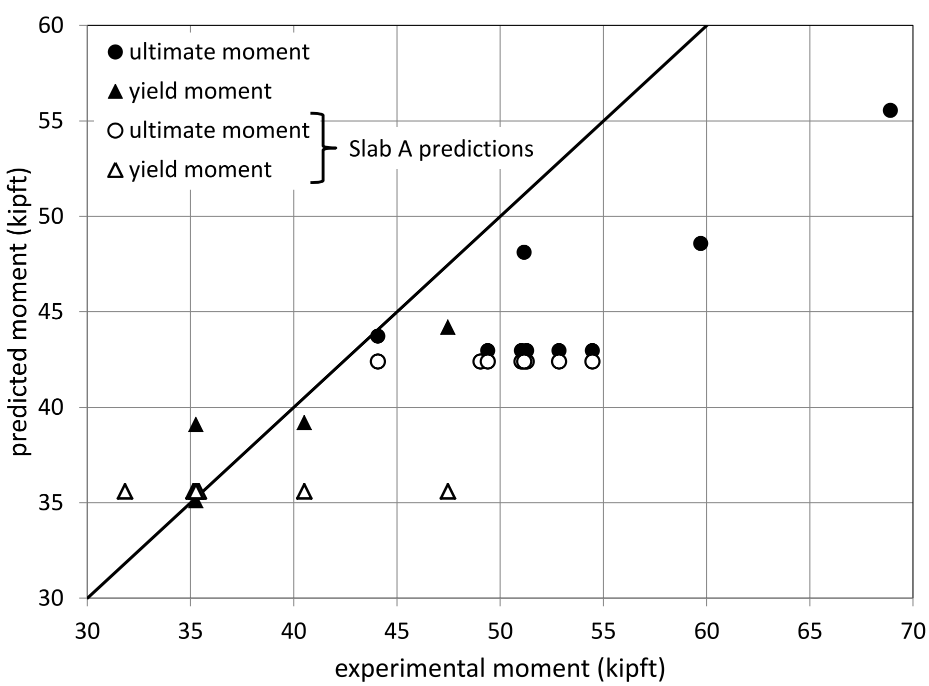

Figure 29: Experimental vs. predicted capacities of laboratory slabs.

Predictions of yield capacity (triangles in Figure 29) were very close, and generally marginally below the experimentally observed values. Since actual reinforcing bar yield strength (f_y = 67.8 ksi (467 MPa)) was used, this good agreement should be expected. Clearly, if nominal material capacities were used (i.e.: f_y = 60 ksi (414 MPa)), the prediction of yield capacity would be that much more conservative. The only slab in which the predicted capacity (39.3 kipft (53.2kNm)) exceeded the experimentally observed capacity (35.3 kipft (47.9kNm)) was Slab H which was tested in the inverted position with the overlay in the tension region of the cross-section.

Prediction of ultimate slab capacity (circles in Figure 29) and slab failure mode (see Table 9) are similarly uniformly conservative, although not excessively so. The comparison of yield and ultimate capacities validate the use of a simple plane sections analysis (in this case implemented using RESPONSE) for predicting slab capacity regardless of the presence of an overlay.

Figure 30 shows the entire moment-curvature response of all laboratory slabs (see Figures 19 through 28 for individual curves). Prior to cracking, all slabs, with the exception of Slab AAA, exhibit comparable stiffness and cracking loads (see Figure 30b). Slab AAA was unintentionally cracked during removal from the formwork prior to testing therefore no uncracked behavior is present. Nonetheless, the cracked behavior of Slab AAA is comparable to the other slabs. Post-cracking behavior of all slabs was comparable and, as described previously, the yield and ultimate behaviors were all similar.

The deeper Slabs C and B show similar although appropriately stiffer behavior. This is an important observation since not only did the LMC overlaid slabs perform similarly to monolithic slabs, the LMC when used to increase the original slab depth, served to also increase the capacity of the original slab. In this study, Slabs C and B, having depths of 8 and 8.5 in. (203 and 216 mm), respectively, exhibited yield capacities 1.27 and 1.49 times greater than the 7.5 in. (191 mm) control Slab A. This increase in strength is offset to some extent by the increase in slab self-weight, 1.07 and 1.13 times, respectively. Additionally it must be noted that the self-weight of any *additional* slab thickness must be considered as an imposed load (DW in the AASHTO loading parlance) rather than as a dead load (DC) since this additional load does result in stress in the reinforcing steel. Nonetheless, Slabs C and B were effectively strengthened by increasing their depth with the LMC overlay.

Superimposed on Figure 30 is the analytical prediction for Slab A. As is typically seen, the analytical model results in a stiffer behavior than is exhibited experimentally. Once again, this is due to necessary simplification of the analytical model. In this case, the assumption of ‘perfect bond’ between reinforcing steel and concrete may significantly affect the stiffness in these under-reinforced members.

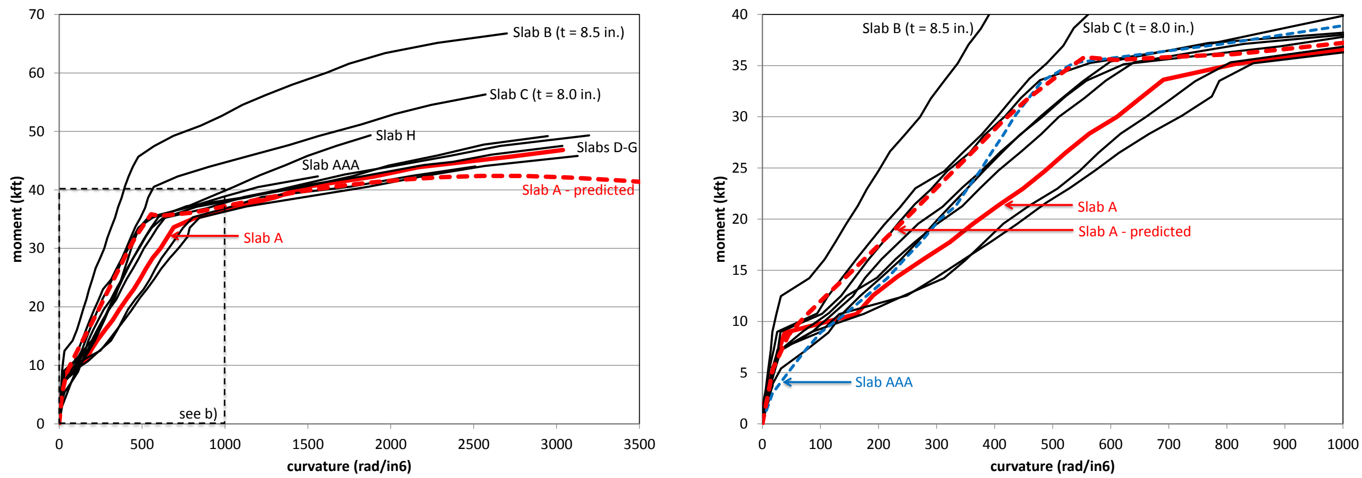

a) moment-curvature curves for all slabs b) moment-curvature response showing 'elastic' range.

Figure 30: Moment-curvature responses of all laboratory specimens.

Figure 31 shows the calculated post-cracking neutral axis depth for all laboratory slabs along with the predicted values for Slab A. Data for individual slabs is provided in Figures 19 through 28. Experimental values tracked each other and the predicted values very well. Once cracking occurs, the neutral axis shifts upward (theoretically, prior to cracking the neutral axis is located at the slab mid depth (3.75 in. (95 mm)) for the laboratory slabs) to a location approximately 5 in. (127 mm) above the soffit. As loading progresses cracking propagates, although since the steel and concrete remain essentially elastic, the neutral axis remains relatively constant as stresses are able to redistribute in the slab section. Yield of the reinforcing steel is evident by an upward 'bump' in the neutral axis (around 35 kipft (47.5 kNm)) and a subsequent continued upward shift as cracking continues to propagate with no further redistribution of stresses in the tension steel possible.

The most important observation in Figure 31 is that there is no obvious effect on the LMC interface. For most slabs, the interface is below the cracked section neutral axis (see Figures 19-28) and above the uncracked neutral axis (approximately 3.75 in. (95 mm) above soffit) and has no obvious effect on slab behavior.

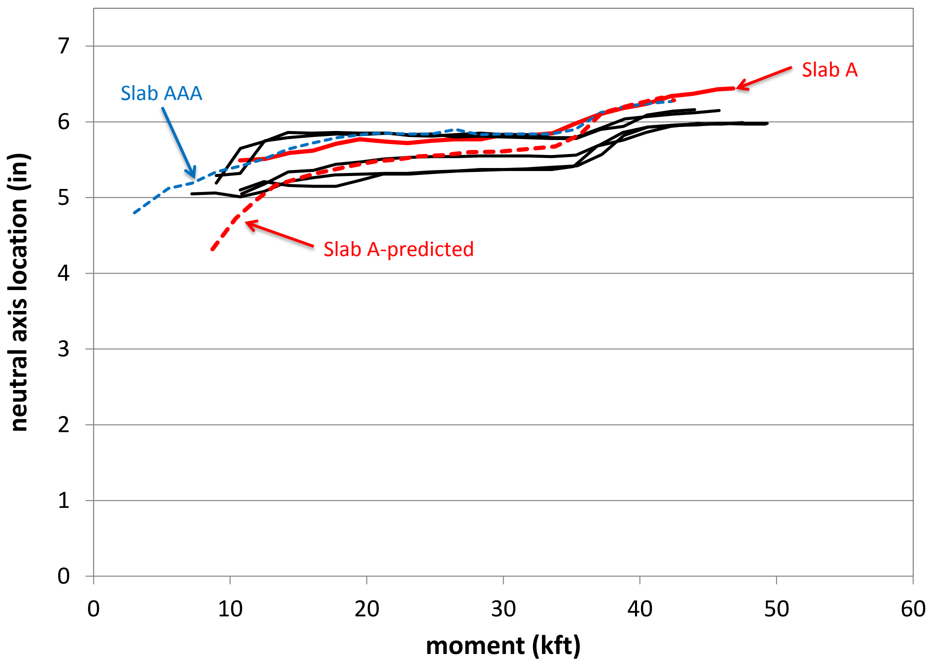

Figure 31: Post-cracking-height of neutral axis vs. moment of laboratory slabs.

3.3.2 Strain Profiles

The strain profiles presented in Figures 19-28 did not exhibit any apparent discontinuity associated with the LMC interface. Full composite behavior – no different from that of a monolithic slab – was observed in all cases. With the exception of when cracking patterns altered strain profiles (see Figure 18), all specimens had a linear strain response through the interface region, indicating no relative movement (slip) between the LMC and concrete substrate.

3.3.3 Crack Patterns

Composite action was also assessed qualitatively by evaluating crack propagation. Flexural cracks propagated upward from the soffit, through the interface, to the neutral axis. If continuity at the interface was not established, one would expect the cracks to be diverted at the interface (analogous to light refracting in water) rather than remain on the same trajectory. In all Figures 19-28 d and e, the cracks are uniformly observed to be unaffected by the presence of the interface.

3.3.4 Stresses at LMC Interface

As discussed earlier, the objective of this study was to establish whether or not composite action was achieved between the substrate and LMC overlay. At the crux of this issue is what magnitude of shear stress is transmitted across the interface. For a homogeneous elastic material, the transverse shear stress is calculated as VAy/It where V = internal shear; A = area of material above interface; y = distance from centroid of A to centroid of gross section; I = moment of inertia of gross section; and, t = width of cross-section at the interface. While this calculation may be valid prior to cracking, it may not be used once the concrete is cracked since A, y and I all vary and the material may no longer be considered elastic. For cracked concrete, the shear carried across the interface is that required to equilibrate the tension-compression couple developed between the reinforcing steel and compression block concrete. Therefore, for an under-reinforced section controlled by reinforcing steel yield, the maximum value of shear that must be transmitted is $T = A_s f_y$. This is resisted at the section at the top of the tension zone by the area of concrete in the shear span; i.e.; the slab width by half the span (*b x L/2*). This is shown schematically in Figure 32.

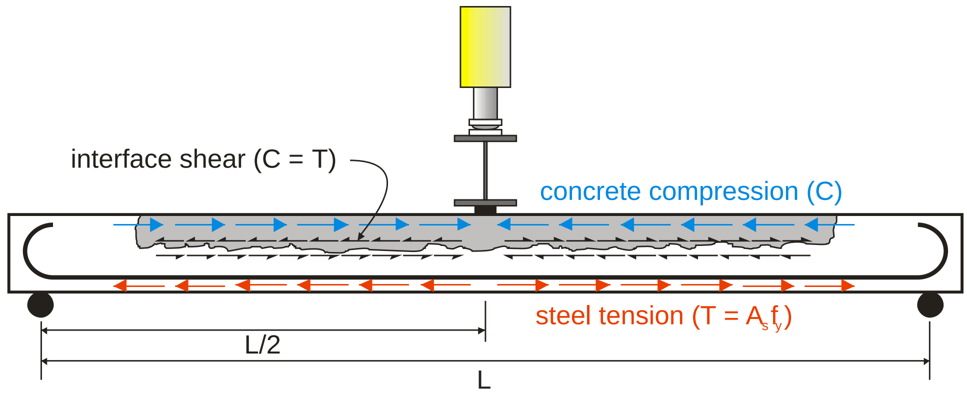

Figure 32: Shear forces at interface of laboratory slabs.

For the laboratory-cast slabs considered in this study, the shear that must be transmitted is developed by the yield of the 4 #5 longitudinal bars:

$T = A_s f_y$ = 4(0.31 in^2)(67.8 ksi) = 84 kips (374 kN)

This is resisted over the horizontal area of the concrete in the shear span:

$A_c = b(L/2)$ = 22 in. x 84 in./2 = 924 in^2 (5.96 x 10^5 mm^2)

Resulting in an interfacial shear stress of 84 kips/924 in^2 = 91 psi. (0.63 MPa).

The concrete shear resistance along a match-cast interface was discussed in Section 1.3.2 and a number of values given in Table 1. For the LMC interfaces in this study, the 'implied aggregate interlock capacity' (Table 1) ranges from 240 psi (1.66 MPa) (AASHTO 2010) to 390 psi (2.69 MPa) (Harries et al. 2012). Similarly, suggested minimum interface tension strengths range from 100 psi (0.689 MPa) (Wenzlick 2002) to 200 psi (1.38 MPa) (Basham 2004), where these values are considered to be at most one half of the shear capacity (Silfwerbrand 2009). As reported in Chapter 4, the average pull-off strength achieved for the laboratory slabs having LMC exceeded 300 psi (2.07 MPa) and the direct tension capacity of Slab A was found to be 373 psi (2.58 MPa). Therefore, by any measure, the shear stress required to yield the reinforcing steel in the laboratory slabs (91 psi (0.63 MPa)) is considerably less than the anticipated (or indirectly measured) capacity of the interface.

Another way of looking at the shear transfer is to consider the maximum reinforcing bar tension force (*T*) that could be resisted by the slab. Considering the AASHTO-implied lowest value of interface shear resistance, 240 psi (1.66 MPa), the slab longitudinal tensile reinforcement ratio, $\rho = A_s/hb$ would have to be increased from the existing value of 0.0075 to almost 0.02 before interface stresses approached the implied capacity. Such a heavily reinforced slab (equivalent to #5 bars at 2 in. (50 mm) or approximately #8 bars at 5.5 in. (140 mm) in a 7.5 in. (190 mm) deep slab) is unlikely for a bridge deck. Nonetheless, this line of enquiry does identify older heavily reinforced 'slab bridges' having no shear reinforcement as poor candidates for overlay repair since the interface stresses may be higher.

3.3.5 Effect of Varying Concrete and LMC Strengths

Good practice dictates that the LMC overlay should be designed to closely match the material properties of the substrate concrete (Silfwerbrand 2009). For the laboratory slabs reported in this study, the compressive strengths at the time of testing of the LMC and substrate concrete differed by less than 100 psi (0.69 MPa) – less than 1.5% of the compressive strength (Table 7).

Using the same RESPONSE model presented previously, a parametric study was conducted in which all parameters but LMC and substrate concrete strength were maintained constant. The model was generated using the cross-sectional geometry of the laboratory slabs with the LMC interface located at the slab mid depth (3.75 in. (95 mm)) thereby ensuring the LMC constituted the entire compression zone even prior to cracking. The LMC and substrate concrete strengths were combined in every combination from 3000 to 8000 psi in 1000 psi increments (20.7 to 55.2 MPa in 6.9 MPa increments).

As should be expected for under-reinforced slabs, varying the concrete strength between the overlay and substrate had very little effect on yield or ultimate capacity. Yield moments varied by a maximum of only 3% and ultimate moments by 7%, for all combinations tested. Ultimate moments were improved as substrate concrete strength was increased, but exhibited no similar trend as a result of the increase of overlay strength. This result reflects the under-reinforced nature of the slabs being governed by the steel tension response and the fact that the effects of tension-stiffening were included in the model (Bentz 2000). The results of the analytical model are also supported by the experimental results of the Marshall Ave. slabs (Appendix C), where altering LMC and substrate compressive strengths had no noticeable detrimental effects on slab behavior.

4 PULL-OFF TESTS

A pull-off testing program was conducted on both laboratory specimens and field cut specimens (Marshall Ave. Specimens). The laboratory specimens' results are presented in this chapter, while the Marshall Ave. specimen results are presented in Appendix C.

4.1 EXPERIMENTAL PROGRAM

A series of standard ASTM C1583 pull-off tests using 50 mm (1.97 in.) diameter disks (dolly) were conducted on the overlaid slabs following flexural testing to determine bond strength and performance. The test procedure consisted of a) wet cutting a circular hole using a 2 in. (51 mm) diameter core barrel in order to isolate the pull-off specimen (Figure 33a); b) surface preparation and adhesion of a 50 mm (1.97 in.) diameter aluminum dolly to the surface by means of a two-part epoxy; and c) applying direct tensile loading to the sample until failure. A Dyna Z-15 test apparatus, shown in Figure 33b, was used for this test. The cut used to isolate the test specimen was extended 0.5 in. (13 mm) beyond the substrate-overlay interface, into the substrate concrete, for all tests.

a) core drill set-up

b) Dyna Z-15 test apparatus

Figure 33: Set-up for pull-off testing.

Due to the nature of the pull-off tests, a number of different failure modes can result; these are described as follows:

Failure Mode A: adhesive failure in which the dolly comes off the overlay surface. While this is a 'bad test' in the sense that it does not provide a measure of interface capacity, such a failure may still be interpreted as a 'lower bound' capacity of the overlay-substrate system. In some cases, such failures may be retested, although specific note of this must be made since the initial test may affect subsequent failure loads.

Failure Mode L: cohesive tensile failure in the overlay LMC.

Failure Mode S: cohesive tensile failure in the substrate concrete.

Failure Mode I: failure at the overlay-substrate interface. For a failure to be described as being a 'perfect adhesive failure'; the exposed surface on the dolly is 100% overlay, while the exposed surface left in the core hole is 100% substrate. Typically, a Mode I failure will follow a tortuous path along the interface. By convention, the failure will be described in terms of the proportion of overlay material found on the dolly, *%LMC*. The proportion of concrete on the dolly is then 1-*%LMC*. The proportions in the core hole will be inverted. The LMC and substrate have a different appearance: the substrate contains larger coarse aggregate (see Figure 34e) and the LMC is slightly green in color (Figures 34a and b); therefore assessing these proportions is not terribly difficult. Wetting the sample can help to differentiate the surfaces of a mode I failure. Representative failures are shown in Figure 34.

a) failure mode I having *%LMC* ≈ 50%.

b) failure mode I having *%LMC* ≈ 50%. Poor bond or void at interface of LMC is evident near center of specimen.

c) failure mode S – failure is entirely in substrate; fractured aggregate is evident indicating that this failure is ***not*** an I failure with *%LMC* = 0%.

d) failure mode L – failure is entirely in overlay as evident by fracture of small aggregate.

e) core hole following test (Slab B, test 20) clearly showing interface region delineated by small aggregate in LMC and large aggregate in substrate concrete. Failure is mode S, well below the interface level at the bottom of the cored hole.

Figure 34: Representative failure modes.

4.2 RESULTS

Results of the entire pull-off test program are reported in Appendix B. A summary of pull-off test results organized by depth of LMC application is presented in Table 10. Table 10 also contains 7- and 28-day tests of the LMC-substrate bond made on Slab B, having an average LMC depth of 1.2 in. (30 mm) With the exception of these, all tests were conducted at a time at which the substrate concrete age exceeded 132 days and the LMC age exceeded 52 days. Finally, tests on slabs A, G, and AAA were attempted to assess the tensile strength of the substrate, LMC, and AAA overlay respectively. Values reported in Table 10 exclude Mode A failures unless otherwise noted.

Table 10: Summary of pull-off test results.

Slab	Overlay depth (in.)	n	f_t (psi)	COV	Notes
B	1.2	3	216	0.19	7-day tests
B	1.2	2	523	0.01	28-day tests
B	1.2	4	373	0.09	28-day tests having Mode A failure (lower bound results)
tests conducted following flexure tests (substrate age > 132 days; LMC age > 52 days)					
B	1.2	3	254	0.20	
C	2.1	5	368	0.18	
D	2.5	4	332	0.15	Mode S and I failures
D	2.5	6	367	0.20	includes Mode A (lower bound) failures
E	2.6	5	291	0.32	
F	3.5	4	288	0.15	Mode L and I failures
F	3.5	8	340	0.20	includes Mode A (lower bound) failures
G	3.8	4	244	0.18	
AAA	3.7	5	221	0.27	Mode I failures
direct tension tests without interface					
A	NA	3	373	0.06	substrate concrete direct tension tests
G	NA	4	373	0.18	LMC overlay direct tension tests; initial Mode A failures
G	NA	2	448	0.08	LMC overlay direct tension tests; Mode L retests
AAA	NA	3	373	0.08	AAA overlay direct tension tests

4.3 DISCUSSION

In general, the results shown in Table 10 conform to expectations for the pull-off tests and no major issues were found with the LMC-substrate concrete bond which is generally classified as being quite good. With the exception of the 7-day and 28-day tests on slab B, all pull-off tests were conducted after the flexural tests were completed. Although all pull-off tests were made near the slab ends which should be relatively undamaged, the possibility of damage resulting from the flexural tests negatively impacting the pull-off test results cannot be discounted. This might explain several seemingly anomalous results; for instance, the post-flexural test results for slab B (254 psi (1.75 MPa)) were significantly lower than the 28-day tests (523 psi (3.61 MPa). Additionally, variation of test results fell well within what can be expected for a standard pull-off test.

Figure 35 shows the relationship between the pull-off capacity, f_t, and the depth of the LMC overlay. This data includes all samples with failure Modes S, L, and I from slabs B, C, D, E, F, and G, along with the substrate concrete tensile tests from slab A. The dashed line in the figure indicates the assumed 320 psi

(2.21 MPa) tensile strength of the substrate concrete. The average pull-off tensile strength for the substrate concrete was 373 psi (2.57 MPa) ($4.6\sqrt{f_c'}$) which falls within the 320-400 psi (2.21-2.76 MPa) range predicted based on split cylinder and modulus of rupture tests (see Section 3.1.4.1). All but two tests exceed the 200 psi threshold recommended by Basham (2004) and all easily exceed the 100 psi (0.69 MPa) threshold recommended by Wenzlick (2002) as acceptance criteria for overlay-to-substrate tensile bond capacity. As can be seen in Figure 35, there appears to be no correlation between pull-off strength and the depth of the LMC overlay. All of the results are distributed around the tensile capacity of the substrate concrete. Thus, the data suggests that there is a sound bond between the substrate concrete and the LMC overlay over the range of depths of overlay investigated in this study.

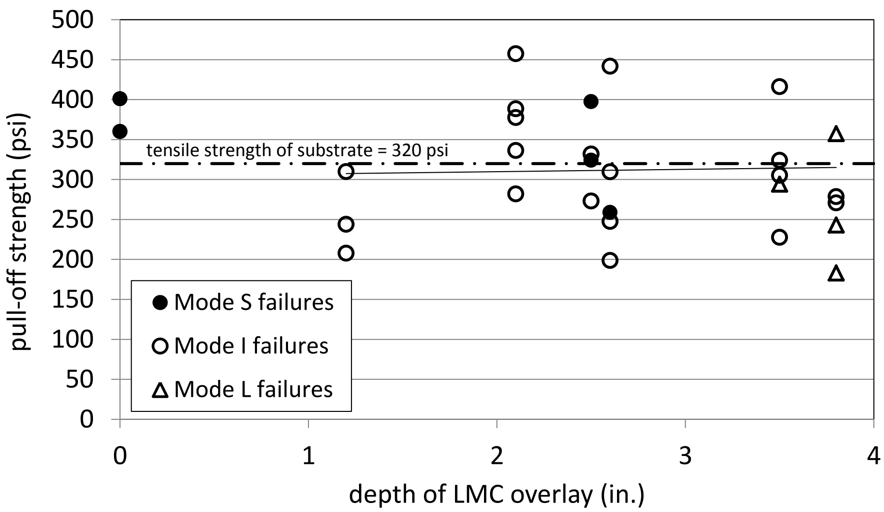

Figure 35: Results of pull-off strength tests vs. depth of LMC overlay.

Slab B, having the thinnest overlay and some evidence of overlay separation in the final failure (see Figure 20f), was selected for further investigation. Additional pull-off tests were conducted to determine pull-off strength along the span of the slab: from the undamaged support region to the heavily damaged midspan. Figure 36a shows the location of each test on the slab. In the figure, the first number listed is the test number, and the number in parentheses is the pull-off strength in psi (average values are reported for the 7-day tests and tests 10-12; see Appendix B for complete test data). Figure 36b plots the pull-off strengths for tests 10-20 versus their location along the span. Clearly, the pull-off strength decreases as the test locations approach the heavily damaged midspan region. Nonetheless, the poor pull-off results near midspan tend to be Mode S failures (Figure 36b), indicating that the damage is concentrating below the interface in the substrate corresponding with the location of the neutral axis (see Figure 20c). While these results indicate that the interface region has been damaged as a result of the compression failure of the slab, the damage is not preferentially located along the interface. This behavior is in contrast to that has been observed by Cole et al. (2002), shown in Figure 3. Finally, it is noted, that the applied load to cause failure of Slab B was approximately 2.6 times that of the STRENGTH I design requirement.

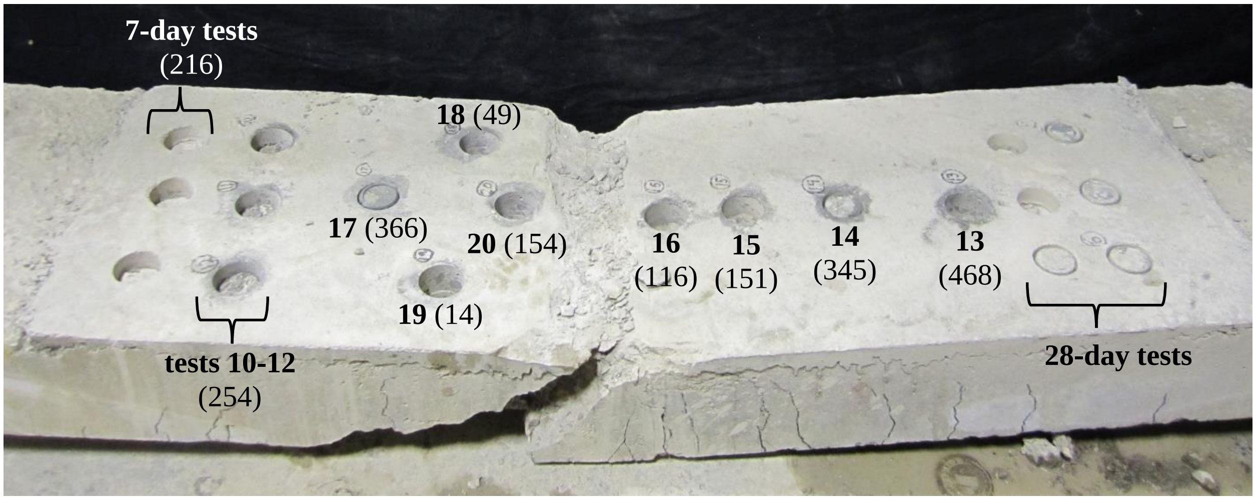

a) layout of Slab B tests (numbers indicate: **test number** (pull-off strength in psi))

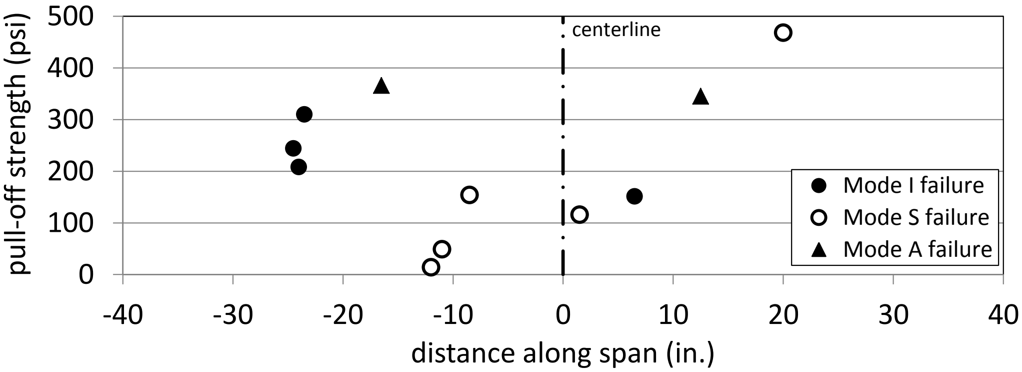

b) Pull-off strength vs. distance from support for Slab B tests

Figure 36: Pull-off strength results from Slab B.

Although the LMC slabs did not indicate any issues with the bond between the LMC overlay and the substrate concrete, interface issues were identified for slab AAA, having an AAA overlay. The five pull-off tests listed for slab AAA in Table 10 were all Mode I failures having an average pull-off strength of 221 psi (1.53 MPa), with no single test exceeding 271 psi (1.87 MPa). These values are significantly lower than the tensile pull-off strength of either the substrate concrete or the AAA overlay (both measured to be 373 psi (2.57 MPa)). Such results suggest that there was an issue with the bond between the AAA overlay and the substrate concrete and the bond capacity is not comparable to the tensile strength. These interface bond issues can be seen visually; several of the failure planes contained voids, indicating that there was incomplete bond between the two layers (see Figure 37). Such voids were not present in samples from LMC-substrate interface failures.

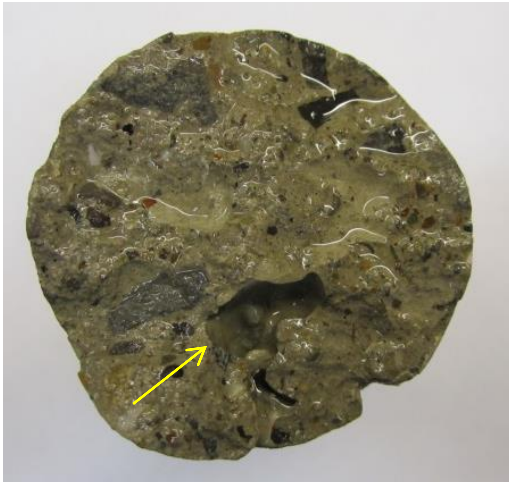

a) slab AAA, test 3

b) slab AAA, test 5

Figure 37: Slab AAA samples containing voids in failure plane.

5 RECOMMENDATIONS AND CONCLUSIONS

The primary objective of this study was to assess the validity of *PennDOT Publication 15 Section 5.5.5.1*, specifically that "a latex overlay is not considered structurally effective", in terms of the structural response of the bridge superstructure. Experimental evidence from this study clearly demonstrates that the LMC overlay is structurally effective in terms of load carrying capacity. Several parameters were varied amongst test specimens in the experimental program: overlay depth, removal of concrete 'shadows' under primary reinforcement bars, and the direction of bending (positive and negative moments). The LMC-repaired slabs acted as monolithic slabs in all cases – laboratory slabs and decommissioned Marshall Ave. slabs – and the capacity was uniform regardless of LMC depth. The capacity of the LMC-repaired slabs tested in positive flexure exceeded their predicted ultimate capacities in all cases. Additionally, the LMC-repaired slab capacity exceeded the ultimate capacity of the control slab in all cases. Finally, it was demonstrated based on fundamental mechanics and shear friction theory that LMC interface stresses are relatively low and unlikely to exceed reasonable values of capacity for properly constructed LMC overlay repairs. Therefore the following revisions are proposed relative to PennDOT *Publication 15*:

PennDOT *Pub. 15M*-Section 5.5.5.1 Superstructures –Current (May 2012)	**Proposed Revisions**
"Minimum load carrying capacity for rehabilitated bridges shall be same as for new design using LRFD/DM-4 method. Analysis should include 0.030 ksf for future wearing surface. A latex overlay is not considered structurally effective. Special approval of the Chief Bridge Engineer is required for any deviation."	"Minimum load carrying capacity for rehabilitated bridges shall be same as for new design using LRFD/DM-4 method. Analysis should include 0.030 ksf for future wearing surface. ~~A latex overlay is not considered structurally effective.~~ <u>A latex overlay shall be considered structurally effective, provided the overlay is deeper than 1.25 inches</u>. Special approval of the Chief Bridge Engineer is required for any deviation."

The proposed revision assumes that the overlay in question has been constructed to an appropriate standard using 'best practices'. PennDOT Publication 408-Sections 1040, 1041 and 1042 provide guidance on the overlay construction practices. Based on this study the following revisions and additions are proposed to PennDOT *Publication 408*:

PennDOT *Pub. 408* –Current (April 2011)	Proposed Revisions
1040.3 CONSTRUCTION (c) Equipment. Power driven hand tools for removal of deteriorated concrete are required and are subject to the following restrictions: Do not use pneumatic hammers with more weight than nominal 30-pound class. Do not operate pneumatic hammers or mechanical chipping tools at an angle in excess of 45 degrees relative to the surface of slab. Do not place pneumatic tools in direct contact with reinforcing steel. Triple-headed tampers fitted with star drills not less than 2 inches in diameter in the tamper sockets may be used in the vertical position. Use hand tools such as hammers and chisels, or small air chisels to remove final particles of unsound concrete or to provide necessary clearances around reinforcement bars.	1040.3 CONSTRUCTION (c) Equipment. 1. Removal of Deteriorated Concrete. Of the following types, hydrodemolition methods are preferred: 1.a Water Blasting (Hydrodemolition) Equipment. Capable of removing partially loosened chips of concrete and removing rust and corrosion from reinforcement bars. Water blasting equipment must have a minimum rated capacity of 4,000 pounds per square inch. 1.b Power driven hand tools for removal of deteriorated concrete are ~~required and are~~ permitted subject to the following restrictions: Do not use pneumatic hammers with more weight than nominal 30-pound class. Do not operate pneumatic hammers or mechanical chipping tools at an angle in excess of 45 degrees relative to the surface of slab. Do not place pneumatic tools in direct contact with reinforcing steel. Triple-headed tampers fitted with star drills not less than 2 inches in diameter in the tamper sockets may be used in the vertical position. Use hand tools such as hammers and chisels, or small air chisels to remove final particles of unsound concrete or to provide necessary clearances around reinforcement bars.
1042.3 CONSTRUCTION (f) 3. QC and Acceptance Testing	*add new section as follows:* 3.c Pull-Off Tests. Pull-off tests *should* be conducted on a representative number of samples, in accordance with ASTM C1583. The Inspector will select acceptance samples (n=1) according to PTM No. 1. When reporting values, both a failure strength and a failure mode must be reported for each individual sample. Acceptance criteria is determined at the owner’s discretion.

In addition to the proposed revisions to *Publications 15* and *408*, a number of additional conclusions were drawn from this study:

- The anticipated capacity of an LMC overlaid deck may be estimated as that of the original full-depth deck. Experimental capacities were seen to exceed this value in all cases. Simple plane sections analyses of either the original full-depth deck or LMC-repaired deck are suitable for obtaining these capacities.
- The LMC interface has essentially no impact on the behavior of the repaired slabs. No evidence of 'buckling' or slip failure was observed. No evidence of the interface affecting crack propagation was observed.
- The interface shear capacity is expected to exceed the demand for bridge slabs typical of slab-on-girder bridges. Nonetheless, older heavily reinforced 'slab bridges' having no shear reinforcement are believed to be poor candidates for overlay repair since the interface stresses may be higher. In such cases, an interface analysis as described in Section 3.3.4 should be conducted.

This study has demonstrated the effectiveness of PennDOT Method 2 LMC overlays for Type 1 and 2 bridge deck repairs. The LMC clearly contributes to the load carrying capacity of the rehabilitated deck slab. With this conclusion, it is envisioned that more bridges that would otherwise be subject to complete deck replacement may be viable candidates for overlay repair. This, it is believed, will conserve resources directed to an individual bridge and significantly speed the deck rehabilitation process.

5.1 SUMMARY OF BEST CONSTRUCTION PRACTICES

The proposed revisions to *Publication 15* are made with the recommendation that several other parameters be followed in order to ensure a quality LMC overlay repair:

Best construction practices, described at length in the literature review, are followed. Briefly these include:

- Attention should be given to the surface condition of interface before placement of the overlay. This includes proper moisture conditioning and cleaning all debris and laitance from the interface. Cleanliness of the interface was mentioned in numerous works as being one of the more critical issues that control overlay performance.
- Although no effect of having concrete 'shadows' below the bars were observed in Slab F*, it is nonetheless recommended that all shadows, were they occur, be removed.
- Like all concrete construction, care should be taken in the placement process to avoid segregation. At the same time compaction should allow for all air voids to be filled without causing segregation.
- LMC overlays should be allowed to cure for an appropriate length of time and under the recommended conditions.
- Available literature and anecdotal evidence suggests that hydrodemolition is the preferred method of concrete removal, although alternative methods of concrete removal (pneumatic hammers) were not assessed in this study.

5.2 PULL-OFF TESTING

It is recommended that a pull-off testing program be establish for quality assurance purposes in accordance with ASTM C1583. A similar program was presented in Chapter 4.

The table below highlights best practices regarding the direct tension pull-off test, as used to determine bond strength and/or tensile strength of a concrete substrate-overlay system. The best practices are presented as a commentary on *ASTM C1583 Standard Test Method for Tensile Strength of Concrete Surfaces and the Bond Strength or Tensile Strength of Concrete Repair and Overlay Materials by Direct Tension (Pull-off Method)*. Only sections of ASTM C1583 on which comments are made are presented.

ASTM C1583	Commentary
6. Apparatus	
6.1 *Core Drill*, for prepping test specimen.	A wet cutting drill is recommended.
6.2 *Core Barrel*, with diamond impregnated bits – nominally 50 mm [2.0 in.] inside diameter.	While a 2 in. [50 mm] inside diameter barrel is preferred, other diameter drill barrels are acceptable, so long as barrel size and disk size match as closely as possible. Cores smaller than 2 in. [50 mm] are not recommended.
6.3 *Steel Disk*, nominally 50 mm [2.0 in.] diameter and at least 25 mm [1.0 in.] thick.	Either steel or aluminum disks (dollies) are acceptable (ASTM D7522, ICRI 2004). Disk thickness must exceed one-half disk diameter (ICRI 2004). Disk must be as close in size to drilled core as possible, but never larger.
6.4 *Tensile Loading Device*, with a load-indicating system and nominal capacity of 22 kN [5,000 lbf] and capable of applying load at the specified rate. The loading device includes a tripod or bearing ring for distributing the force to the supporting surface.	Although the standard does not specify, a device similar to Dyna Z15 (having tripod reaction legs) is recommended. (see Appendix A of ASTM D7522 for schematic). The 22 kN capacity is not critical provided the loading device has the capacity to conduct the test; the Dyna Z15, for example has a capacity of only 16 kN [3600 lbf]. Benefits of this device are that it is "small, mobile (for use in any location), allows assurance that the pull-off takes place at right angles, and allows for jerk-free increases in load" (Vaysburd 1999). Testing device types B-F, presented in ASTM D4541, are not recommended for concrete applications of pull-off testing on highway bridges. Bearing ring testers require a flat even surface which may require additional grinding of the surface around the core on bridge decks. Additionally, tined deck surfaces can affect the operation of automated bearing ring testers.

ASTM C1583	Commentary
6.4.2 A coupling device shall be used to connect the steel disk to the tensile loading device. The coupling device shall be designed to withstand the tensile load capacity without yielding, and to transmit the tensile force parallel to and in line with the axis of the cylindrical test specimen without imparting torsion or bending to the test specimen.	The coupling device is typically a component of a commercial test device.
7. Materials 7.1 Epoxy adhesive material for bonding the steel disk to the test specimen. It shall be a fast-curing paste or gel meeting the requirements of Specification C881/C881M for Type IV, Grade 3, except that a shorter gel time is permitted.	A two-part epoxy adhesive works very well for this test. Loctite® 21425 Fast Cure Epoxy has been used extensively and successfully by the research team.
8. Sampling 8.2 The field test site shall be large enough so that all methods to be used in the full-scale repair or overlay operation, including surface preparation, are used for preparing test specimens. The test site shall be at least 1 m by 1 m [3 ft. by 3 ft.]. It shall be selected to be representative of actual field conditions. 8.3 If concrete cover is less than 20 mm [3/4 in.], do not locate test specimens directly over bars in the layer of reinforcement nearest to the surface.	It is important to select individual test locations within the test site that do not have excessive surface roughness, so as to minimize adhesive failures. Under no circumstances should the top of the specimen receive any mechanical treatment (grinding ,etc.) (Austin et al. 1995). It is recommended that whenever practicable, testing over reinforcing steel should be avoided. Often overlay interfaces are below the reinforcing bar layer, in which case tests must be conducted in such a manner to avoid all reinforcing steel.
10. Preparation of Test Specimen 10.1 Using the coring equipment, drill a circular cut perpendicular to the surface. For tests of substrate concrete, drill to a depth of at least 10 mm [0.5 in.]. For tests if repair or overlay materials, drill to at least 10 mm [0.5 in.] below the concrete-overlay interface. The test specimen is left intact, attached to the substrate. Measure the diameter of the test specimen in two directions at right angles to each other. Record the average diameter to the nearest 0.2 mm [0.01 in.]	Achieving the proper drilling depth is one of the most critical aspects of the testing procedure. The value of 0.5 in. [10 mm] cited in the standard is a minimum; it may be advisable to drill deeper. ICRI (2004) recommends drilling at least 1 in. [25 mm] or half the disk diameter (whichever is greater) into the underlying concrete substrate. Vaysburd (1999) also recommends a cut depth of 1 in. [25 mm] into the substrate, and notes that shallower cuts may increase stress concentrations at the bond interface. It is very important to have the drill securely fixed to the drilling surface. Any disturbances could cause damage to the test area, including premature core during drilling.

ASTM C1583	Commentary
10.2 Remove any standing water; clean the surface of any debris from the drilling operation and allow to dry.	Compressed air or water can be very effective for cleaning test surface in preparation of applying disk. It is important to avoid excessive mechanical action (such as grinding) as a means of site preparation (Austin et al. 1995).
10.3 Attach the steel disk to the top of the test specimen using the epoxy adhesive. Ensure that the disk is centered with the test specimen and that the axis of the disk is parallel to the axis of the test specimen. Cure the epoxy adhesive following manufacturer's instructions. Do not allow the adhesive to run down the side of the test specimen into the annular cut; if this occurs, the specimen is not tested and another is prepared. At temperatures below 20°C [70°F], it is permitted to gently heat the steel disk to no more than 50°C [120°F] to facilitate spreading of the adhesive and to accelerate curing. The test specimen shall not be heated with a direct flame.	Be sure to apply adhesive to both the concrete surface and the disk (with more adhesive usually required on the concrete surface than the disk). Nonetheless, the amount of adhesive used should result in the thinnest adhesive line possible considering the roughness of the specimen surface. It is critical to avoid twisting while attaching disk to sample (ASTM D4541, D7234) as this may affect adhesive performance. When applying disk to a vertical or overhead surface, disk must be held firmly in place for a sufficient amount of time to allow the adhesive to have an initial cure and to ensure there is no subsequent creep or movement. It is crucial to allow the adhesive adequate time to cure. Heating the disk can marginally increase the rate of initial cure.
11. Test Procedure	
11.2 Apply the tensile load to the test specimen so that the force is parallel to and coincident with the axis of the specimen.	Any deviation from perpendicularity can induce moment in the sample and cause premature failure. As mentioned previously, the recommended Dyna Z15 testing device, or similar tripod-based devices, can greatly help to avoid this issue.
11.3 Apply the tensile load at a constant rate so that the tensile stress increases at a rate of 35 ± 15 kPa/s [5 ± 2 psi/s].	Appropriate rate of loading is very important; similar rates are recommended by many sources (ASTM D7522, ICRI 2004, Vaysburd 1999, Austin et al. 1995). This rate of application should be maintained until failure is observed. It is important to avoid ending the test too early. Upon failure, there will typically be a "popping" sound. However, such sounds can sometimes occur earlier in the test, due to mechanical realignment within the test set-up. Automated test devices often mistake these events as specimen failure. Bearing ring devices are particularly susceptible to realignment during testing as the bearing stresses redistribute around the ring. After failure is believed to have occurred, the loading rate should be maintained for several seconds to ensure

ASTM C1583	Commentary
	that failure has indeed occurred (the machine should read "0" load). For these reasons, it may be preferable to use a testing device with a manual rate of load application, rather than an automatic device. Such automatic devices will occasionally record failure prematurely.
11.4 Record the failure load and the failure mode. Record the failure mode as *(a)* in the substrate, *(b)* at the bond line between the substrate and the repair or overlay material, *(c)* in the repair or overlay material, or *(d)* at the bond line between the repair or overlay material and the epoxy adhesive used to bond the steel disk. If failure occurs at the bond line between the steel disk and epoxy adhesive, discard the test result and perform another test.	Due to the nature of the pull-off tests, a number of different failure modes can result; these may be conventionally described as follows: *Failure Mode A*: adhesive failure in which the dolly comes off the overlay surface. While this is a 'bad test' in the sense that it does not provide a measure of interface capacity, such a failure may still be interpreted as a 'lower bound' capacity of the overlay-substrate system. *Failure Mode O*: cohesive failure in the overlay. *Failure Mode S*: cohesive failure in the substrate. *Failure Mode I*: failure at the overlay-substrate interface. For a failure to be described as being a 'perfect adhesive failure'; the exposed surface on the dolly is 100% overlay, while the exposed surface left in the core hole is 100% substrate. Typically, a Mode I failure will follow a tortuous path along the interface. By convention, the failure will be described in terms of the proportion of overlay material found on the dolly. Although the standard appears to permit retesting tests of Mode A failures, it is required to explicitly note such retests in any report. The initial adhesive failure may have resulted in damage to the sample.

5.2.1 Acceptance Criteria for Pull-off Testing

Acceptance criteria in both the available literature and test guidance for pull-off testing fall between 100 and 200 psi (0.70 to 1.4 MPa). Values observed in this study averaged 373 psi (2.57 MPa) for the laboratory specimens (Chapter 4), 285 psi (1.97 MPa) for the Marshall Ave slabs (Appendix C), and from 202 psi (1.40 MPa) and 348 psi (2.43 MPa) for *in situ* tests as part of this study (Table 4).

If the pull-off strength exceeds 200 psi, it is believed that the interface shear capacity will be adequate and the overlay will behave in a fully composite manner with the substrate concrete. For pull-off capacities less than 200 psi, the mode of failure is telling. If the failure remains in the substrate (Mode S), the interface is stronger than the substrate and the shear capacity is at least that of the residual substrate concrete. In such a case, composite behavior of the overlay is likely. Pull-off tests indicating an interface failure (Mode I) are cause for further investigation. Pull-off tests less than 100 psi, regardless of failure mode should not be accepted.

5.3 AREAS OF FURTHER STUDY

5.3.1 Performance of LMC Materials

There a number of recent developments in LMC materials aimed at providing faster construction of LMC overlays and reducing the susceptibility of LMC to exhibit plastic shrinkage cracks. These include the development of 'very-early strength' LMC (Sprinkel 1988) and the introduction of chopped glass and/or carbon fibers into the LMC mix design (Issa et al. 2007). Ohama (2001) has also proposed and demonstrated the concept of 'self-repairing' epoxy-modified mortar. Validating the use of these improved LMC materials – particularly in the relative harsh environment (freeze-thaw, chloride exposure, etc.) of Pennsylvania – may extend further the expected life of bridge decks having LMC overlays. Based on extant research, it is believed that an overlay may be fabricated that can be opened to traffic in as little as three hours (Sprinkel 1998) while also exhibiting less plastic shrinkage than conventional LMC overlays.

5.3.2 Substrate Preparation

A number of studies (and subsequently, construction specifications) have suggested that vibration during slab demolition should be limited; therefore hydrodemolition, augmented by light hand tools, is the preferred method for such partial slab demolition. These conclusions are based on limiting microcracking in the substrate concrete. However, most studies have been conducted on 'laboratory specimens' which neglects the existing damage and deterioration of the slab due to its years in service. Additional study of the effects of demolition practices using decommissioned slabs is warranted. Such a study could also better establish the decision threshold between full-depth (Type 3) and partial depth (Type 2) repairs.

5.3.3 Fatigue Performance of LMC Overlays

Although limited study (Silfwerbrand 2009; Cole et al. 2002) is available on the low-cycle fatigue performance of LMC overlaid slabs, there are no known studies addressing more realistic high cycle fatigue loads. In bridge engineering and research practice, high cycle fatigue load protocols typically consider 100% of the design transient service load applied for (at least) two million cycles; this protocol is argued to represent 75 years in service (Appendix E of Shahrooz et al. 2011). The present study (and others) has clearly indicated that the monotonic strength of an LMC overlaid slab is at least that of the original slab and there appears to be no deterioration of the bond between LMC and substrate concrete. The question remains, however: *how does the LMC-concrete interface perform under repeated (fatigue) loads?* The research team has maintained four test slabs in reserve in order to address this question.

It is proposed to test the remaining four slabs leveraging the already-reported monotonic specimens as 'control' slabs in each case. The fatigue test slabs will be designated FA: control slab having no overlay and FB, FD and FF having overlay depths of 1.25, 2.5 and 3.5 inches, respectively. The monotonic 'control' slabs for these are then Slabs A, B, D and F, respectively. The fatigue protocol will consist of 2 million cycles of applied load resulting in the slab moment ranging from 0.75 kipft/ft to 5.69 kipft/ft as described in Section 3.1.6. Following this fatigue regime – assuming that the slab has not failed – the slab will be tested monotonically to failure in a manner identical to the control slabs presented in this report. From this study, either the anticipated fatigue life, or the residual capacity following fatigue conditioning may be established for LMC-overlaid slabs.

REFERENCES

ACI Committee 318 (2011). *Building Code Requirements for Structural Concrete (ACI318-11) and Commentary (ACI 318R-11)*. Farmington Hills, MI, American Concrete Institute.

ACI Committee 548 (2011). *Specification for Latex-Modified Concrete Overlays (ACI548.4-11)*. Farmington Hills, MI, American Concrete Institute.

ACI Committee 548 (2009). *Report on Polymer-Modified Concrete (ACI548.3R-09)*. Farmington Hills, MI, American Concrete Institute.

ACI Committee 546 (2004) *Concrete Repair Guide*. Farmington Hills, MI, American Concrete Institute.

Alhassan, M. A. and Issa, M. A. (2010) Long-term Protection of Bridge-deck Systems with Structural Latex-Modified Concrete Overlays. *PCI Journal*, 122-137.

American Association of State Highway and Transportation Officials (AASHTO) (2010). *AASHTO LRFD Bridge Design Specifications*, 5th edition.

American Society for Testing and Materials (ASTM) (2009). *D4541-09 Standard Test Method for Pull-Off Strength of Coatings Using Portable Adhesion Testers*. ASTM, West Conshohocken, PA.

American Society for Testing and Materials (ASTM) (2009). *D7522-09 Standard Test Method for Pull-Off Strength for FRP Bonded to Concrete Substrate*. ASTM, West Conshohocken, PA.

American Society for Testing and Materials (ASTM) (2010). *C881-10 Standard Specification for Epoxy-Resin-Base Bonding Systems for Concrete*. ASTM, West Conshohocken, PA.

American Society for Testing and Materials (ASTM) (2012). *D7234-12 Standard Test Method for Pull-Off Adhesion Strength of Coatings on Concrete Using Portable Pull-Off Adhesion Testers*. ASTM, West Conshohocken, PA.

ASTM International (2013). *C1583-13 Standard Test Method for Tensile Strength of Concrete Surfaces and the Bond Strength or Tensile Strength of Concrete Repair and Overlay Materials by Direct Tension (Pull-off Method)*. ASTM, West Conshohocken, PA.

ASTM International (2013) *C42-13 Standard Test Method for Obtaining and Testing Drilled Cores and Sawed Beams of Concrete*, West Conshohocken, PA. 7 pp.

ASTM International (2012) *C39-12 Standard Test Method for Compressive Strength of Cylindrical Concrete Specimens*, West Conshohocken, PA. 7 pp.

ASTM International (2012) *C1152-12 Standard Test Method for Acid-Soluble Chloride in Mortar and Concrete*, West Conshohocken, PA. 4 pp.

ASTM International (2012) *D4580-03 Standard Practice for Measuring Delaminations in Concrete Bridge Decks by Sounding*. West Conshohocken, PA. 4 pp.

ASTM International (2010) *C78-10 Standard Test Method for Flexural Strength of Concrete (Using Simple Beam with Third-Point Loading)* West Conshohocken, PA. 4 pp.

ASTM International (2011) *C496-11 Standard Test Method for Splitting Tensile Strength of Cylindrical Concrete Specimens*, West Conshohocken, PA. 5 pp.

ASTM International (2009) *D7522-09 Standard Test Method for Pull-Off Strength for FRP Bonded to Concrete Substrate*, West Conshohocken, PA. 6 pp.

ASTM International (2009) *D7522-09 Standard Test Method for Pull-Off Strength for FRP Bonded to Concrete Substrate*, West Conshohocken, PA. 6 pp.

ASTM International (2009) *ASTM D4541 Standard Test Method for Pull-Off Strength of Coatings Using Portable Adhesion Testers*, West Conshohocken, PA. 16 pp.

Austin, S., Robbins, P., Pan, Y. (1995). "Tensile bond testing of concrete repairs." *Materials and Structures*, **28**, 249-259.

Bartlett, F.M. and MacGregor, J.G. (1994) Effect of Core Diameter on Concrete Core Strengths," *ACI Materials Journal*, **91**(5), pp. 460-470.

Basham, K. (2004) *Testing and Evaluation of Concrete Repair Materials for the Cheyenne Airport Taxiways*. Cheyenne: State of Wyoming Department of Transportation; U.S. Department of Transportation.

Bentz, E.C. (2000) *Sectional Analysis of Reinforced Concrete Members-PhD Thesis*, Department of Civil Engineering, University of Toronto, pp. 310.

Bertrand, J. (2012) Performance of latex-modified bridge overlays after 20+ years of service. *Preservation Engineering – Stone, Masonry and Concrete*. ICRI Spring Convention, Quebec City. April 2012.

Bertrand, J. and Sprinkel, M. (2009) *History and case studies of latex modified concrete (LMC) in USA and Quebec*. American Concrete Institute. Section du Québec et de l'est de l'Ontario. Progress in concrete seminar, December 2009, Montreal.

Birkeland, P.W., and Birkland, H.W. (1966) Connections in Precast Concrete Construction. *Journal of the American Concrete Institute* **63**(3), 345-368.

Cole, J., Shahrooz, B. M. and Gillum, A. J. (2002) Performance of Overlays under Static and Fatigue Loading. *ASCE Journal of Bridge Engineering*, **7**(4), 206-213.

Eveslage, T., Aidoo, J., Harries, K. A. and Bro, W. (2010) Effect of Variations in Practice of ASTM D7522 Standard Pull-Off Test for FRP-Concrete Interfaces. *ASTM Journal of Testing and Evaluation*, **38**(4), 424-430.

Federal Highway Administration (FHWA) (2011) *Deck Structure Type*. Retrieved October 24, 2012.

Federal Highway Administration (FHWA) (1978) Styrene-Butasiene Latex Modifiers for Bridge Deck Overlay Concrete, *Report No. FHWA-RD-78-35*. April 1978.

Fowler, D., and Trevino, M. (2011) Overlay Design Process, *Bonded Cement-Based Material Overlays for the Repair, the Lining or the Strengthening of Slabs or Pavements*, RILEM State-of-the-Art Report, Vol. 3, 5-16.

Germann Instruments, Inc. (2012) *Bond-Test*, Evanston, IL.

Gillum, A. J., Cole, J., Turer, A. and Shahrooz, B. M. (1998) *Bond Characteristics of Overlays Place Over Bridge Decks Sealed with HMWM or Epoxy*, University of Cincinnati, College of Engineering. Cincinnati Infrastructure Institute.

Gillum, A. J., Shahrooz, B. M. and Cole, J. (2001) Bond Strength Between Sealed Bridge Decks and Concrete Overlays. *ACI Structural Journal*, **98**(6), 872-879.

Harries, K.A., Kasan, J. and Aktas, C. (2009) *Repair Methods for Prestressed Concrete Bridges*, Report No. FHWA-PA-2009-008-PIT 006. 170 pp.

Harries, K.A., Zeno, G. and Shahrooz, B.M., (2012) Toward an Improved Understanding of Shear Friction Behavior, *ACI Structural Journal*, Vol 109, No. 6, pp 835-844.

International Concrete Repair Institute (ICRI) (2004). *Guideline No. 03739 Guide to Using In situ Tensile Pull-Off Tests to Evaluate Bond of Concrete Surface Materials*, ICRI, Des Plaines, IL.

Issa, M.A., Alhassan, M.A. and Ramos, J. (2007) Glass Fiber-Reinforced Latex-Modified Concrete Using a Volumetric Mixer for Production of Overlays. *Concrete International*, Vol. 29, No. 3, pp 48–52.

Kahn, L. F., and A. D. Mitchell (2002). Shear Friction Tests with High Strength Concrete. *ACI Structural Journal*, **99** (1), 98-103.

Ohama, Y. (2001) Recent Progress in Research and Development Activities of Concrete-Polymers Composites in Japan. *Proceedings of the Tenth International Congress on Polymers in Concrete*, Hawaii

PennDOT *Publication 15: Design Manual Part 4: Structures*, May 2012. accessed via: ftp.dot.state.pa.us/public/PubsForms/Publications/PUB 15M.pdf

PennDOT *Publication 408: Construction Specifications*, April 2011. accessed via: ftp.dot.state.pa.us/public/bureaus/design/pub408/pub 408-2011.pdf

RILEM (2011) *Bonded Cement-Based Material Overlays for the Repair, the Lining or the Strengthening of Slabs or Pavements*, State-of-the-Art Report of the RILEM Technical Committee 193-RLS, Bissonnette, B., Courard, L., Fowler, D.W. and Granju, J.-L. (editors)/ RILEM State-of-the-Art Reports, Vol. 3. Reunion Internationale des Laboratoires et Experts des Materiaux, Systemes de Construction et Ouvrages, Bagneux, France.

Shahrooz, B.M., Miller, R.A., Harries, K.A. and Russell, H.G. (2011) Design of Concrete Structures Using High-Strength Steel Reinforcement, *NCHRP Report 679*, Transportation Research Board, 83 pp + appendices.

Silfwerbrand, J. (2009) *Bonded Concrete Overlays for Repairing Concrete Structures. Failure, Distress and Repair of Concrete Structures*, Woodhead Publishing Limited, Oxford UK, 208-243.

Silfwerbrand, J., Beushausen, H. and Courard, L. (2011) Bond, *Bonded Cement-Based Material Overlays for the Repair, the Lining or the Strengthening of Slabs or Pavements*, RILEM State-of-the-Art Report, Vol. 3, 59-79.

Sprinkel, M. (2009) *A Short History of Latex Modified Concrete for Bridge Repairs*, American Concrete Institute. Section du Québec et de l'est de l'Ontario. Progress in concrete seminar, December 2009, Montreal.

Sprinkel, M. (2003) High Performance Concrete Overlays for Bridges, *Proceedings of the Prestressed Institute Convention/National Bridge Conference/Federal Highways Administration Symposium on High Performance Concrete*, Orlando FL, October 2003.

Sprinkel, M. (1998) *Technical Assistance Report Very-Early-Strength Latex-Modified Concrete Overlay*, Virginia Transportation Research Council Report TAR 99-TAR3.

Sprinkel, M. (1988) High Early Strength Latex Modified Concrete Overlay, *Transportation Research Record 1204*, TRB, National Research Council, Washington, D.C., 1988, pp. 42-51.

Vaysburd, A. M. and McDonald, J. E. (1999) *An Evaluation of Equipment and Procedures for Tensile Bond Testing of Concrete Repairs*, US Army Corp of Engineers, Washington, DC.

Vaysburd, M. and Bissonnette, B. M. (2011) Practice and Quality Assurance, *Bonded Cement-Based Material Overlays for the Repair, the Lining or the Strengthening of Slabs or Pavements*, RILEM State-of-the-Art Report, Vo. 3, 157-170.

Wenzlick, J. D. (2002) *Hydrodemolition and Repair of Bridge Decks*, Missouri Department of Transportation, Research, Development and Technology. Jefferson City.

Zeno, G.A. (2009). *Use of High-Strength Steel Reinforcement in Shear Friction Applications-Master's Thesis.* University of Pittsburgh, Swanson School of Engineering. Watkins-Haggart Structural Engineering Laboratory.

APPENDIX A– BRIDGES HAVING LMC IDENTIFIED IN DISTRICT 11.

Data presented in this appendix is mentioned in section 2.1. All data comes from the PennDOT bridge management system (BMS).

BMS	Facility	Feature Intercepted	Length	Deck Area	WS Thickness	Year Reconst.	Inspection Date	WS cond.
02 0028 0080 0981	SR 0028 SH	RAMP B	32	1,258	2.20	0	12/13/2012	8
02 0028 0220 2488	SR 0028 SH	GAMMA DRIVE (TWP RD 505)	175	9,678	1.50	2001	11/8/2011	6
02 0028 0240 0000	SR 0028 SH	POWERS RUN ROAD SR 1009	242	10,285	1.20	2001	10/30/2011	7
02 0028 0260 0801	SR 0028 NB	COAL CO RD & BARGE BASIN	1,087	36,415	1.20	2004	9/6/2012	7
02 0028 0260 2109	SR 0028 NB	LR 02244-GUYS RUN ROAD	143	6,221	2.00	2008	12/9/2011	8
02 0028 0261 1084	SR 0028 SH	COAL CO RD & BARGE BASIN	992	33,232	0.50	2004	9/5/2012	7
02 0028 0261 2263	SR 0028 SB	LR 02244-GUYS RUN ROAD	143	6,221	1.20	2008	12/9/2011	8
02 0028 0270 0000	SR 0028 NB	DEER CREEK	176	8,888	1.30	2008	12/23/2011	6
02 0028 0270 1046	SR 0028 NB	LR 679-SR 910	190	8,227	0.50	2008	4/18/2012	7
02 0028 0271 0000	SR 0028 SB	DEER CREEK	176	7,603	1.20	2008	12/23/2011	8
02 0028 0271 1085	SR 0028 SB	LR 679-TR 910	190	8,227	0.50	2008	4/18/2012	8
02 0028 0290 1112	SR 0028 NB	PA TURNPIKE	187	10,865	0.50	2008	5/30/2012	9
02 0028 0291 1327	SR 0028 SB	PA TURNPIKE	196	8,330	0.50	2008	5/30/2012	8
02 0028 0310 1477	SR 0028 NB	LR 02169-YUTES RUN RD	112	6,508	1.20	2008	12/8/2011	7
02 0028 0311 1744	SR 0028 SB	LR 02169--YUTES RUN RD	114	4,845	1.20	2008	12/8/2011	7
02 0028 0360 0000	ALLEGHENY VAL. EX	CRAWFORD RUN ROAD	326	14,344	1.50	2008	6/7/2011	6
02 0028 0361 0208	ALLEGHENY VAL EX	CRAWFORD RUN ROAD	326	14,344	1.50	2008	6/7/2011	6
02 0028 0370 0568	ALLEGHENY VAL EX	BAILEYS RUN RD.,CREEK	444	19,536	1.00	2008	8/8/2011	6
02 0028 0371 0878	ALGY.VALY. EX	BAILEYS RUN RD.,CREEK	440	24,640	1.50	2008	8/8/2011	6
02 0028 0430 1987	SR 0028 SH	LR 02220-BURTNER ROAD	153	6,732	0.50	2005	9/1/2011	6
02 0028 0433 1947	SR 0028 SH	LR 02220-BURTNER ROAD	153	6,732	0.50	2005	9/1/2011	7
02 0028 0460 2380	SR 0028 SH	LR 02222 & LITTLE BULLCR	339	14,645	0.50	2005	11/21/2011	7

BMS	Facility	Feature Intercepted	Length	Deck Area	WS Thickness	Year Reconst.	Inspection Date	WS cond.
02 0028 0461 2413	SR 0028 SH	LR 02222,LITTLE BULL CRK	365	15,768	0.50	2005	11/21/2011	7
02 0028 0490 0373	SR 0028 SH	FREEPORT/MILLERSTOWN RD	230	10,120	0.50	2005	9/9/2011	8
02 0028 0491 0344	SR 0028 SH	FREEPORT/MILLERS TOWN RD	220	9,680	0.50	2005	9/9/2011	8
02 0050 0190 0090	WASHINGTON AV	CHARTIERS CREEK	367	14,497	0.50	1974	10/24/2012	8
02 0065 0003 0000	SR 0065 SB	REEDSDALE,N.SHORE ALL.RV	1,153	38,164	3.00	2011	3/30/2012	9
02 0065 0004 0000	SR 0065 SH	ALLEGHENY AVE, RP.B SB	133	11,438	1.50	0	5/4/2012	5
02 0065 0005 0000	SR 0065 SH	ALLEHGHENY AV.& RP.B SB	133	8,446	1.50	0	5/4/2012	6
02 0065 0140 1735	OHIO RIVER BL	GLENFIELD ROAD	142	10,792	0.50	2010	8/25/2011	8
02 0079 0524 0409	RAYMONDP SHAFER HW	TR 50	184	7,820	1.20	1998	1/14/2013	8
02 0079 0524 1139	SR 0079 SH	WLE RR,CHARTIERS CREEK	574	27,839	1.20	1998	4/25/2011	8
02 0079 0525 0486	RAYMONDP SHAFER HW	TR 50	187	9,350	1.50	1998	1/14/2013	7
02 0079 0525 1150	SR 0079 SH	W&LE RR,CHARTIERS CREEK	578	28,033	1.20	1998	4/26/2011	8
02 0079 0544 2310	RAYMOND P SHAFE HW	THOMS RUN RD,FLOOD CHANN	344	16,856	0.50	2005	8/19/2011	6
02 0079 0610 0467	RAYMOND P.SHAFER H	CLEVER RD	219	9,636	1.50	2001	7/9/2012	7
02 0079 0611 0496	RAYMOND P SHAFE HY	CLEVER RD	264	11,616	1.50	1982	7/9/2012	7
02 0079 0650 0000	RAYMOND P SHAFE HW	CSX RR,NS RR, OHIO RIVER	4,544	368,064	0.50	2010	10/4/2012	7
02 0079 0660 0615	RAYMOND P SHAFE HW	GLENFIELD RD,KILBUCK RUN	445	19,580	1.00	2008	7/11/2011	8
02 0079 0661 0760	RAYMOND P SHAFE HW	GLENFIELD RD,KILBUCK RUN	448	19,712	0.50	2008	7/12/2011	8
02 0079 0690 0106	RAYMOND P SHAFE HW	RED MUD HOLLOW RD.	164	6,970	0.50	2008	11/1/2011	7
02 0079 0691 0194	RAYMOND P SHAFE HW	RED MUD HOLLOW RD	194	8,342	0.50	2008	11/1/2011	6
02 0079 0765 0152	RAYMOND P SHAFE HW	I76,PA TURNPIKE	238	10,710	3.00	2009	8/16/2012	7
02 0279 0008 0000	1039 NB	SR279 SB RP SR 8041 RP D	452	13,831	3.00	0	4/27/2012	8
02 0279 0008 0425	FORT DUQUESNE BR	FT DUQ BR SB,ALLEG RVR	921	56,642	3.00	0	5/30/2012	8
02 0279 0009 0351	I 279 RAMP F	I-279 NB RAMP D ALLGY RI	351	10,706	0.50	1985	3/30/2012	7
02 0279 0009 2108	FORT DUQ BR SB	FT DUQ BRDG NB, ALLEGH R	921	56,642	3.00	0	5/30/2012	8
02 0366 0032 0400	RAMP A,TARENTUM BR	4TH AVE,RAMPD, NS RR	576	17,856	1.50	1986	5/3/2011	6
02 0366 0033 0890	TARENTUM BR,RMP.B	NS RR,4TH AVE,ROSS ST	612	23,134	1.50	1986	5/3/2011	6
02 0376 0584 0097	AIRPORT PY	CLIFF MINE RD,MONTOUR RN	304	29,184	0.50	2009	8/27/2012	6
02 0376 0650 0000	PARK WAY WEST PY	W.BUSWAY,ARCH,BELL,R R	510	38,505	1.00	1975	8/28/2011	6

BMS	Facility	Feature Intercepted	Length	Deck Area	WS Thickness	Year Reconst.	Inspection Date	WS cond.
02 0376 0650 1095	PARKWAY WEST PY	SR 50;WLE RAILWAY	768	57,984	3.00	1976	8/28/2011	6
02 0376 0654 0281	PENN LINCOLN PW	WHISKEY RUN, BELL RD	622	45,717	1.50	1976	6/4/2011	5
02 0376 0670 0490	PENN LINCOLN PY	POPLAR AVENUE	115	9,200	2.00	1976	12/16/2011	4
02 0376 0730 1965	PARKWAY EAST SH	CSX RR,SWINEBURN,FRAZIER	1,015	96,933	2.00	1981	9/18/2011	7
02 0376 0744 0762	PARKWAY EAST	FORWARD AVE, RAMP H	99	9,187	0.50	1981	10/14/2011	8
02 0376 0754 0000	SR 376 SH	COMMERCIAL ST. & NINE MI	863	61,704	2.00	2007	6/24/2011	7
02 0376 0764 0000	PARKWAY EAST	LR 763 RAMP B	174	15,138	0.50	2007	10/20/2011	8
02 0376 0764 0513	PARKWAY EAST	BRADDOCK AVE	201	14,372	2.00	2007	8/17/2011	8
02 0376 0774 2445	PENN LINCOLN PY	ARDMORE BLVD.	290	25,375	2.00	2008	6/17/2011	8
02 0376 0780 0125	PENN LINCOLN PY	SR 8012-RAMP A	57	4,845	1.50	2008	8/23/2011	7
02 0376 0780 0641	PENN LINCOLN PY	LR 763-RAMP G	80	6,840	1.50	1971	8/29/2011	8
02 0376 0790 1628	PARKWAY EAST	BEULAH ROAD	176	13,728	3.00	2008	8/25/2011	8
02 0376 0800 0915	PARKWAY EAST	LR 187,RAMP A,W.B.	78	6,903	3.50	1976	1/9/2013	7
02 0376 0800 2406	PENN LINCOLN PY	LR 395-RODI ROAD NB&SB	332	34,196	0.50	1976	10/22/2012	7
02 0376 0804 1997	PARKWAY EAST	SUNSET;OLD WM PENN;CREEK	546	54,600	3.50	2010	8/28/2012	6
02 0376 0820 0342	PARKWAY EAST SH	LR 744,UNION RR,THOMPSON	706	72,153	0.50	2009	9/17/2012	8
02 0376 0830 0726	PARKWAY EAST	OLD WM PENN HWY,LEAK RUN	224	22,736	3.50	2010	5/9/2012	6
02 0376 0834 0952	PARKWAY EAST HW	OLD WILLIAM PENN HIGHWAY	221	22,432	3.50	1976	8/9/2011	6
02 0376 0840 0872	PARKWAY EAST	HAYMAKER ROAD	116	7,308	1.50	2010	1/10/2013	7
02 0376 0841 0913	PARKWAY EAST	HAYMAKER ROAD	105	6,668	1.50	2009	1/10/2013	8
02 0837 0430 0000	EIGHTH AV	BALDWIN ROAD	739	17,367	1.50	0	7/12/2012	6
02 0837 0431 0000	EIGHTH AV	RPS. C&D,RP.CARSON,LOCAL	819	25,389	1.50	0	7/26/2012	7
02 2091 0010 0000	LAUREL ST	PARKWAY EAST	74	3,515	0.50	2008	8/1/2011	5
02 2093 0010 0000	EDGEWOOD AV	PARKWAY EAST	73	3,358	2.00	2008	8/1/2011	7
02 2095 0010 0000	CHESTNUT ST	LR 763,906+78	72	2,880	0.50	2008	8/1/2011	8
02 2097 0010 0000	GREENSBURG PIKE	PARKWAY EAST	173	9,740	2.00	2008	8/15/2011	8
02 2099 0010 0000	GARDEN CITY DR	OVER 376 EB WB	116	6,090	1.20	2009	1/9/2013	8
02 2107 0010 0000	BOWMAN AV	1066,RAMP,G-E,CLIFF ST	374	10,846	0.50	0	4/24/2012	6
02 2114 0011 0785	SR 2114 SH	LR 392 (PA 148)-5TH AVE.	145	5,220	1.50	1983	1/24/2012	6

BMS	Facility	Feature Intercepted	Length	Deck Area	WS Thickness	Year Reconst.	Inspection Date	WS cond.
02 3048 0190 0000	NOBLESTOWN RD	OHIO C.,SR3117,ROBINSON	596	39,038	0.50	2008	5/25/2011	6
02 3069 0110 0135	LIBERTY BR	MON R,I376,0837,2 AV,ARL	2,663	175,758	1.50	1983	9/11/2012	6
02 4003 0020 0000	MCKNIGHT RD	BABCOCK BLVD,GIRDY'S RUN	221	15,028	2.00	0	5/21/2012	9
02 4022 0020 0000	MOUNT NEBO RD	I-79 NB-SB	286	10,725	0.50	2008	8/11/2011	8
02 4049 0060 0175	NICHOLSON RD	I79 NB&SB	328	15,744	1.50	2008	8/25/2011	8
02 8002 0260 0000	RAMP G RD,TO LIB.	LIBERTY BRDG APPROACH RD	588	17,052	1.50	1984	7/27/2012	6
02 8002 0280 0000	CROSSTOWN BL	FORBES,DIAMOND,RPS.J&G	976	23,912	1.50	1984	8/28/2012	7
02 8006 0250 0159	RAMP D RD, EXIT 7B	HODGE ST	63	1,827	0.50	2007	9/21/2011	9
02 8008 0510 0569	RAMP AD RD	LR 763	93	4,511	2.00	2007	8/4/2012	7
02 8008 0750 0000	RAMP E RD	LR 763 RAMP G	42	1,827	0.50	2007	9/29/2011	9
02 8012 0280 1906	RAMP D RD	ARDMORE BLVD.	138	4,623	0.50	2008	7/28/2011	8
02 8012 0280 2164	RAMP D RD	LR 763-RAMP A	53	1,776	1.50	2008	8/23/2011	7
02 8012 0750 0550	RAMP A RD	LR 763 RAMP F	58	2,604	3.00	2008	8/23/2011	7
02 8012 0750 1423	RAMP A RD	LR 120-ARDMORE BLVD-TR.8	147	6,615	0.50	2008	7/8/2011	8
02 8015 0010 0000	RAMP-D RD	OHIO RIVER BACK CHANNEL	1,370	46,580	0.50	2010	12/4/2012	7
02 8017 0260 0403	LOCAL RAMP RD	LOCAL RAMP TO SR 65 NB	148	4,292	0.50	2010	11/7/2011	9
02 8017 0760 0910	79NB RAMP TO 65 NB	652 RAMP A1,LR 02123	420	14,364	0.50	2010	10/23/2012	8
02 8017 0770 0000	RAMP B1 RD	65 NB-SB,RAMP A1,RAMP R	485	16,587	0.50	2010	10/11/2012	8
02 8020 0760 0112	RAMP D RD	RODI RD.,N.B.	47	1,598	1.50	1977	1/18/2011	9
02 8031 0010 0000	RAMP A RD	PARKWAY WEST	184	6,532	3.50	1976	8/9/2012	6
02 8041 0260 0072	RAMP J RD	LR 1039 RAMP C	55	1,375	0.50	1988	6/29/2012	9
02 8041 0530 0140	RAMP H RD	LR 1039 RAMPS C,K,& D	615	15,068	3.00	1988	12/28/2012	7
02 8041 0760 0244	RAMP C RD	LR 1039 RAMP F	36	1,026	3.00	2001	1/11/2012	7
02 8041 0770 0043	RAMP E RD	LR 1039 RAMP F	30	855	3.00	2001	1/11/2012	8
02 8045 0250 0000	RAMP A RD	SR 65 REEDSDALE ST	1,420	36,210	3.00	0	12/21/2011	7
02 8059 0500 0000	RAMP A RD	RAMP C,D-RP. NB TO CARSO	323	13,695	1.50	0	7/19/2011	7
02 8059 0520 0000	RAMP B RD	RPS.C&D,NB CARSON RAMP	175	3,850	1.50	0	7/19/2011	7
02 8086 0010 0383	RAMP F RD	1066, 392,LOCAL STREETS	893	33,934	1.50	1983	10/25/2011	7
02 8086 0260 0407	RAMP G RD	LR 1066	165	6,270	1.50	1983	8/2/2012	6

BMS	Facility	Feature Intercepted	Length	Deck Area	WS Thickness	Year Reconst.	Inspection Date	WS cond.
02 8086 0260 0704	RAMP G RD	LR 1066 RAMP E	126	4,284	1.50	1983	8/3/2012	7
04 0018 0720 0000	FOURTH AV	CREEK	506	34,560	0.50	1995	7/9/2012	6
04 0051 0220 0000	PENNSYLVANIA AV	04136,641 RP.A,& LOCAL	988	59,774	0.50	1997	8/15/2011	6
04 0051 0230 1222	PENNSYLVANIA AV	SR 4042 (MARKET ST)	127	9,017	1.20	2011	8/1/2012	8
04 0065 0170 3360	OHIO RIVER BL	8TH STREET	58	3,828	1.50	0	4/12/2011	7
04 0168 0250 1507	SHIPPINGPORT HI RD	SERVICE ROAD NUC PLANT	120	5,184	0.50	2009	3/21/2011	8
04 0168 0260 0000	SHIPPINGPORT-HI RD	N/S RR ,SERVICE RD,OHIOR	1,616	58,984	1.30	2010	9/12/2012	9
04 0376 0340 0000	BEAVER VALLEY EXPR	LR 04004, BRADYS RUN PK.	1,360	60,112	1.00	2011	5/25/2012	7
04 0376 0341 1360	BEAVER VALLEY EXPR	LR 04004,BRADYS RUN PK.	1,360	59,840	1.20	2011	5/18/2012	8
04 0376 0390 1899	BEAVER VALLEY EX	TR 18	178	18,601	1.20	2001	5/10/2011	7
04 0376 0430 2403	BEAVER VALLEY EX	TWP. RD. 461	152	6,460	0.50	-1	5/17/2011	7
04 0376 0431 2546	BEAVER VALLEY EX	TWP. RD. 461	137	5,823	0.50	-1	5/17/2011	7
04 0376 0435 1601	BVR V EXPWY I-376	RELOCATED RACCOON CREEK	390	14,625	0.50	1982	4/13/2012	6
04 0376 0444 1193	BEAVER VALLEY EX	SR 3016-GREEN GARDEN RD	163	8,900	1.50	-1	5/16/2011	7
04 0376 0445 1411	BEAVER VALLEY EX	SR 3016-GREEN GARDEN RD	167	7,098	1.30	2002	5/16/2011	7
04 0376 0460 2020	BEAVER VALLEY EX	SR 3024	140	6,160	2.50	2008	5/24/2011	7
04 0376 0461 2122	BEAVER VALLEY EX	CLOSED SR 3024	106	4,664	1.50	-1	5/24/2011	7
04 0588 0280 1067	RIVERVIEW RD	CSX, CONNOQUENESSING CRK	478	22,944	1.50	2010	7/31/2012	8
04 3016 0230 1153	KENNEDY BL	LOGTOWN RUN	26	1,628	1.20	1989	7/16/2012	6
04 8007 0260 0466	RAMP J RD	TR 18	97	4,171	1.60	0	4/19/2011	7
37 0065 0290 0000	WASHINGTON RD	SR 0422-BEN FRANKLIN HW	264	23,232	0.50	2004	6/1/2011	6
37 0168 0200 1337	MORAVIA ST	LR 1055-US 422 EB & WB	299	26,312	0.50	2004	9/18/2012	5
37 0208 0130 1709	PULASKI RD	LR 1023-PA TR 60	271	17,344	1.20	2003	1/15/2013	6
37 0224 0170 0000	STATE ST	LR 1023 & RAMP K	289	30,923	1.20	0	5/21/2012	8
37 0376 0060 2301	BEAVER VALLEY EX	TWP RD 605	158	6,826	1.30	0	6/22/2011	5
37 0376 0061 2609	BEAVER VALLEY EX	TWP RD 605	175	7,560	0.50	2005	6/22/2011	5
37 0376 0094 1508	BEAVER VALLEY EX	RIVER ROAD	193	8,338	0.50	0	6/28/2011	7
37 0376 0095 1816	BEAVER VALLEY EX	RIVER ROAD	193	8,338	1.50	0	6/28/2011	7
37 0376 0120 0576	BEN FRANKLIN HW	LR 37061-US 422 BUSINESS	292	16,702	0.50	0	4/6/2011	6

BMS	Facility	Feature Intercepted	Length	Deck Area	WS Thickness	Year Reconst.	Inspection Date	WS cond.
37 0376 0121 0869	BEN FRANKLIN HW	LR 37061-US 422 BUSINESS	292	16,702	0.00	0	4/6/2011	8
37 0422 0340 0000	BENJAMIN FRANKL HW	SR 2001,BRANCH OF BIG RN	404	17,776	0.50	2009	9/7/2011	9
37 0422 0341 0000	BENJAMIN FRANKL HY	SR 2001,BRANCH OF BIG RN	404	17,776	1.20	2009	9/7/2011	9
37 1002 0080 0000	MAITLAND LANE	NESHANNOCK CREEK	202	7,151	0.50	2012	9/28/2012	9
37 1014 0040 0000	BRENT NORTH LIB RD	LR 1021,I79 NB&SB	179	6,086	0.50	2008	9/26/2012	6
37 1016 0090 1622	NORTH LIBERTY DR.	I-79	235	7,990	0.50	2008	5/24/2011	8
37 1020 0020 1294	POLLOCK STORE RD	I-79,N.B. & S.B.	224	7,504	1.20	2008	10/27/2011	7
37 2021 0010 0000	MARTHA ST	LR 1055-US 422	299	13,754	1.20	2008	4/14/2011	8
37 4012 0010 0698	MITCHELL RD	LR1023-PA 60 NB&SB	305	19,520	1.20	2008	8/30/2012	7
37 4016 0010 0000	KINGS CHAPEL RD	LR 1023-TR 60	259	12,432	0.50	2008	6/21/2011	8
37 8008 0010 1536	BENJAMIN FRANKLIN	BUSINESS RT. 422	258	8,824	1.00	0	4/6/2011	5

APPENDIX B– PULL-OFF TEST DATA

Slab	test	f_t (psi)	failure mode	*%LMC*	Slab	test	f_t (psi)	failure mode	*%LMC*	Slab	test	f_t (psi)	failure mode	*%LMC*
7 day tests					B	10	244	I	25%	F	1	294	L	-
B	1	182	I	50%	B	11	208	I	75%	F	2	228	I	50%
B	2	261	S	-	B	12	310	I	75%	F	3	324	I	67%
B	3	205	I	33%	B	13	468	S[1]	-	F	4	367	A[1]	-
28 day tests					B	14	345	A[1]	-	F	4r	416	I[1]	25%
B	4	337	A[1]	-	B	15	151	I[1]	25%	F	5	349	A[1]	-
B	5	405	A[1]	-	B	16	116	S[1]	-	F	5r	405	A[1]	-
B	6	400	A[1]	-	B	17	366	A[1]	-	F	6	413	A[1]	-
B	7	520	I	25%	B	18	49	S[1]	-	F	7	442	A[1]	-
B	8	526	S	-	B	19	14	S[1]	-	F	8	305	I	33%
B	9	350	A[1]	-	B	20	154	S[1]	-					
following flexure tests										G	1	258	A[1]	-
A	1	384	A[1]	-	C	1	114	A[1]	-	G	1r	357	L[1]	-
A	2	224	S[1]	-	C	1r	336	I	50%	G	2	144	A[1]	-
A	3	206	S[1]	-	C	2	377	I	25%	G	3	279	I	75%
A	4	163	A[1]	-	C	3	282	I	33%	G	4	243	L	-
A	4r	219	A[1]	-	C	4	389	I	50%	G	5	183	L	-
A	5	155	S[1]	-	C	5	457	I	50%	G	6	271	I	33%
A	6	193	S[1]	-						G (LMC only)	7	273	A	-
A	7	363	A[1]	-	D	1	119	A[1]	-	G (LMC only)	8	387	A	-
A	8	192	S[1]	-	D	2	123	A[1]	-	G (LMC only)	8r	424	L	-
A	9	213	S[1]	-	D	3	53	A[1]	-	G (LMC only)	9	402	A	-
A	10	178	A[1]	-	D	3r	397	S	-	G (LMC only)	9r	472	L	-
A	10r	337	A[1]	-	D	4	324	S	-	G (LMC only)	10	430	A	-
A	11	140	A[1]	-	D	5	332	I	67%	G (LMC only)	10r	290	A[1]	-
A	11r	242	A[1]	-	D	6	273	I	50%					
A	12	99	A[1]	-	D	7	486	A[1]	-	AAA	1	119	I	
A	12r	360	S	-	D	8	391	A[1]	-	AAA	2	230	A[1]	
A	13	401	S	-						AAA	3	271	I	
A	14	360	S	-	E	1	201	A[1]	-	AAA	4	256	I	
					E	2	442	I	33%	AAA	5	224	I	
					E	3	199	I	75%	AAA	6	234	I	
					E	4	310	I	25%	AAA (overlay)	7	347	L	
					E	5	259	S	-	AAA (overlay)	8	361	A[1]	
					E	6	248	I	50%	AAA (overlay)	9	405	L	
										AAA (overlay)	10	365	L	

[1] excluded from average values reported
r indicates retest of Mode A failure

APPENDIX C- MARSHALL AVE. SPECIMENS

Figure C1 shows a schematic representation of the decommissioned bridge deck from which the Marshall Ave. slabs were cut. The existing deck was 44 years old at the time of decommissioning. Slabs were cut perpendicular to the longitudinal axis of the bridge (spanning between stringers). However, the one-way flexural direction of this deck was in the longitudinal direction – between floor beams. Thus the slabs, as delivered were tested in the their ‘weak’ bending direction. Nonetheless, the slab behavior still provides insight into how overlays applied to older decks may perform in the field.

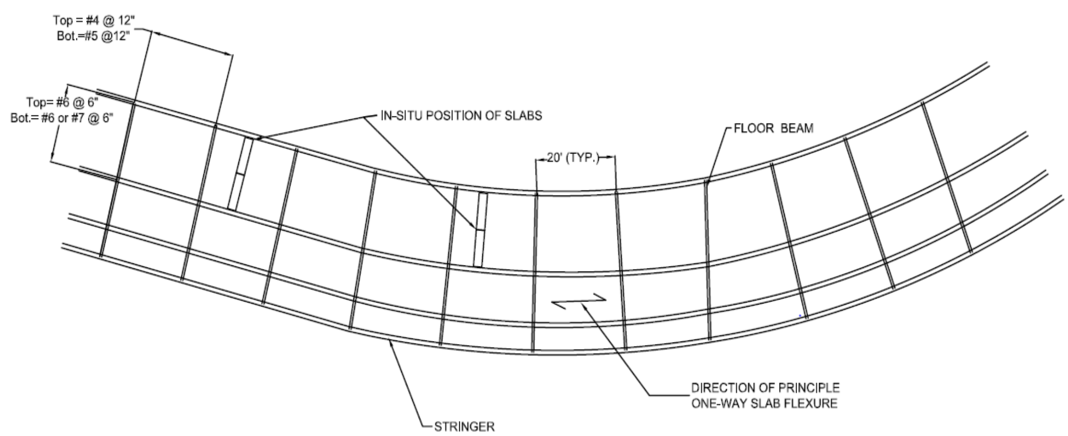

Figure C1: *In situ* location of Marshall Ave. slabs.

C.1 Test Program

The test setup for the Marshall Ave. slabs was identical to the test setup used for the laboratory cast concrete slabs, with the exception that the Marshall Ave slabs were tested over 72 in. (1829 mm) span lengths, instead of 84 in. (2133 mm). Some of the Marshall Ave slabs exhibited damage at their ends that would have been under the supports if tested at the longer span. Figure C2 shows the general geometry of each Marshall Ave. specimen tested. The slabs were delivered and tested in their inverted orientation when compared to their *in situ* position. This was necessary to facilitate testing without requiring additional repairs to the slabs. The position does not change the analysis procedures, only the expected capacities of the specimens.

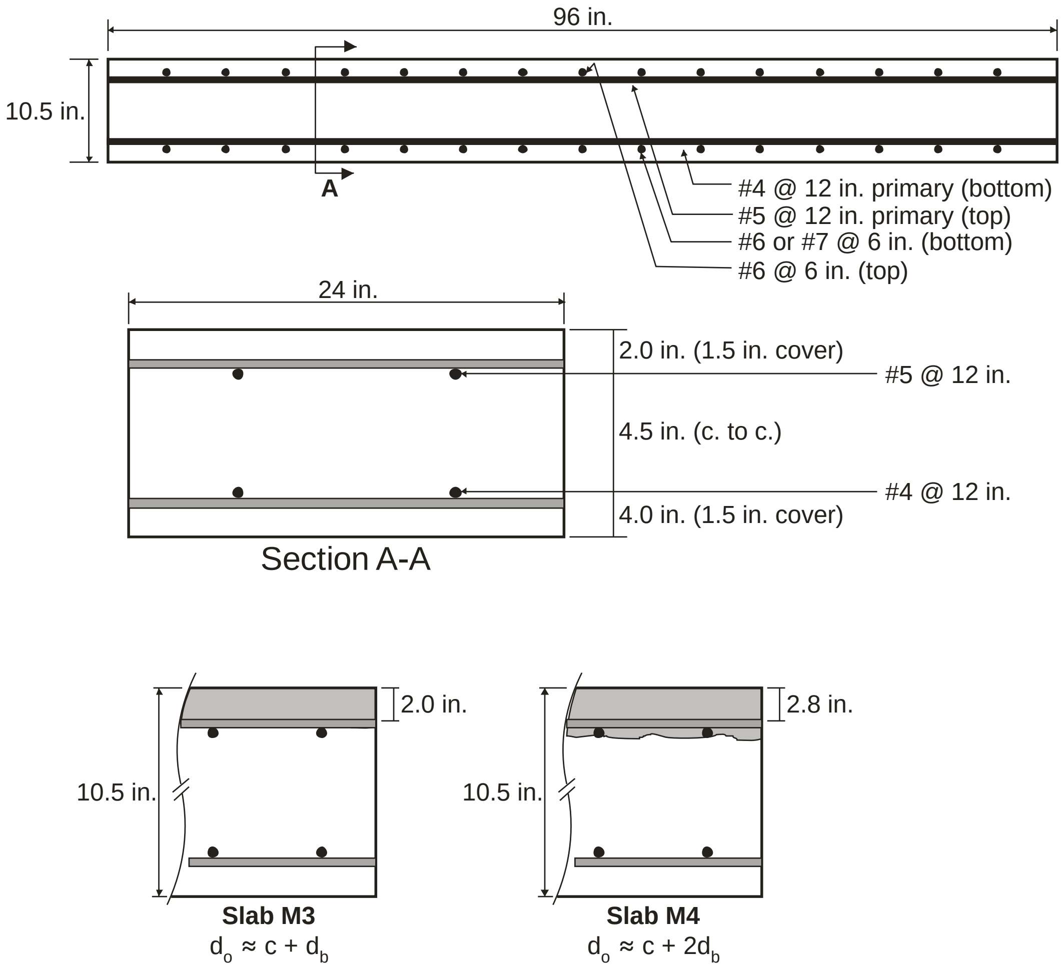

Figure C2: Schematic details of Marshall Ave. slabs.

C.2 Material Properties

Three 2 in. (51 mm) cores recovered from the slabs had an average compression strength of 5017 psi with a standard deviation of 714 psi. Using cored and small diameter samples typically yields results that are lower and more scattered than *in situ* strength (Bartlett and Macgregor 1994). The latex modified concrete (LMC) material properties are listed in Table 7.

A portion of primary reinforcement bar was extracted from one of the Marshall Ave. slabs. Yield and ultimate strength were experimentally-determined to be 43.0 and 66.7 ksi, respectively.

C.3 Flexural Test Results

Table C1 summarizes Marshall Ave. test results in the same format as Table 9. Detailed test results, in the same format as Figures 19-28 are shown in Figures C3 to C5.

		Marshall Ave. - Slabs			
	RESPONSE	**M1**	**M2**	**M3**	**M4**
depth of slab (in.)	10.5	10.5	10.5	10.5	10.5
depth of overlay (in)	none	none	none	2.0	2.8
load at first crack (kips)		existing cracking indicating that service loads had exceeded cracking capacity			
moment at first crack (kipft)					
load at reinforcing yield (kips)	6.5	7.15	7.84	9.51	9.50
moment at reinforcing yield (kipft)	9.7	10.73	11.76	14.27	14.25
deflection at reinforcing yield (in.)		0.031	0.094	0.188	0.094
curvature at reinforcing yield (rad/in^6)	356	37.0	n.a.	374.5	376.3
ultimate load (kips)	10.7	14.13	14.20	15.13	17.90
ultimate moment (kipft)	16.0	21.20	21.30	22.70	26.85
deflection at ultimate load (in.)		3.25	3.00	3.50	4.75
failure mode	flexure	flexural	flexural	flexural	flexural

Table C1: Results summary- Marshall Ave. slabs.

Slabs M1 and M2 were intended to act as control specimens (no overlay applied). Repaired slabs M3 and M4 exhibited approximately 127% increase in load to cause reinforcing steel yield and 117% increase in ultimate load. All observed loads were notably greater than those predicted from plane sections behavior. Subfigures a in Figures C3 to C5 plot moment vs. curvature showing curves for both experimental and RESPONSE predictions. The RESPONSE predictions are based on the geometry of each individual slab. Since these slabs were field-cut the geometry varies from slab to slab. Due to significant existing cracking in slab M2, it was not possible to obtain reliable strain profiles and thereby curvature values for this specimen; therefore only observed loads are reported in Table C1.

All observations and data from the Marshall Ave. slabs corroborate the conclusions drawn based on the laboratory specimens described in Chapter 3.

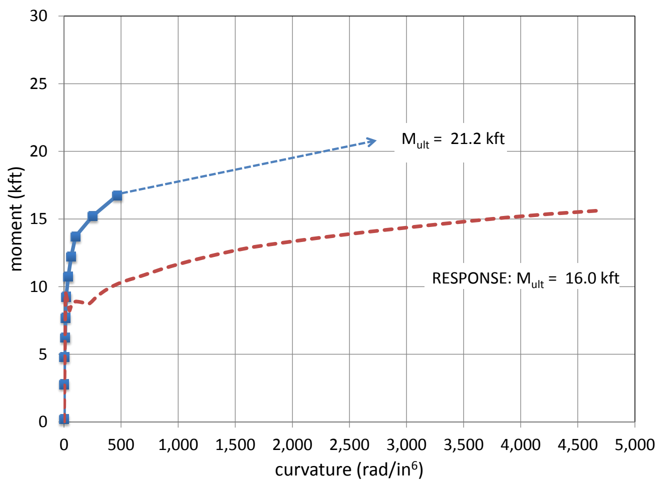

a) moment-curvature plot

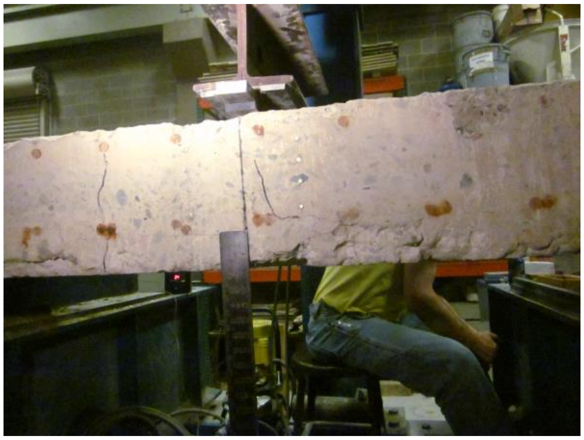

d) reinforcement yield (10.7 kipft)

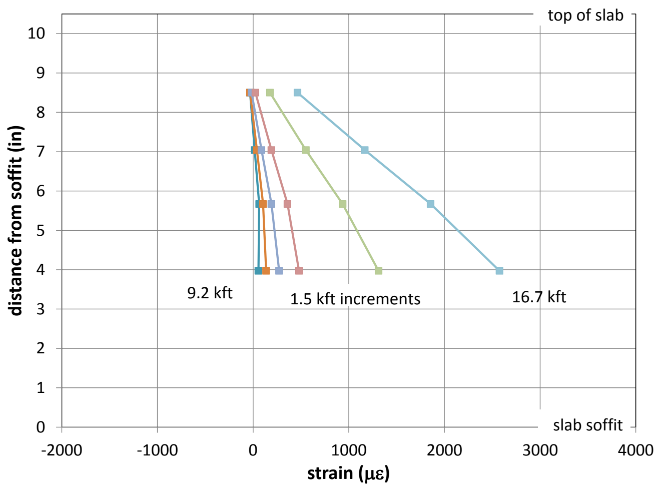

b) strain profiles

e) final DEMEC reading (16.7 kipft)

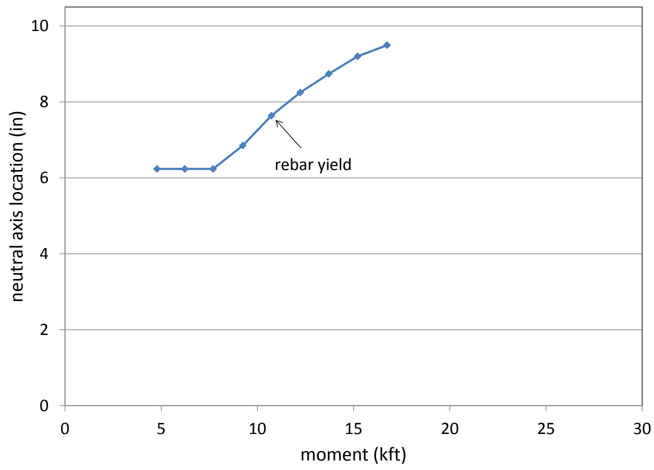

c) location of neutral axis

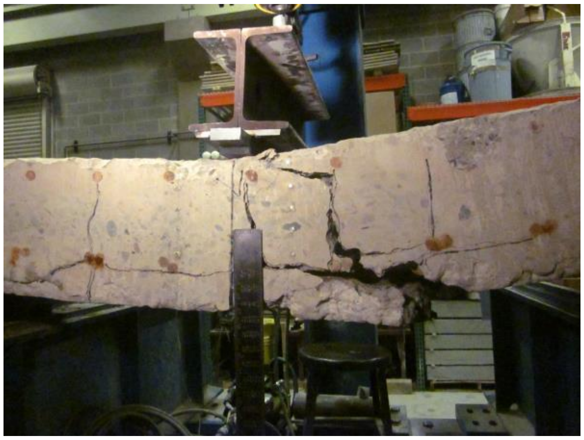

f) ultimate load (21.2 kipft)

Figure C3: Slab M1 results.

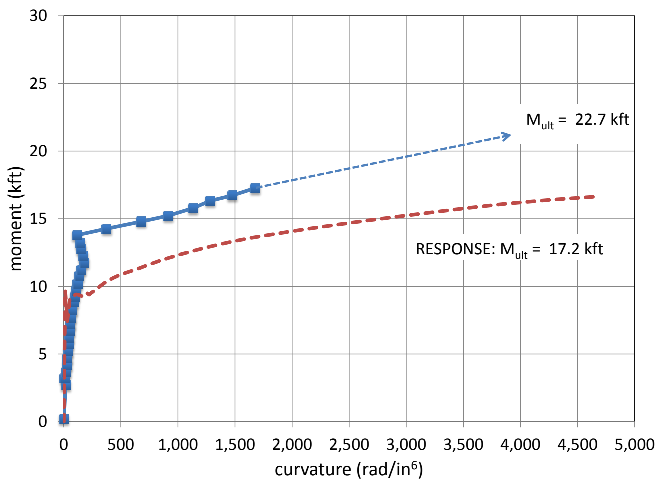

a) moment-curvature plot

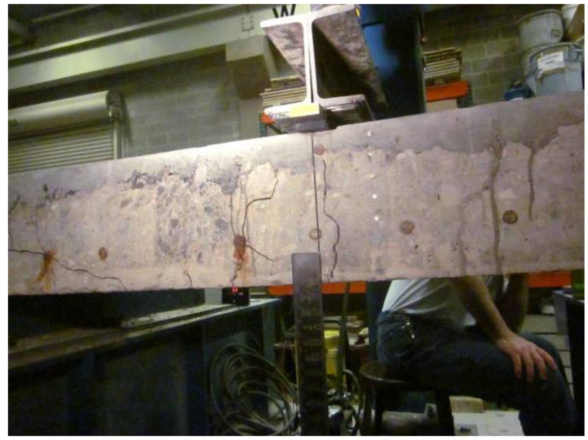

d) reinforcement yield (14.3 kipft)

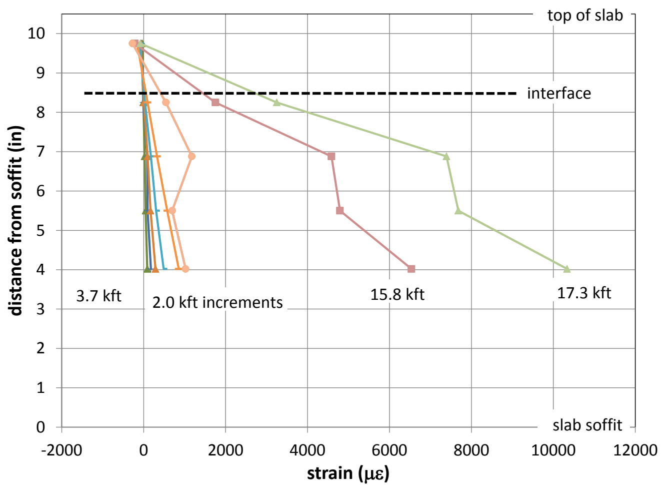

b) strain profiles

e) final DEMEC reading (17.3 kipft)

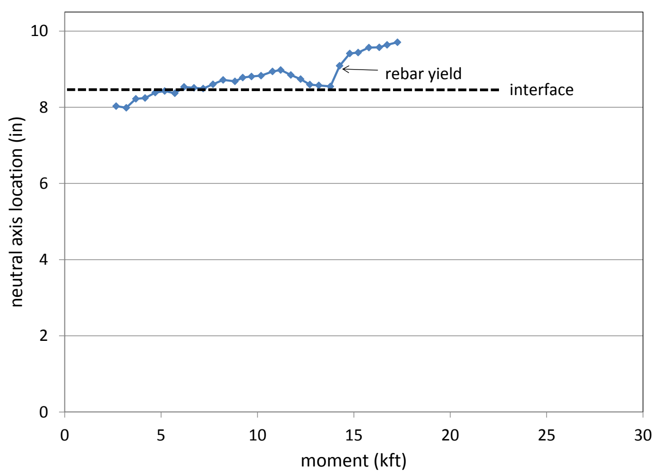

c) location of neutral axis

f) ultimate load (22.7 kipft)

Figure C4: Slab M3 results.

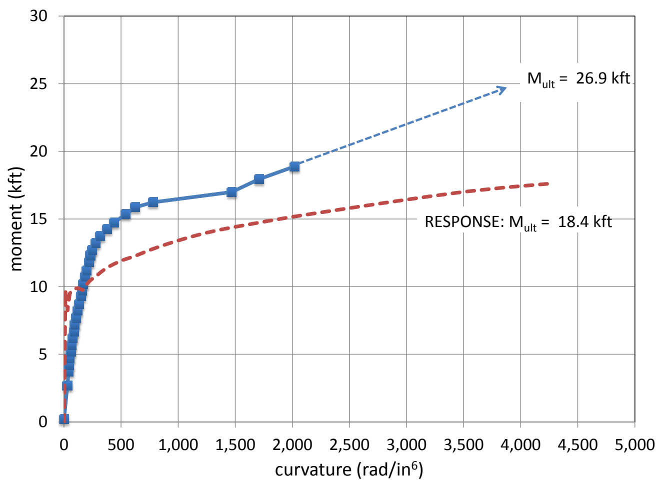

a) moment-curvature plot

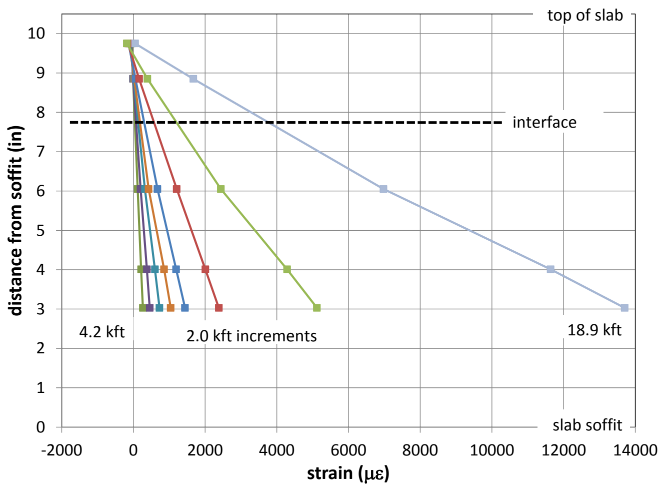

b) strain profiles

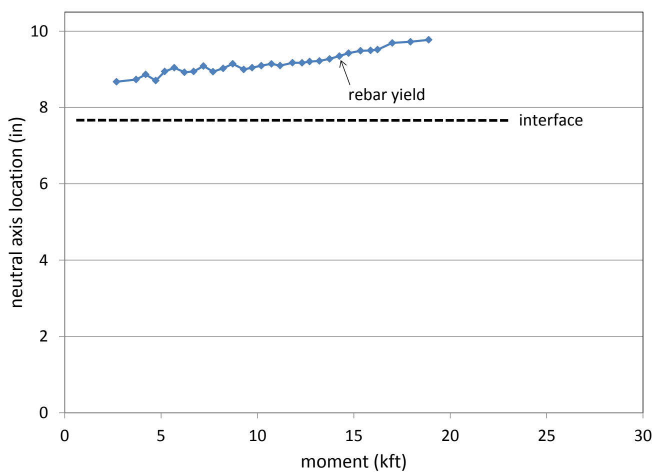

c) location of neutral axis

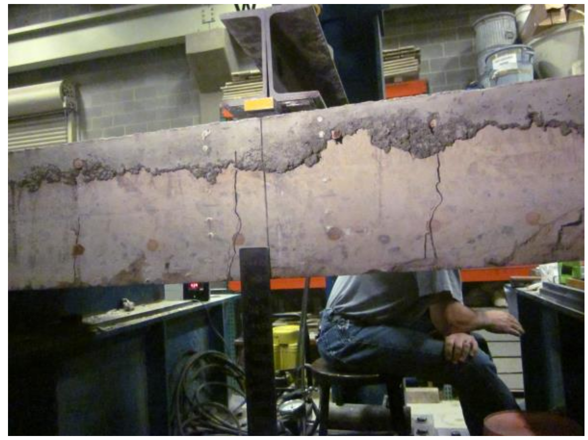

d) reinforcement yield (14.3 kipft)

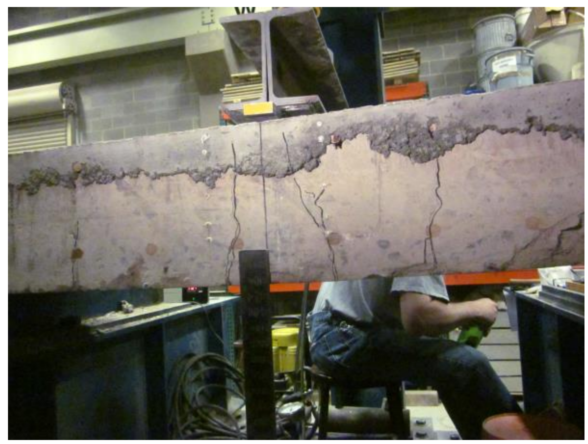

e) final DEMEC reading (18.9 kipft)

f) ultimate load (26.9 kipft)

Figure C5: Slab M4 results

C.4 Pull-off Test Results

Limited pull-off tests were also conducted on the Marshall Ave. slabs. A summary of results is presented in Table C2 in the same format as Table 10. Table C3 provides all pull-off results in a manner similar to that shown in Appendix B for the laboratory specimens.

Results are comparable to those of the laboratory-cast specimens reported in Chapter 4 and corroborate all conclusions drawn. The direct tensile strength of the Marshall Ave. substrate concrete is marginally greater than the laboratory specimens, this should be expected since the concrete is considerably older.

Table C2: Summary of Marshall Ave. slab pull-off tests.

Slab	Overlay depth (in.)	n	f_t (psi)	COV	Notes
HD1	2.0	5	280	0.26	
HD2	2.8	4	293	0.14	Mode S and I failures
HD2	2.8	6	286	0.14	includes Mode A failures
HD2	NA	3	397	0.13	substrate concrete direct tension tests

Table C3: Marshall Ave. pull-off tests.

Slab	**test**	**f_t (psi)**	**failure**	***%LMC***	**Slab**	**test**	**f_t (psi)**	**failure**	***%LMC***
HD1	1	273	S	-	HD2	1	305	A[1]	-
HD1	2	296	I	25%	HD2	2	233	S	-
HD1	3	197	A[1]	-	HD2	3	308	S	-
HD1	4	374	S	-	HD2	4	241	A[1]	-
HD1	5	283	I	25%	HD2	5	305	I	50%
HD1	6	171	I	50%	HD2	6	324	I	33%
HD1	7	312	I[1]	25%	HD2 (substrate)	7	412	S	-
HD1	8	333	I[1]	33%	HD2 (substrate)	8	341	S	-
HD1	9	87	S[1]	-	HD2 (substrate)	9	440	S	-

[1] excluded from average values reported

APPENDIX D– REPORT SUBMITTED BY SIVA CORROSION SERVICES

August 8, 2013

Kent A. Harries Ph.D., P. Eng.
Associate Professor of Structural Engineering and Mechanics
Department of Civil and Environmental Engineering
University of Pittsburgh
742 Benedum Hall
Pittsburgh, PA 15261

Subject: Structural Evaluation of Slab Rehabilitation by the Method of Hydrodemolition and Latex Modified Overlay

Reference: Task 3 - Assessment of Field Conditions

1. Introduction

Siva Corrosion Services, Inc. (SCS) was retained by University of Pittsburgh (Pitt) to participate in the research project "Structural Evaluation of Slab Rehabilitation by Method of Hydrodemolition (HD) and Latex Modified Overlay (LMC)". SCS was assigned Task 3 of the project regarding field assessment of LMC overlays. The goal of this task was to document the in-situ performance of the HD-LMC deck rehabilitation method for five selected bridge decks.

HD-LMC rehabilitation has been performed on 149 bridge decks in PennDOT District 11. Pitt selected five bridges for field evaluation based on overlay conditions. Table 1 summarizes the locations and age of each bridge. These five bridges have LMC overlays varying from 4 to 15 years old.

Table 1. List of Selected Bridges for Task 3

Bridge ID	Bridge Location	Lane Closure	Year of Construction	Year of LMC Overlay
A	SR28 over Powers Run Rd	NB-Left Lane & Shoulder	1970	2002
B	SR28 over SR910	SB-Right Lane & Shoulder	1970	2008
C	SR79 over Route 50	SB-Left Lane & Shoulder	1965	1998
E	SR79 over Red Mud Hollow Rd	NB-Right Lane & Shoulder	1971	2009
F	SR837 to Homestead Ramps	NB-Right Lane & Shoulder	1966	2004

After reviewing relevant information on selected bridge decks, SCS performed the following evaluations per the scope of work:

Field Evaluations:

- Schedule and coordinate traffic control (provided by PennDOT)
- Select test locations based on visual condition of the decks
- Locate reinforcement and record rebar cover using Ground Penetrating Radar (GPR)
- Drill and extract two 4-inch diameter cores with rebar per bridge (10 total)
- Perform pull-off adhesion testing at three locations per bridge (15 total); collect concrete cores from adhesion test locations for laboratory testing
- Patch core locations with PennDOT approved cement-based mortar

Laboratory Evaluations:

- For 4-inch diameter cores, assess:
    - Bond between LMC and Substrate
    - Amplitude of LMC-Substrate interface
    - Presence/Absence of original concrete immediately below embedded reinforcement
    - Degree of corrosion of embedded steel
    - Sample and test chloride content at two locations (at immediately below the LMC-in the original concrete and at rebar depth) per core
    - Overlay depth and rebar depth
- For 2-inch diameter cores, assess:
    - Bond between LMC and Substrate
    - Amplitude of LMC-Substrate interface
    - Sample and test chloride content at two locations (at immediately below the LMC-in the original concrete and at rebar depth) per core
    - Overlay depth

2. Field Evaluations

2.1 Test Locations

A total of five cores were extracted per bridge (two 4-inch diameter cores with rebar and three 2-inch diameter cores without rebar). Coring locations were selected in the field based on the condition of the bridge deck. Locations of the cores were distributed throughout the bridge deck in 'problem areas' and 'sound areas' to obtain representative samples. Drawings in Appendix A display the locations of each core on all five bridge decks.

2.2 Extracting Cores

A delamination survey was performed on each deck using chain drag within traffic control area. No delamination was identified. Hammer sounding was performed at all core locations to confirm that no delamination was present. All 4-inch diameter cores were extracted from areas exhibiting cracking (problem areas) with one top mat rebar included in the core. All 2-inch diameter cores were extracted from sound areas that were free of delamination or cracking. Two-inch diameter cores were used for pull-off testing before extraction. Two-inch cores did not include reinforcement.

GPR was used to identify reinforcement and measure concrete cover at all core locations. GPR is a non-destructive instrument that emits electromagnetic waves into concrete, asphalt, soil, and other mediums. Radar waves reflect off of objects (such as rebars, strands, conduits, voids, water, etc.) embedded within the tested medium. Radargrams (images produced from a GPR scan) are interpreted to identify these objects. After calibration, depth of targets can be determined.

After each core was extracted, it was labeled using a permanent marker, clearly marking the top and bottom of the cores in the field. The core was then wrapped in burlap, sealed in a plastic bag, and later transported to SCS laboratory for further testing. All core holes were patched with a Penn DOT approved, non-ferrous, non-shrink, fast-setting cement based mortar (Euclid – Speed Crete Green Line).

2.3 Pull-off Tests

In order to quantitatively assess the bond quality between the LMC overlay and substrate, SCS performed three pull-off tests per bridge (at 2-inch diameter core locations) in accordance with ICRI Guideline No. 03739 "Guide to Using In-Situ Tensile Pull-Off Tests to evaluate Bond of Concrete Surface Materials".

At each 2-inch diameter core location, SCS drilled the core to a depth of approximately 3.5 inches, vacuumed out all standing water/contaminants, ground smooth the deck surface to facilitate good adhesion between the test dolly and concrete, and allowed the concrete to dry completely. When the concrete surface was wet, a hairdryer was used to promptly dry the surface. After the surface was dry, a 2-inch diameter aluminum dolly (rigid disk) was adhered to the drilled core surface using Devcon 5 Minute Epoxy Gel. The adhesive was allowed to cure for at least one hour (per manufacturer's instruction) before a pull-off test was performed. A Defelsko PosiTest Adhesion Tester was used to perform the pull-off tests in the field. A slow, steadily increasing force was applied to the dolly in the vertical direction (along the centerline of the cores) until failure was achieved. The failure mode (per ICRI 03739) and failure stress were recorded. After adhesion testing was performed, core holes were drilled deeper as necessary and 2-inch diameter cores were extracted for further laboratory testing. Figure 1 shows a typical core location before and after pull-off testing.

Figure 1. Pull-off test at Bridge A-L5. Rigid disc attached to the drilled core (Left); Core failed at substrate during pull-off testing (Right).

The purpose of pull-off adhesion testing is to quantify the condition of the bond between the overlay and substrate. If poor materials or poor surface preparation procedures are used during repairs, a good bond may not be achieved. This will result in lower pull-off stresses and could possibly lead to poor performance of the overlay.

During pull-off testing, failures will occur at the weakest material, bond, or at an internal flaw such as delamination. Figure 2 describes each possible failure mode per ICRI 03739. When failure occurs at the rigid disk or entirely within the substrate or overlay material (Failure Modes 1, 2 & 6), this indicates that the bond strength is greater than the measured stress. If failure occurs at or partially at the overlay-substrate interface (Failure Modes 3, 4 & 5), the recorded stress is an approximate measure of the bond strength between the overlay and substrate.

During pull-off testing at all five bridges, only failure modes 1, 3, 5, and 6 were observed. Since failure never occurred within the LMC overlay, the LMC is the strongest material in the composite system. Pull-off adhesion results are summarized in Appendix B.

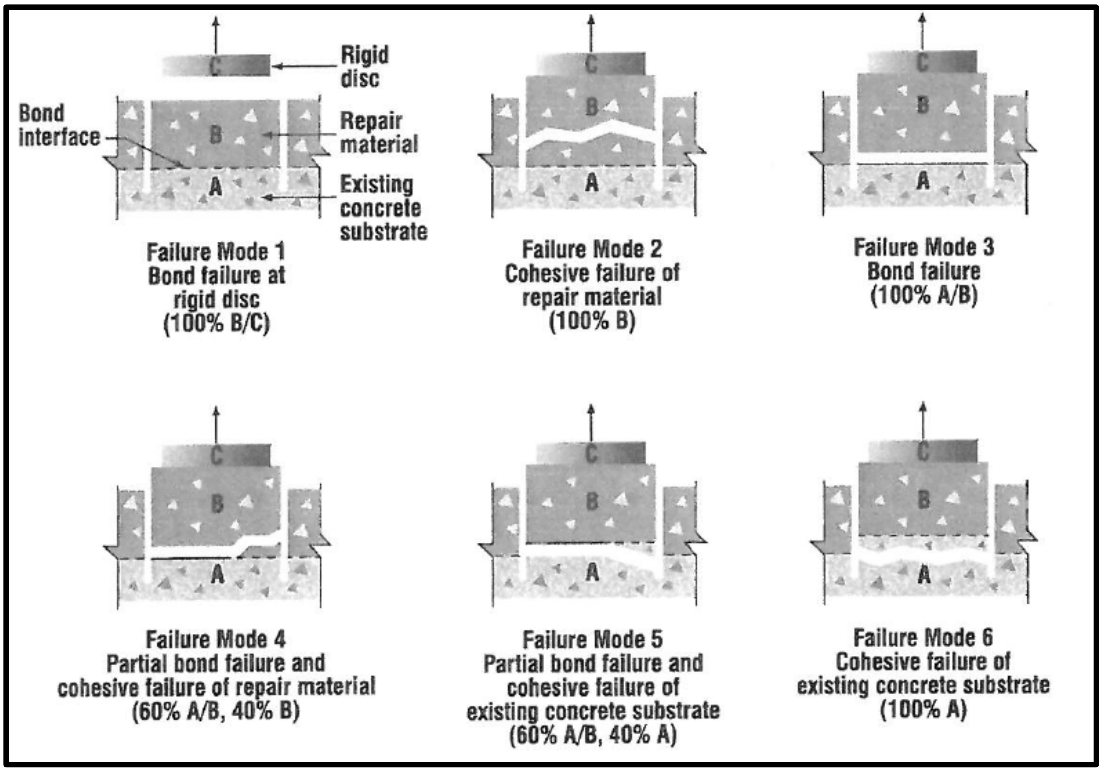

Figure 2. Pull-Off Failure Modes per ICRI 03739

It should be noted that at one of fifteen test locations (7%), the LMC overlay extended beyond the depth of coring. It is possible that at this location partial or full-depth concrete repairs were performed before the overlay placement, leading to deeper than average overlay depths.

At three other adhesion locations, the depth of initial coring did not extend beyond the overlay-base concrete interface (since the overlay depth was deeper than the average). At these locations, the bond strength registered in the field is not reflective of the actual bond strength between the overlay and base concrete. However, visual evaluation of the cores indicated that the bond between the overlay and base concrete was excellent. Due to limited lane closure times and the time required to prepare, test, and repair test locations, it was not possible to perform additional adhesion testing at these locations. SCS corrected for greater overlay depths by drilling deeper at other adhesion test locations to include the overlay-base concrete interface.

No established criterion exists for evaluating the performance of HD-LMC overlay repairs using pull-off testing. Too little data is available from the current field study to develop a statistically significant acceptance criterion. However, ICRI 03739 suggests that values less than 175 psi may indicate poor bonding.

The minimum recorded pull-off stress was 132 psi. However, this failure occurred within the substrate of Bridge C, indicating that the bond strength is greater than the substrate (> 132 psi). The lowest recorded bond strength (Failure Modes 3-5) was 153 psi. All other bond strengths were 199 psi or greater. This indicates that the overlay is well-bonded to the base concrete in 82% (9 of 11) of the deck.

3. Laboratory Evaluations

3.1 Core Evaluations

All extracted cores were transported to the SCS laboratory for visual evaluation and chloride content analysis. For each core, the length, overlay depth, rebar depth, and bond interface amplitude were recorded. Additionally, cracking, corrosion, and bond quality in each core were assessed. After visual evaluations were completed, powder samples were collected and tested per ASTM C1152.

3.2 Overlay and Bond Condition

The overlay depth varied from 1.4 inches to over 5.1 inches; at this location, the overlay extended beyond the depth of the core. The average overlay depth was 2.9 inches with a standard deviation of 0.9 inches. Hydrodemolition is expected to result in varying overlay depth. The amplitude of the overlay-substrate interface varied from 0.3 inches to 1.4 inches, with an average of 0.6 inches. Measurements for each core are summarized in Appendix C.

The bond quality appeared good in 17 of 24 cores. Of the remaining 7 cores, 4 exhibited complete or partial failure at the bond interface during pull-off testing, and 3 (out of 10 4-inch cores with rebars) exhibited cracking due to reinforcement corrosion, see Figure 3.

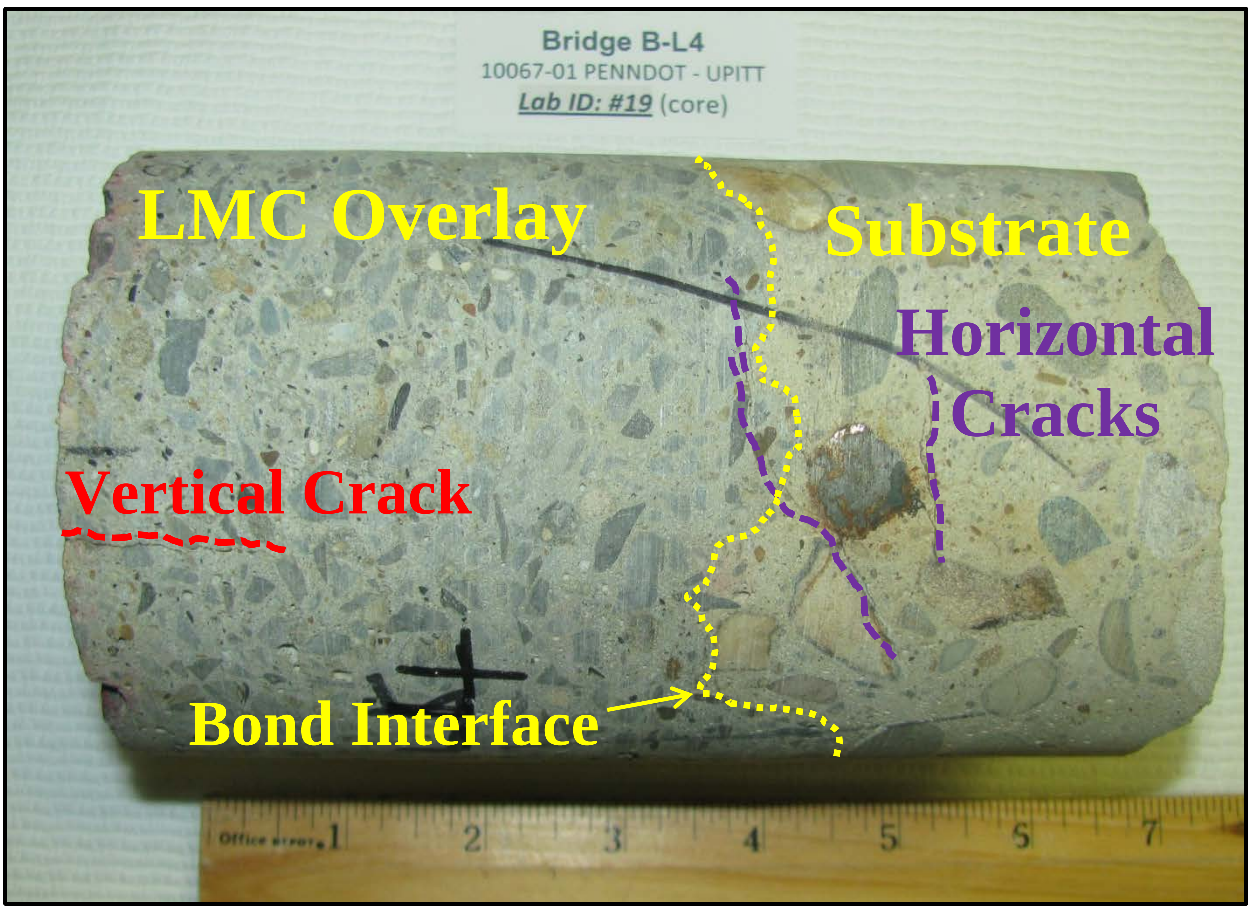

Figure 3. Core with vertical crack and horizontal cracking due to reinforcement corrosion.

SIVA CORROSION SERVICES, INC.
NDT • Corrosion • Materials Specialists

3.3 Cracking Defects and Reinforcement Corrosion

A total of ten 4-inch diameter cores were drilled through a top mat rebar in areas exhibiting cracking (i.e. problem area). Vertical crack depths varied from 0.8 inches to the full depth of the core. Vertical cracking was generally confined to the overlay (8 out of 10 cores). In addition to vertical cracking, 8 of 10 cores failed at the rebar level during extraction. Crack, overlay, and rebar depth are summarized in Appendix D. All fifteen 2-inch diameter cores were drilled in areas of sound concrete without cracking or reinforcement.

Rebars were extracted from all 4-inch diameter cores. Rebar conditions were documented with photographs (see Appendix E) and diameter losses of the rebar were recorded (see Appendix D). Nine out of ten (90%) rebars exhibited diameter loss due to corrosion, varying from 3% to 25%. This corrosion likely caused cracking at the top mat rebar level, which led to failure of the cores at the rebar level during extraction.

The cores that did not break during extraction (cores B-L4 and F-L4) also exhibited substantial rebar diameter losses. The core (B-L4) shown in Figure 3 exhibited horizontal cracking at the rebar level due to corrosion. Since the rebar in core B-L4 was located in the original chloride contaminated concrete (as opposed to overlay concrete with possibly less chloride contamination), continued corrosion of the rebar will occur and lead to delamination and spalling.

The entire core F-L4 (6.8" long) had only overlay material. No original concrete was a part of this core. The rebar from core F-L4 was centered along a vertical crack. Though the vertical crack extended past the rebar, the core was extracted without any horizontal cracking at the rebar level. This indicates that the crack may be structural in nature and that it allowed for corrosion product expansion without delamination. Even though the rebar had a significant section loss (25%), the core was extracted intact. This is due to the fact that corrosion product present on the rebar prior to overlay placement was removed during repairs/overlay placement.

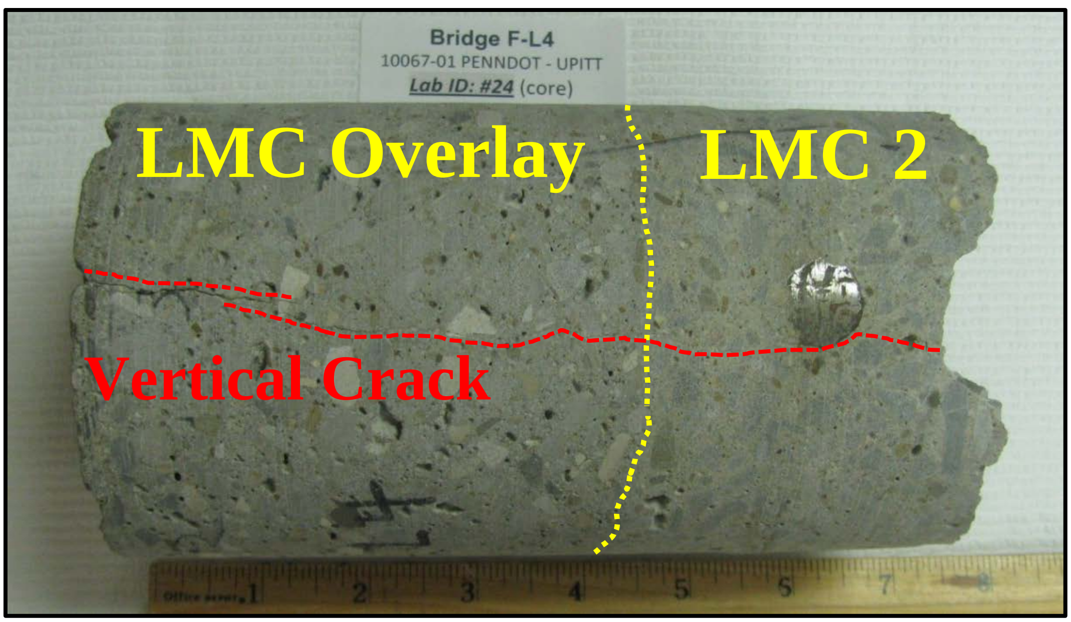

Figure 4. Core with two layers of LMC and full depth vertical crack.

3.4 Overlay and Rebar Depth

The average rebar depth for all five bridges was 4.0 inches with a minimum and maximum cover of 2.4 and 5.6 inches, respectively. The average overlay depth was 2.9 inches. The LMC overlay typically does not extend beyond the top mat steel. Three of fifteen (20%) 2-inch diameter cores exhibited overlay depths greater than the measured rebar depth. It is possible that these are locations where partial or full depth repairs were performed. The LMC depth exceeded the rebar depth in one of ten 4-inch diameter cores (Bridge F – L4). LMC surrounds the rebar and at least 0.5 inches below the rebar (Figure 4).

3.5 Chloride Content

Chloride powder samples were collected at two depths from each core. The goal was to collect one sample immediately below the LMC-substrate interface (in the original concrete), and one sample at the top mat rebar. However, the overlay depth varied relative to the rebar depth. At various locations, the rebar was located below the interface, at the interface, or above the interface. Sample depths were selected based on overlay and rebar depth. Table 2 summarizes the sampling depths for each overlay-rebar depth relationship. Powder samples collected from the cores were prepared and tested in accordance with ASTM C1152 Standard Test Method for Acid-Soluble Chloride in Mortar and Concrete. Chloride contents for each core are summarized in Appendix F.

Table 2. Core Sampling Depths

LMC Overlay - Rebar Relationship	No. of Locations	Sample 1	Sample 2
Rebar deeper than LMC-substrate interface	13	Below Interface	At Rebar Depth
Rebar at LMC-substrate interface	6	At Rebar Depth	Below Rebar
Rebar above LMC-substrate interface	4	At Rebar Depth	Below Interface
No LMC-substrate interface observed*	2	Above Rebar	At Rebar Depth

*At two locations (Bridge E–L5 and Bridge F–L4), cores did not include any substrate concrete. It is possible that full-depth repairs were performed at these locations. For these cores, one sample was collected at the rebar level and one sample was collected 0.5 inches above the rebar.

All vertical cracks terminate nearly two inches before the top mat rebar, except at Bridge F–L4. Chloride content was found to be well above the threshold for corrosion of 350ppm[1] in all samples from 4-inch diameter cores. The high chloride content has led to significant reinforcement corrosion, as observed in extracted cores. Vertical cracking in these cores may have led to accelerated accumulation of chlorides at the rebar level. Chloride likely accumulated in the substrate concrete before HD-LMC rehabilitation. Since HD did not typically remove concrete below the reinforcement, chloride content is high in the substrate. This will lead to corrosion-related concrete damage.

[1] SHRP-S-377 – "Life-Cycle Cost Analysis for Protection and Rehabilitation of Concrete Bridges Relative to Reinforcement Corrosion," Washington, D.C., 1994.

Chloride content at the rebar depth was above the threshold for corrosion in six of fifteen 2-inch diameter cores (40% of the deck area). Chloride contamination at the rebar level is widespread and will lead to corrosion-related concrete damage. No delamination was identified on the inspected bridge decks via chain drag/hammer sounding. However, cores from areas with vertical cracking already exhibited horizontal cracking at the top mat rebar due to corrosion. Chloride data from 2-inch and 4-inch diameter cores indicate that these bridge decks will experience significant corrosion-related concrete damage in the near future (5-10 years). SCS can confirm this by performing service life analysis if the Department so desires.

It should be noted that in 36% of the cases, chloride content did not decrease with increasing depth as expected for a typical diffusion profile. Many samples were taken just below the interface between LMC and substrate concrete. When chloride-free concrete is placed above contaminated base concrete, some chlorides diffuse out of the substrate into the overlay. This may account for chloride contents in some cases being lower at shallower depths than at deeper depth, contrary to a typical chloride profile. The number of chloride samples per core specified in the scope of work is too low to confidently determine the cause of this variation.

4. Conclusion and Discussion

- The overlay depth ranged from 1.4 inches to greater than 5.1 inches. The average overlay depth was 2.9 inches. The amplitude of the overlay-substrate interface varied from 0.3 inches to 1.4 inches, with an average of 0.6 inches.
- The LMC overlay typically did not extend beyond the top mat steel. Only four of twenty-five (16%) cores exhibited overlay depths greater than the top mat rebar depth. In one core where the rebar was embedded in LMC, no substrate concrete was observed immediately behind the rebar.
- The LMC-Substrate bond visually appeared to be in good condition.
- Pull-off adhesion testing indicated that the LMC is typically well bonded to the substrate concrete, based on limited data. The measured bond strength was greater than 175 psi in nine of eleven valid test locations (82%).
- Since hydrodemolition did not remove concrete beyond the top mat rebar level, chloride-contaminated concrete remained in place in original concrete (after HD-LMC deck rehabilitation).
- Chloride content at the rebar level was above the threshold for corrosion in 40% of cores from sound concrete and 100% cores from areas of the decks with vertical cracking. In addition, deicing salt is accumulating at the rebar level at a faster rate due to the presence of vertical cracks. This will increase the rate of concrete damage in the future.
- The high level of chloride contamination will lead to significant corrosion-related concrete damage in 5-10 years.
- Nine of ten rebars (90%) extracted from the deck exhibited diameter losses due to corrosion. Diameter losses ranged from 3% to 25%. Buildup of corrosion product has led to cracking at the top mat rebar level in cores with vertical cracking.
- Since the LMC overlays are less than 15 years old (placed in 1998 or after), the overlays may not achieve a service life of 25 years due to rebar corrosion.
- Chloride profiling and service life modeling to predict the service life of HD-LMC repairs are beyond the scope of work for Task 3.

If you have any questions or need additional information, please do not hesitate to contact me at (610) 692-6551 or Stu@SivaCorrosion.com. Thank you for the opportunity to be of service.

Very Truly Yours,

Stuart Mundth
Project Engineer
Siva Corrosion Services, Inc.

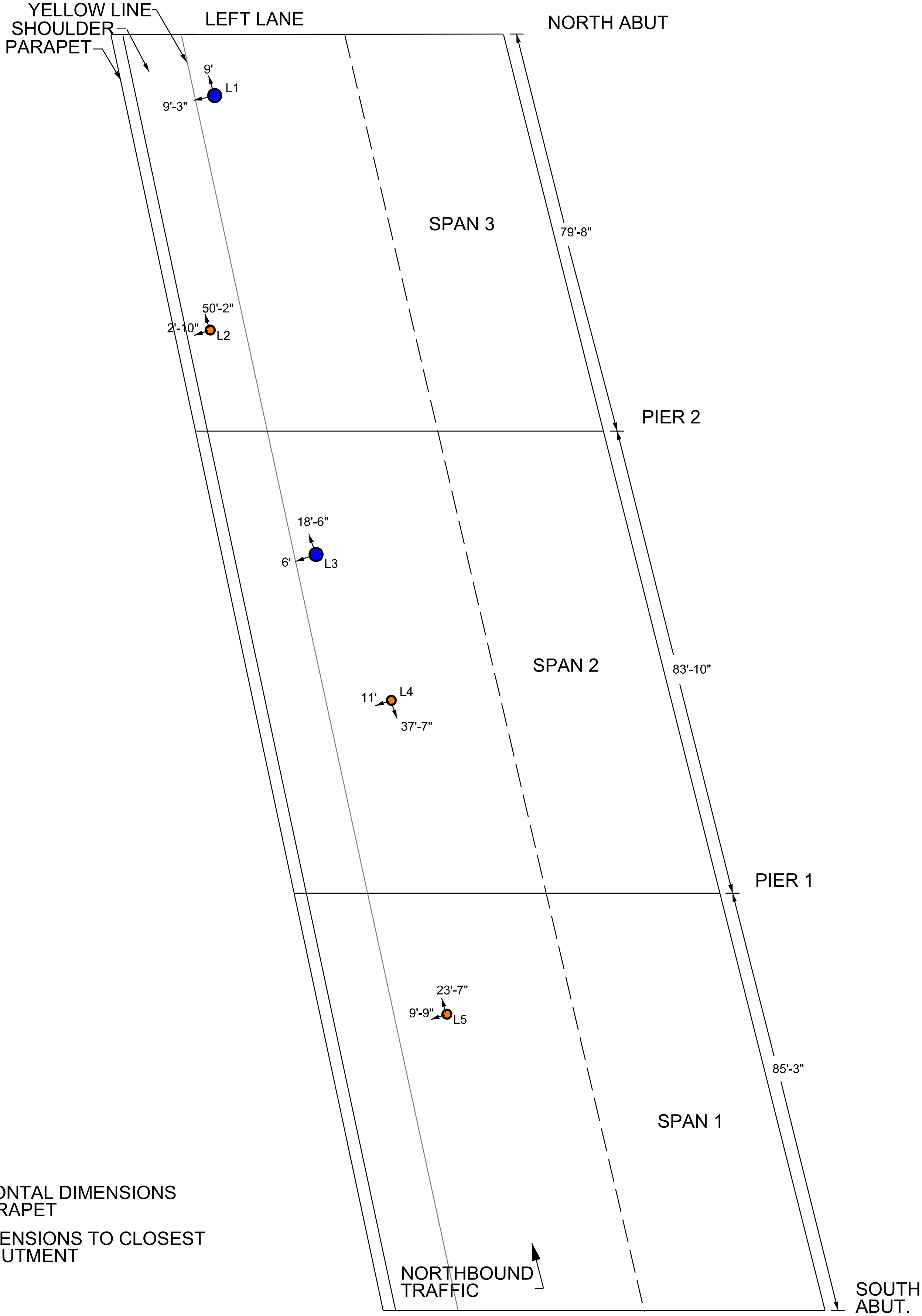

NOTES:
ALL HORIZONTAL DIMENSIONS ARE TO PARAPET

OTHER DIMENSIONS TO CLOSEST PIER OR ABUTMENT

LEGEND:
- 2" CORE
- 4" CORE

SR 28 OVER POWERS RUN RD - NB
SCALE: NTS

SIVA CORROSION SERVICES, INC.
MATERIALS, CORROSION, AND NDT SPECIALISTS

BRIDGE ID NUMBER: A PROJECT NUMBER: 10067-01 PENNDOT	CORE LOCATIONS SHEET 1 OF 5

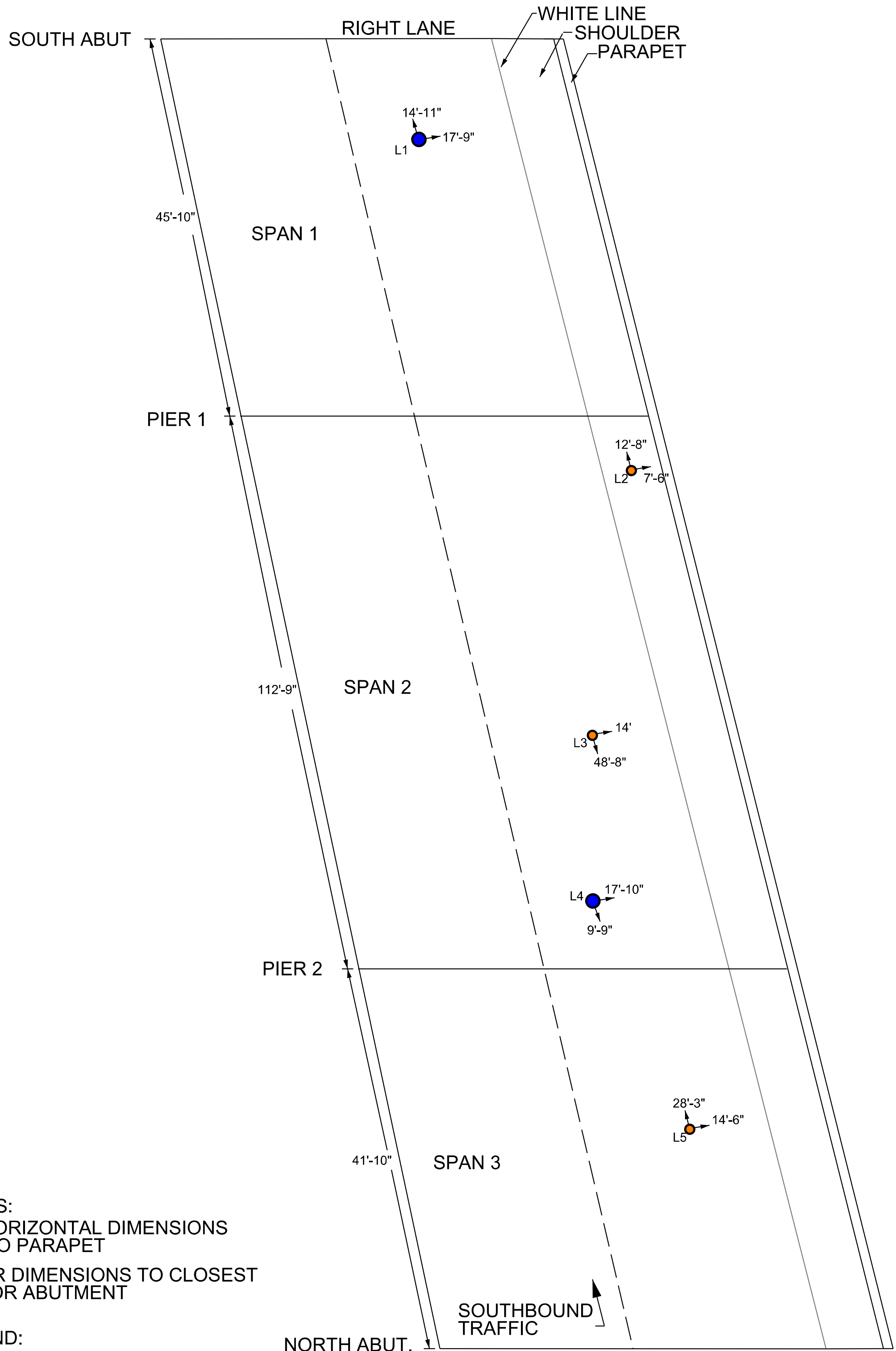

SR 28 OVER SR910 - SB

SCALE: NTS

NOTES:

ALL HORIZONTAL DIMENSIONS ARE TO PARAPET

OTHER DIMENSIONS TO CLOSEST PIER OR ABUTMENT

LEGEND:

- 2" CORE
- 4" CORE

SCS

SIVA CORROSION SERVICES, INC.

MATERIALS, CORROSION, AND NDT SPECIALISTS

BRIDGE ID NUMBER: B PROJECT NUMBER: 10067-01 PENNDOT	CORE LOCATIONS SHEET 2 OF 5

P:\SCS Active Projects - Sharing Folder\10067-01 PennDOT - UPITT - Deck Overlay\5 - Drawings\2_SR28Over910.dgn

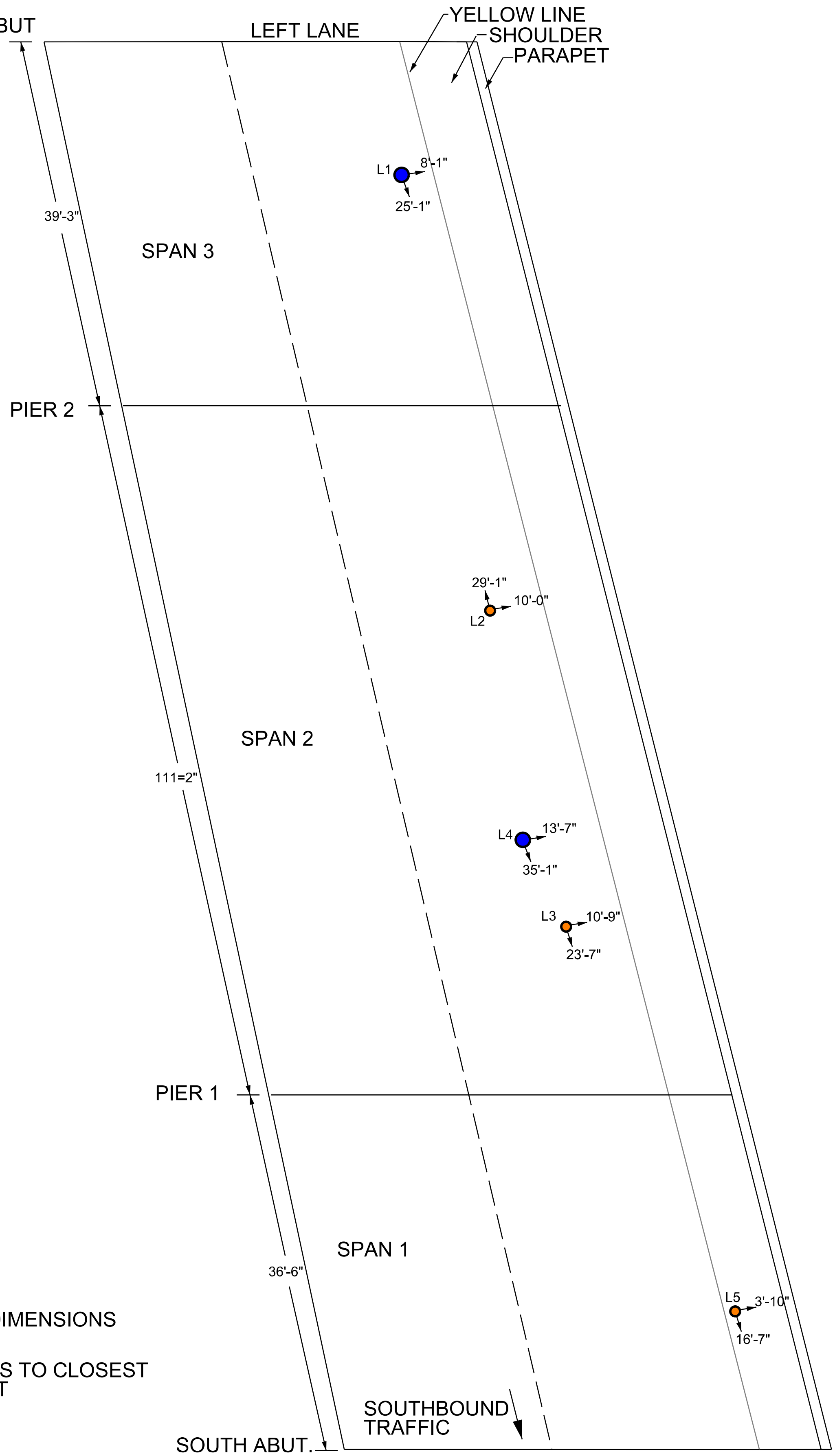

SR 79 OVER RT 50 - SB

SCALE: NTS

NOTES:

ALL HORIZONTAL DIMENSIONS ARE TO PARAPET

OTHER DIMENSIONS TO CLOSEST PIER OR ABUTMENT

LEGEND:

- 2" CORE
- 4" CORE

SIVA CORROSION SERVICES, INC.
MATERIALS, CORROSION, AND NDT SPECIALISTS

BRIDGE ID NUMBER: C PROJECT NUMBER: 10067-01 PENNDOT	CORE LOCATIONS SHEET 3 OF 5

P:\SCS Active Projects - Sharing Folder\10067-01 PennDOT - UPITT - Deck Overlay\5 - Drawings\3_SR79overRt50.dgn

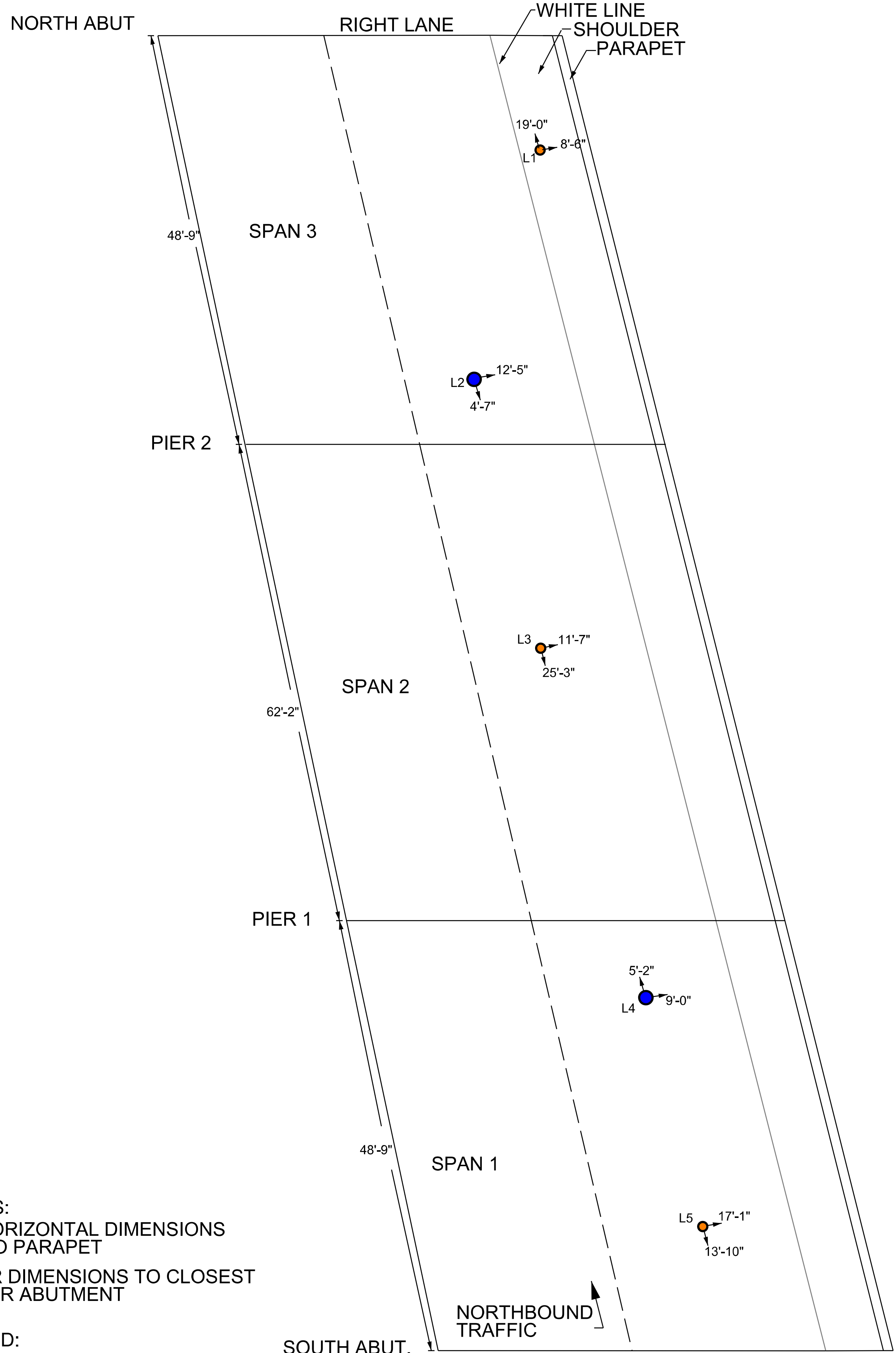

NOTES:
ALL HORIZONTAL DIMENSIONS ARE TO PARAPET

OTHER DIMENSIONS TO CLOSEST PIER OR ABUTMENT

LEGEND:
- 2" CORE
- 4" CORE

SR 79 OVER RED MUD RD - NB
SCALE: NTS

SIVA CORROSION SERVICES, INC.
MATERIALS, CORROSION, AND NDT SPECIALISTS

BRIDGE ID NUMBER: E PROJECT NUMBER: 10067-01 PENNDOT	CORE LOCATIONS SHEET 4 OF 5

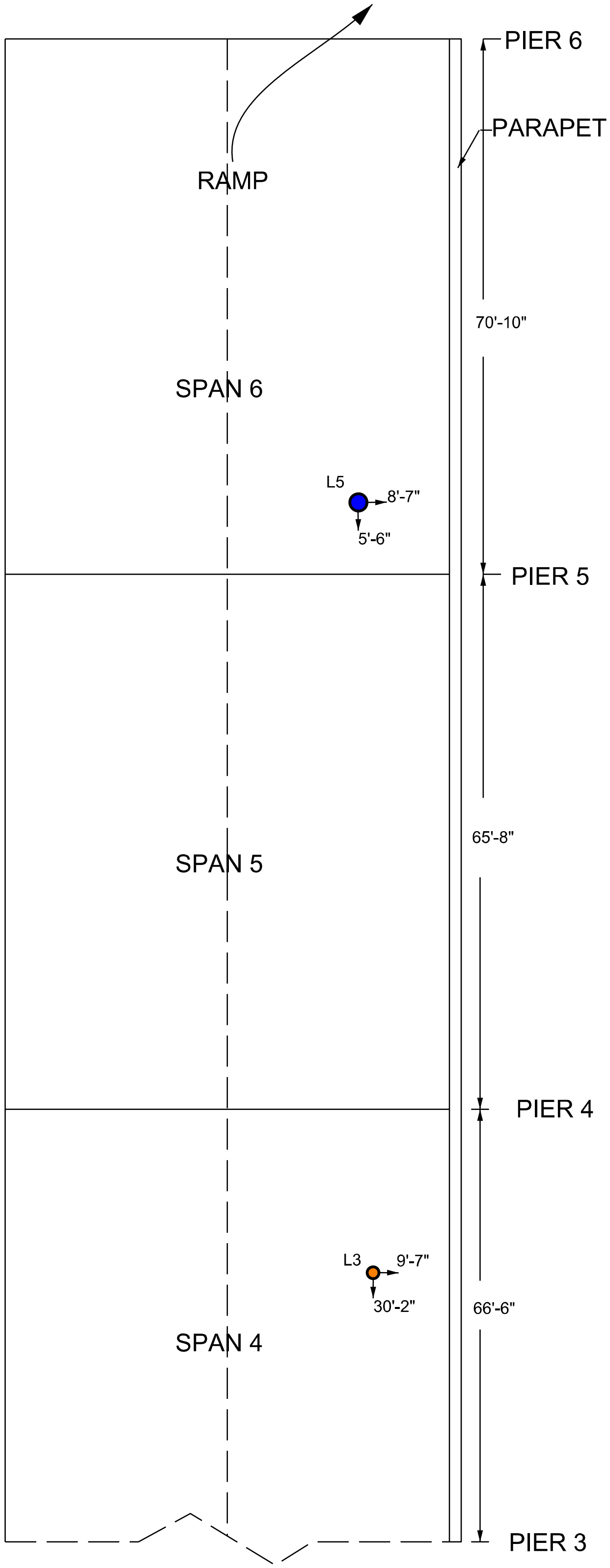

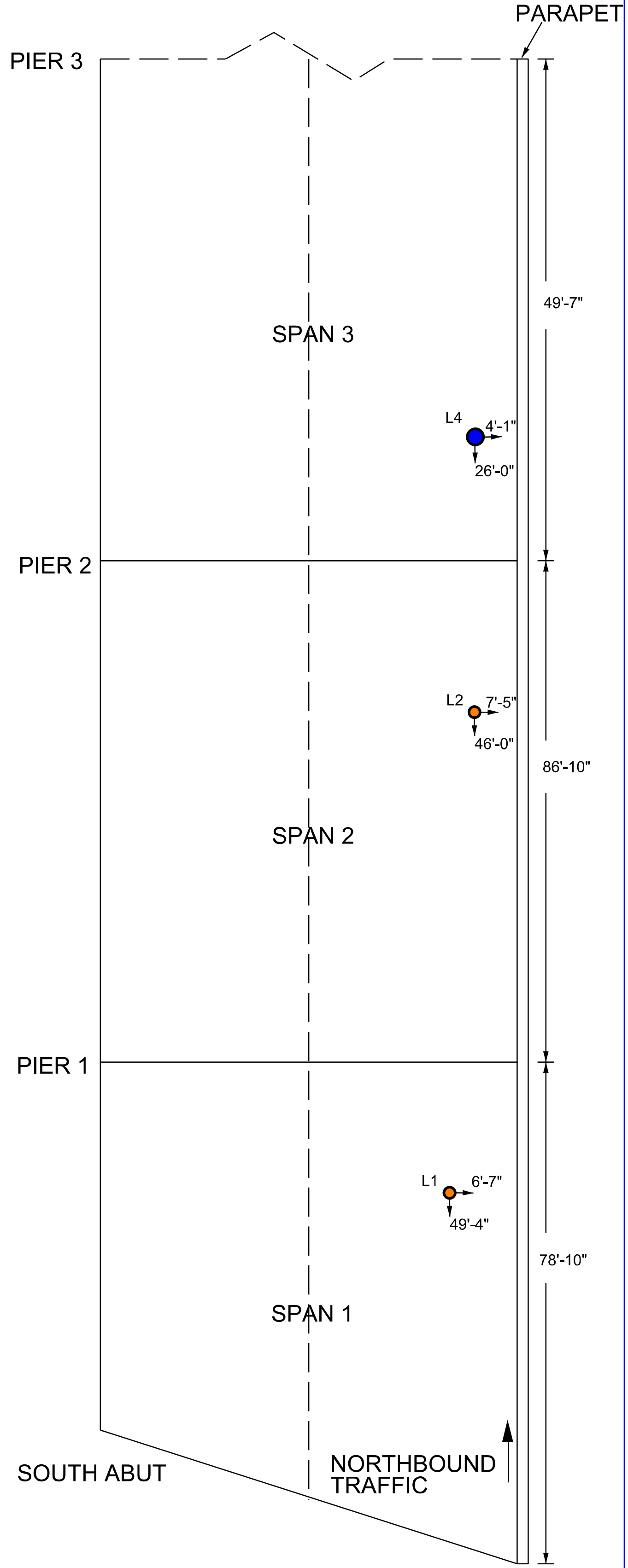

NOTES:
ALL HORIZONTAL DIMENSIONS ARE TO PARAPET

OTHER DIMENSIONS TO CLOSEST PIER OR ABUTMENT

LEGEND:
- 2" CORE
- 4" CORE

SR 837 TO HOMESTEAD RAMP - NB
SCALE: NTS

SIVA CORROSION SERVICES, INC.
MATERIALS, CORROSION, AND NDT SPECIALISTS

BRIDGE ID NUMBER: F
PROJECT NUMBER: 10067-01 PENNDOT

CORE LOCATIONS
SHEET 5 OF 5

P:\SCS Active Projects - Sharing Folder\10067-01 PennDOT - UPITT - Deck Overlay\5 - Drawings\5_SR837ToHomeSteadRamp.dgn

Summary of Pull-Off Test Results

No.	Location ID	Bond Strength (psi)	Pull-off Failure Mode*	Weather Conditions
1	SR28 (Bridge A) - L2	199	5	Morning rain showers
2	SR28 (Bridge A) - L4	331	1	Morning rain showers
3	SR28 (Bridge A) - L5	326	6	Morning rain showers
4	SR28 (Bridge B) - L2	358	6	Raining in early morning
5	SR28 (Bridge B) - L3	352	1	Raining in early morning
6	SR28 (Bridge B) - L5	334	1	Raining in early morning
7	SR79 (Bridge C) - L2	153	3	Sunny; lower 50s (˚F)
8	SR79 (Bridge C) - L3	320	6	Sunny; lower 50s (˚F)
9	SR79 (Bridge C) - L5	132	6	Sunny; lower 50s (˚F)
10	SR79 (Bridge E) - L1**	348	1	Sunny
11	SR79 (Bridge E) - L3**	166	1	Sunny
12	SR79 (Bridge E) - L5**	308	1	Sunny
13	SR837 (Bridge F) - L1**	369	1	Raining in the morning
14	SR837 (Bridge F) - L2	331	5	Raining in the morning
15	SR837 (Bridge F) - L3	237	3	Raining in the morning
	Minimum	132		
	Average	270		
	Maximum	358		

* Pull-off Failure Modes:

Mode 1: Bond failure at rigid disc - Actual bond strength is greater than the recorded value
Mode 2: Cohesive failure of repair material - Failure within LMC overlay material
Mode 3: Bond failure
Mode 4: Partial bond failure and cohesive failure of repair material
Mode 5: Partial bond failure and cohesive failure of existing concrete substrate
Mode 6: Cohesive failure of existing concrete substrate - Bond strength is greater than recorded value

** LMC overlay extends beyond core depth. Failure stress does not reflect interface bond strength.

Summary of Overlay and Bond Conditions

No.	Core ID	Core Dia.	Core Length	Overlay Depth (Min)	Overlay Depth (Max)	Overlay Depth (Avg)	Overlay Amplitude	Bond Condition (Visual)	Notes
1	SR28 (Bridge A) - L2	2	6.0	3.3	4.1	3.7	0.9	Partial Failure	Failure during pull-off testing
2	SR28 (Bridge A) - L4	2	6.0	1.6	2.0	1.8	0.4	Good	
3	SR28 (Bridge A) - L5	2	6.0	2.0	2.8	2.4	0.8	Good	
4	SR28 (Bridge B) - L2	2	5.5	1.8	2.5	2.1	0.8	Good	
5	SR28 (Bridge B) - L3	2	5.8	2.6	3.1	2.9	0.5	Good	
6	SR28 (Bridge B) - L5	2	5.6	1.6	2.0	1.8	0.4	Good	
7	SR79 (Bridge C) - L2	2	6.1	1.9	2.1	2.0	0.3	Failed	Failure during pull-off testing
8	SR79 (Bridge C) - L3	2	5.8	1.8	2.3	2.0	0.5	Good	
9	SR79 (Bridge C) - L5	2	6.1	3.0	3.8	3.4	0.8	Good	
10	SR79 (Bridge E) - L1	2	5.8	3.1	3.9	3.5	0.8	Good	
11	SR79 (Bridge E) - L3	2	5.5	4.0	5.0	4.5	1.0	Good	
12	SR79 (Bridge E) - L5	2	5.1	>5.1	>5.1	>5.1	N/A	NA	Overlay deeper than core depth
13	SR837 (Bridge F) - L1	2	5.8	3.8	4.1	3.9	0.4	Good	
14	SR837 (Bridge F) - L2	2	5.5	2.8	3.0	2.9	0.3	Partial Failure	Failure during pull-off testing
15	SR837 (Bridge F) - L3	2	5.9	3.1	3.4	3.3	0.3	Failed	Failure during pull-off testing
16	SR28 (Bridge A) - L1	4	7.1	2.4	3.4	2.9	1.1	Good	
17	SR28 (Bridge A) - L3	4	7.4	1.4	2.8	2.1	1.4	Good	
18	SR28 (Bridge B) - L1	4	7.0	3.4	4.3	3.8	0.8	Partial Failure	Due to corrosion of the rebar
19	SR28 (Bridge B) - L4	4	6.4	3.3	4.1	3.7	0.9	Cracking	Due to corrosion of the rebar
20	SR79 (Bridge C) - L1	4	7.1	2.1	2.7	2.4	0.6	Good	
21	SR79 (Bridge C) - L4	4	7.3	2.0	2.5	2.3	0.5	Good	
22	SR79 (Bridge E) - L2	4	7.9	3.4	3.8	3.6	0.4	Good	
23	SR79 (Bridge E) - L4	4	7.9	2.4	3.8	3.1	1.4	Good	
24	SR837 (Bridge F) - L4	4	6.8	3.9	4.1	4.0	0.3	Good	
25	SR837 (Bridge F) - L5	4	5.9	2.1	2.8	2.4	0.6	Partial Failure	Due to corrosion of the rebar
				1.4	**>5.1**	**2.9**			

Note: All units are in inches.

Summary of Core Rebar Corrosion

No.	Core ID	Overlay Depth (Avg)	Rebar Depth	Rebar Location	Vertical Crack Depth	Broke at Rebar During Extraction	Nominal Rebar Size	Rebar Diameter Loss (%)	Notes
1	SR28 (Bridge A) - L2	3.6	3.5	Interface	NA	NA	NA	NA	
2	SR28 (Bridge A) - L4	1.8	3.5	Substrate	NA	NA	NA	NA	
3	SR28 (Bridge A) - L5	2.4	4.1	Substrate	NA	NA	NA	NA	
4	SR28 (Bridge B) - L2	2.1	2.6	Substrate	NA	NA	NA	NA	
5	SR28 (Bridge B) - L3	2.9	4.0	Substrate	NA	NA	NA	NA	
6	SR28 (Bridge B) - L5	1.8	3.4	Substrate	NA	NA	NA	NA	
7	SR79 (Bridge C) - L2	2.0	4.5	Substrate	NA	NA	NA	NA	
8	SR79 (Bridge C) - L3	2.0	3.8	Substrate	NA	NA	NA	NA	
9	SR79 (Bridge C) - L5	3.4	4.4	Substrate	NA	NA	NA	NA	
10	SR79 (Bridge E) - L1	3.5	4.7	Substrate	NA	NA	NA	NA	
11	SR79 (Bridge E) - L3	4.5	3.8	Substrate	NA	NA	NA	NA	
12	SR79 (Bridge E) - L5	>5.1	4.8	LMC	NA	NA	NA	NA	
13	SR837 (Bridge F) - L1	3.9	3.0	LMC	NA	NA	NA	NA	
14	SR837 (Bridge F) - L2	2.9	3.3	Substrate	NA	NA	NA	NA	
15	SR837 (Bridge F) - L3	3.3	2.4	LMC	NA	NA	NA	NA	
16	SR28 (Bridge A) - L1	2.9	4.2	Substrate	0.8	Yes	#4	7%	No corrosion observed
17	SR28 (Bridge A) - L3	2.1	4.4	Substrate	1.3	Yes	#4	7%	
18	SR28 (Bridge B) - L1	3.8	3.5	Interface	1.5	Yes	#4	7%	
19	SR28 (Bridge B) - L4	3.7	3.5	Interface	1.1	No	#4	19%	Cracking present due to corrosion
20	SR79 (Bridge C) - L1	2.4	4.6	Substrate	1.6, 2.2	Yes	#5	3%	Two vertical cracks present
21	SR79 (Bridge C) - L4	2.3	4.6	Substrate	0.8	Yes	#5	6%	
22	SR79 (Bridge E) - L2	3.6	5.6	Substrate	0.8	Yes	#4	14%	
23	SR79 (Bridge E) - L4	3.1	5.5	Substrate	1.8	Yes	#4	0%	
24	SR837 (Bridge F) - L4	4.0	4.9	LMC	Full Depth	No	#5	25%	Two layers of LMC were observed
25	SR837 (Bridge F) - L5	2.4	2.6	Interface	0.9	Yes	#5	17%	

Note: All units are in inches.
All rebars are black bars.
Diameter Loss (%) = (Nominal Diameter-Measured Minimum Diameter)/Nominal Diameter * 100
2-inch diameter cores are shown in gray. All other cores are 4-inch diameter.

REBAR COVER		
	Min	2.4
	Max	5.6
	Avg	4.0
	StDev	0.9

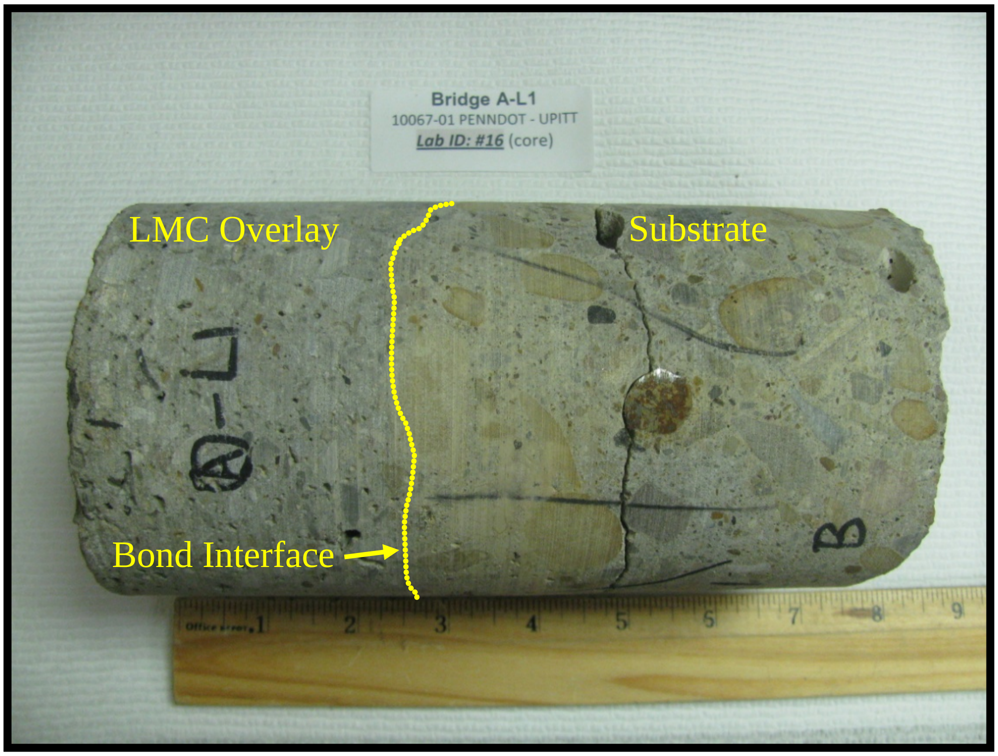

Photograph 1: SR28 (Bridge A) – L1 - Core

Photograph 2: SR28 (Bridge A) – L1 - Rebar

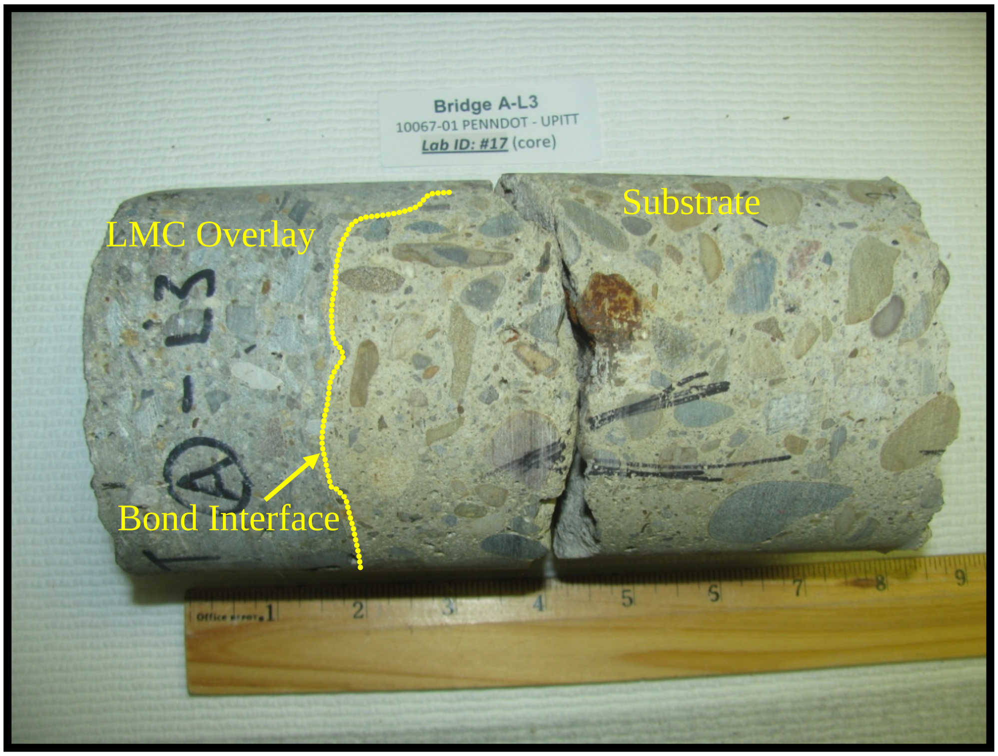

Photograph 1: SR28 (Bridge A) – L3 - Core

Photograph 2: SR28 (Bridge A) – L3 - Rebar

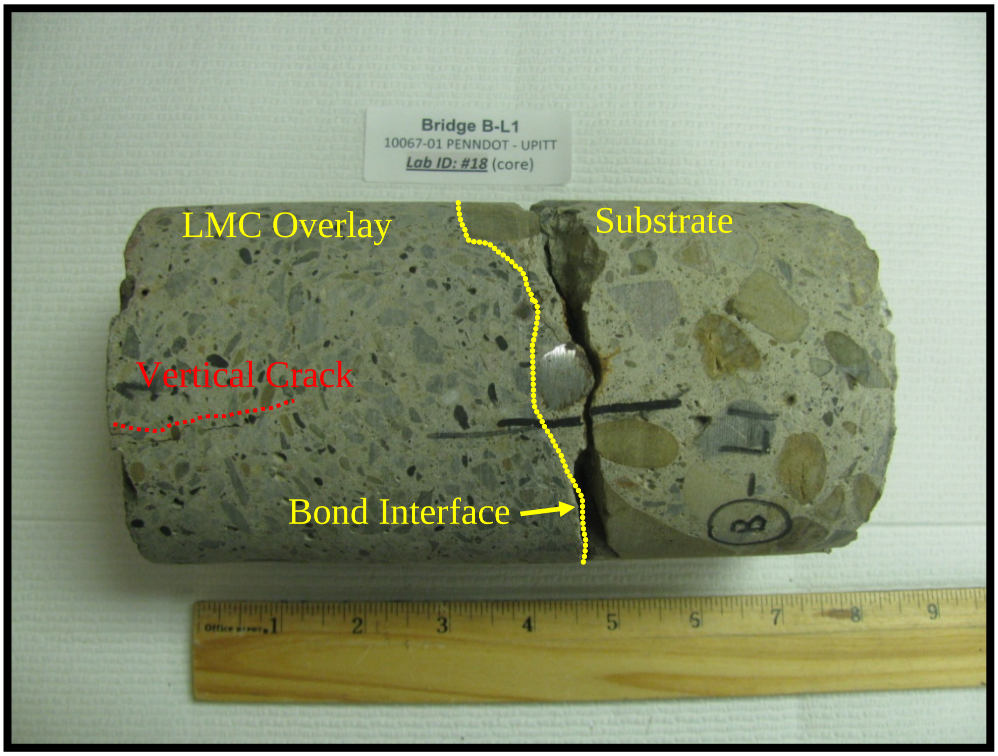

Photograph 1: SR28 (Bridge B) – L1 - Core

Photograph 2: SR28 (Bridge B) – L1 - Rebar

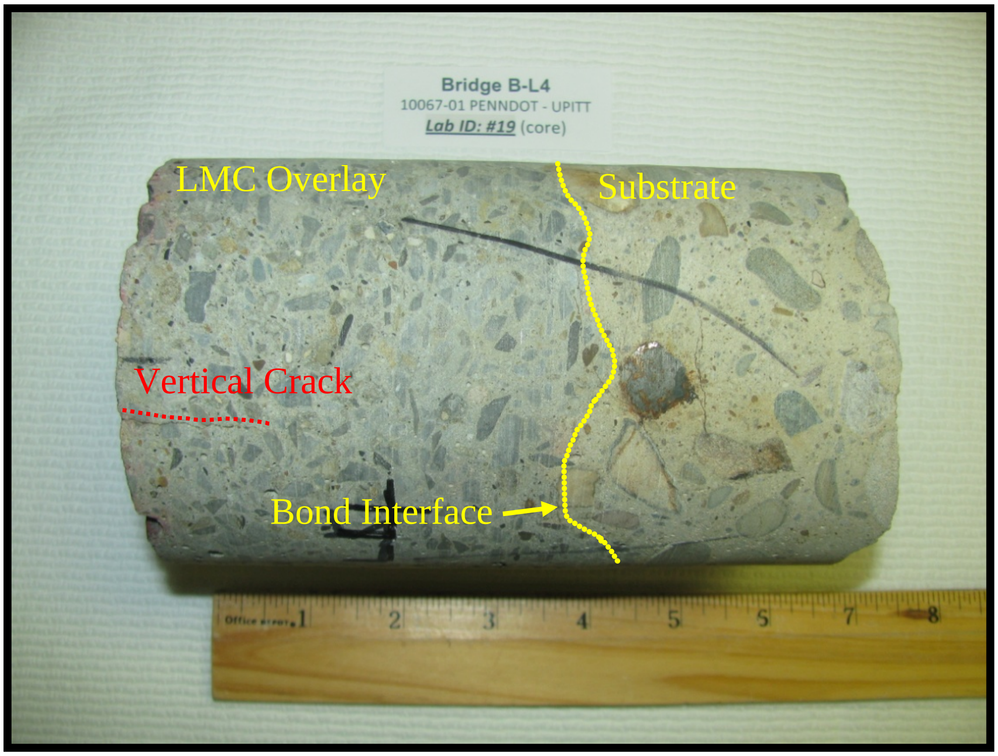

Photograph 1: SR28 (Bridge B) – L4 - Core

Photograph 2: SR28 (Bridge B) – L4 - Rebar

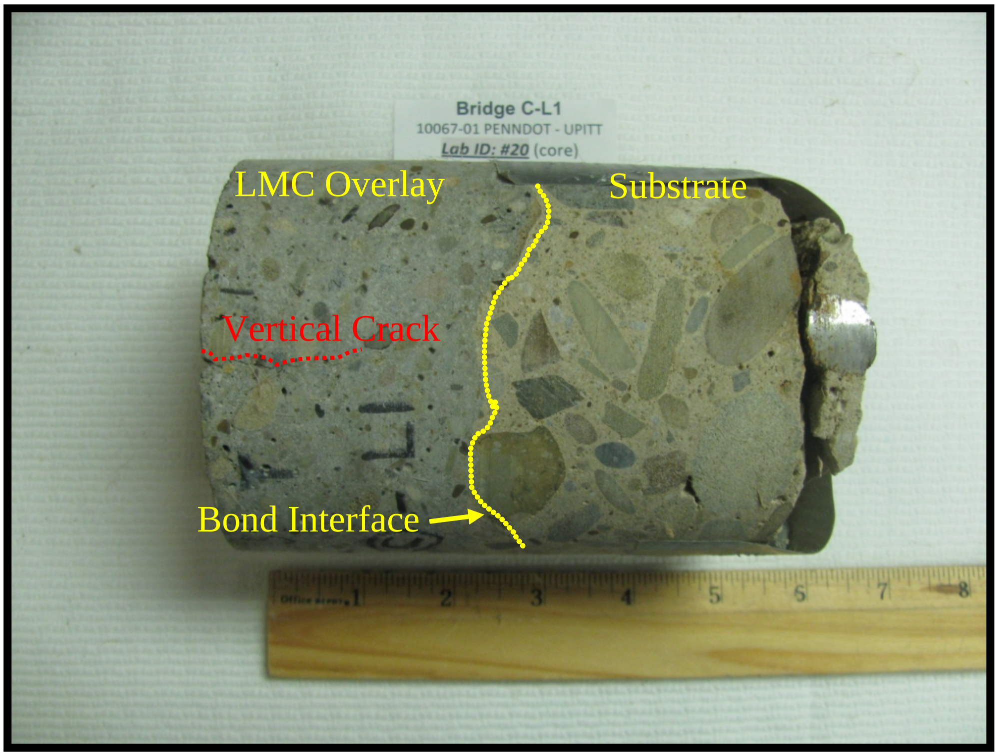

Photograph 1: SR79 (Bridge C) – L1 - Core

Photograph 2: SR79 (Bridge C) – L1 - Rebar

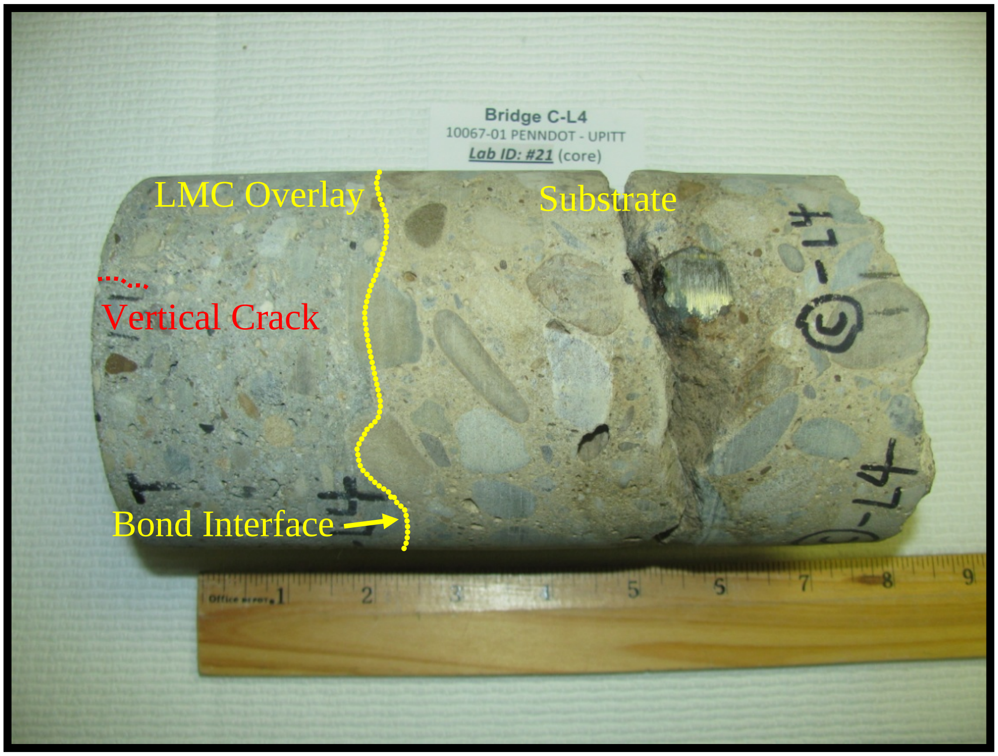

Photograph 1: SR79 (Bridge C) – L4 - Core

Photograph 2: SR79 (Bridge C) – L4 - Rebar

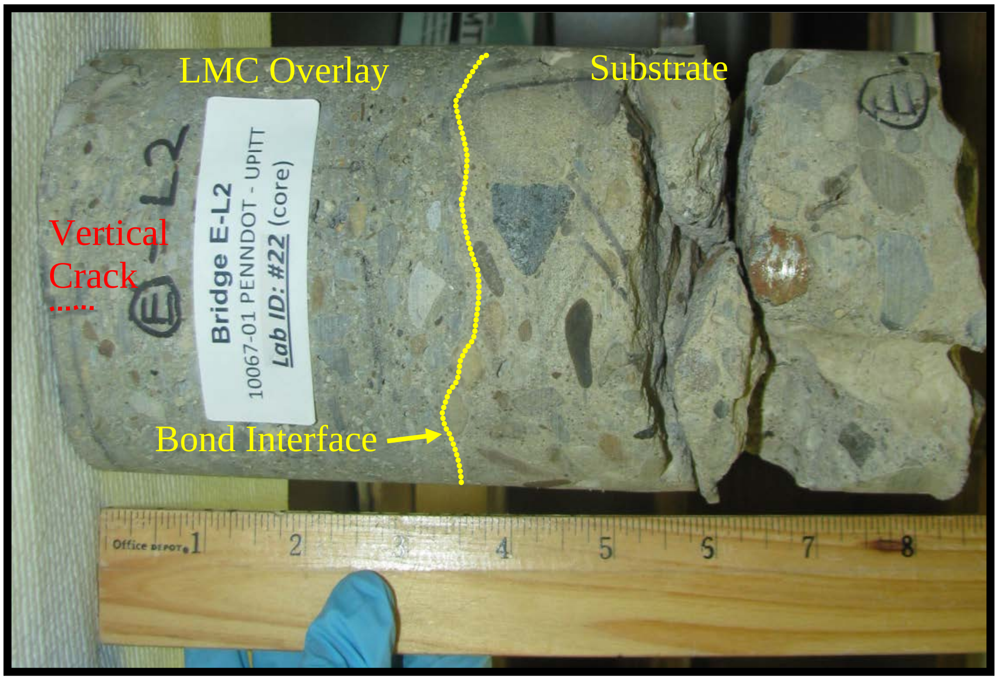

Photograph 1: SR79 (Bridge E) – L2 – Core

Photograph 2: SR79 (Bridge E) – L2 - Rebar

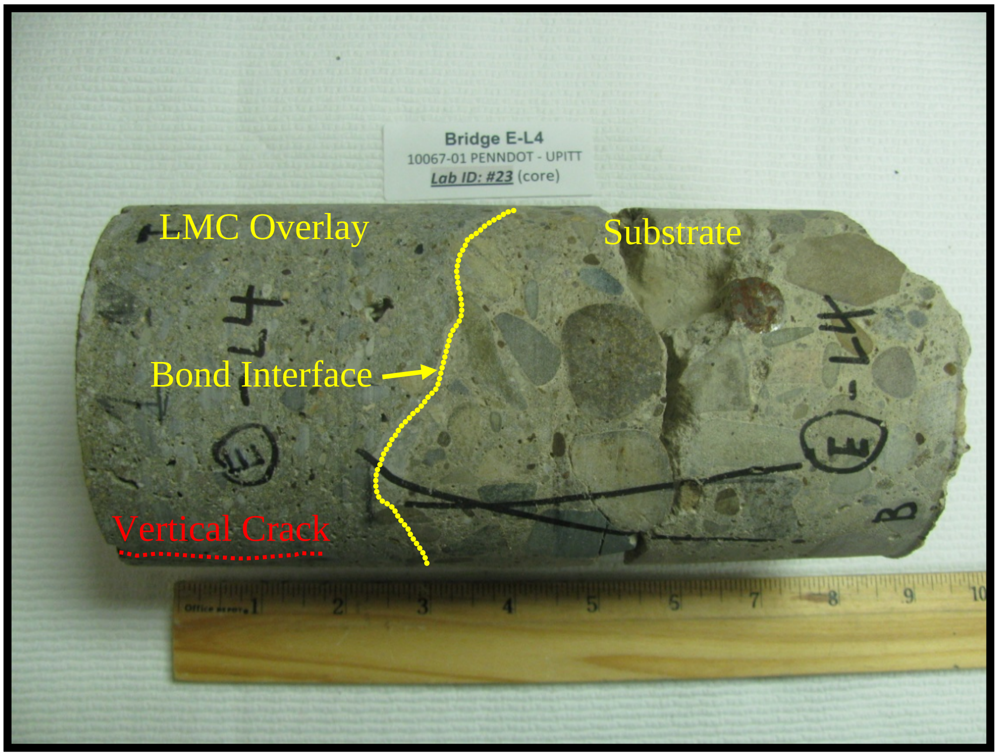

Photograph 1: SR79 (Bridge E) – L4 - Core

Photograph 2: SR79 (Bridge E) – L4 - Rebar

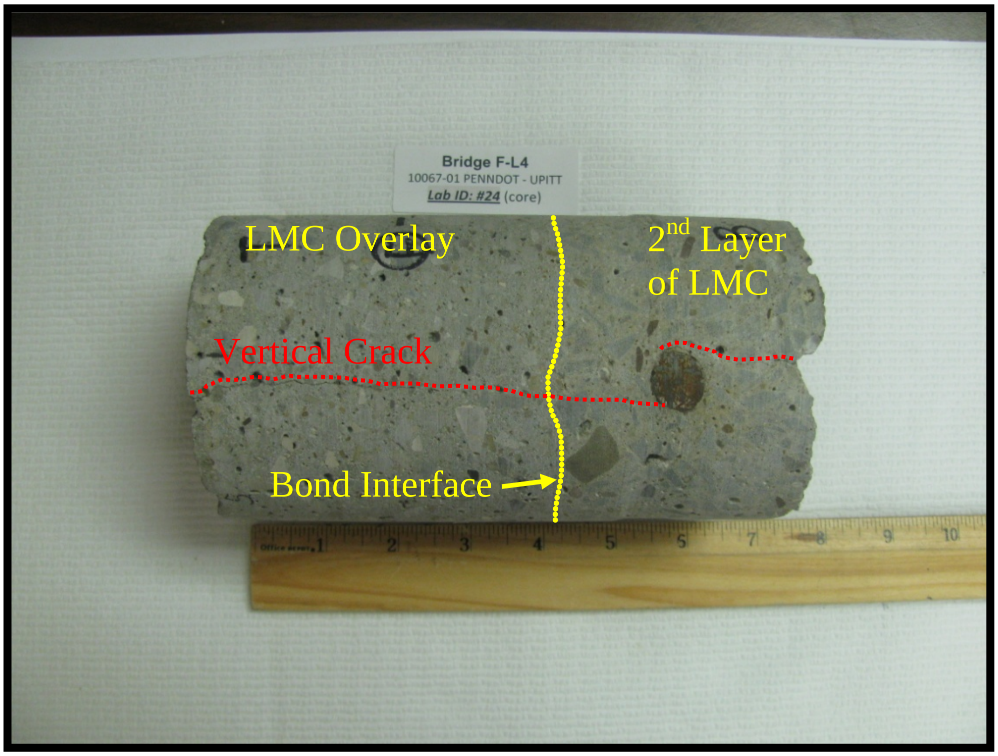

Photograph 1: SR837 (Bridge F) – L4 - Core

Photograph 2: SR837 (Bridge F) – L4 - Rebar

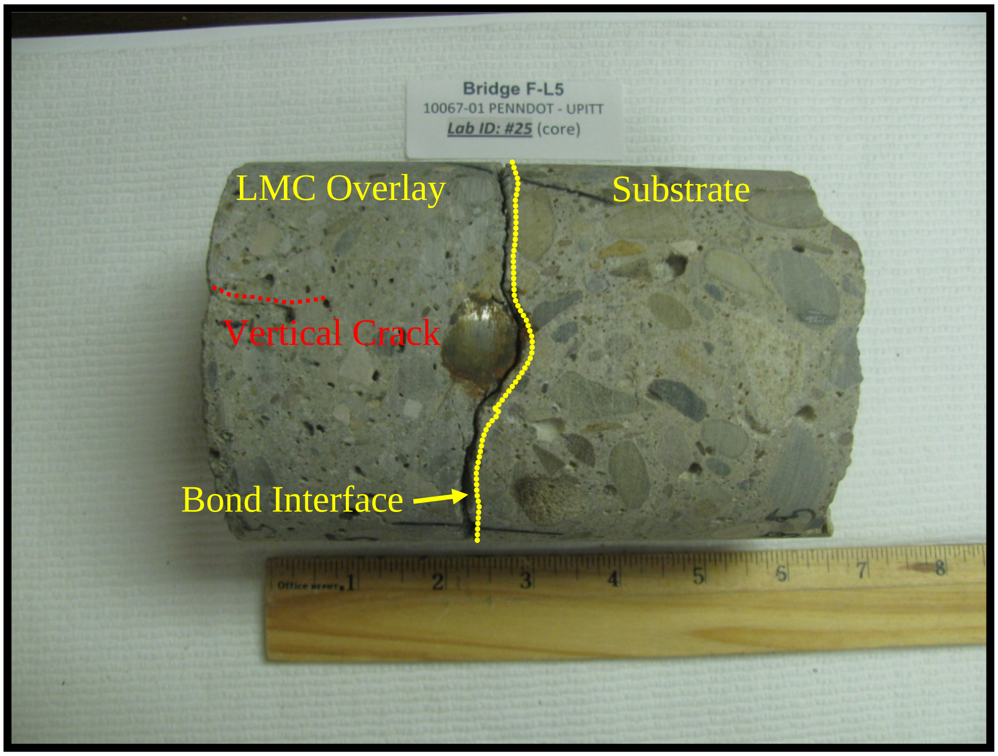

Photograph 1: SR837 (Bridge F) – L5 - Core

Photograph 2: SR837 (Bridge F) – L5 - Rebar

Summary of Core Chloride Content

No.	Core ID	Sample Collected Above Rebar	Sample Collected At Rebar Depth	Sample Collected Below Rebar	Notes
1	SR28 (Bridge A) - L4	**1335**	**409**		
2	SR28 (Bridge A) - L5	**1612**	**1041**		
3	SR28 (Bridge B) - L5	82	59		
4	SR79 (Bridge C) - L2	**647**	160		
5	SR79 (Bridge C) - L3	86	68		
6	SR79 (Bridge C) - L5	**518**	190		
7	SR79 (Bridge E) - L1	**1526**	**1733**		
8	SR28 (Bridge A) - L1	**1660**	**1869**		4-inch core with vertical crack
9	SR28 (Bridge A) - L3	**2630**	**2455**		4-inch core with vertical crack
10	SR79 (Bridge C) - L1	**1818**	**2401**		4-inch core with vertical crack
11	SR79 (Bridge C) - L4	**1763**	**1951**		4-inch core with vertical crack
12	SR79 (Bridge E) - L2	**2108**	**3294**		4-inch core with vertical crack
13	SR79 (Bridge E) - L4	**2202**	**1115**		4-inch core with vertical crack
14	SR28 (Bridge A) - L2		279	257	
15	SR28 (Bridge B) - L2		218	212	
16	SR28 (Bridge B) - L3		79	77	
17	SR837 (Bridge F) - L2		**559**	**498**	
18	SR28 (Bridge B) - L1		**1546**	**1734**	4-inch core with vertical crack
19	SR28 (Bridge B) - L4		**2157**	**1801**	4-inch core with vertical crack
20	SR79 (Bridge E) - L3		**593**	127	
21	SR837 (Bridge F) - L1		315	**877**	
22	SR837 (Bridge F) - L3		155	**803**	
23	SR837 (Bridge F) - L5		**1271**	**1275**	4-inch core with vertical crack
24	SR79 (Bridge E) - L5	143	81		
25	SR837 (Bridge F) - L4	**1532**	**1462**		4-inch core with vertical crack

Note: Values above the threshold for corrosion are highlighted in red type.
Samples collected from LMC are shaded in blue.
Samples collected from immediately below LMC-Base interface are shaded in green.
Samples collected from the base concrete are shaded in yellow.

Above 350 ppm
LMC
Interface (just below LMC)
Base Concrete